Experimental Program to Improve the VTE Distillation Process

United States Department of the Interior

Office of Saline Water • Research and Development Progress Report No. 487

Research and Development Progress Report No. 487 • September 1969

Experimental Program to Improve the VTE Distillation Process

By Dr. A. E. Dukler, and Messrs. L. C. Elliott and C. V. Grana, Houston Research Institute, Inc., Houston, Texas, for Office of Saline Water; Dr. Chung-ming Wong, Director, and Everett N. Sieder, Chief, Distillation Division.

Contract No. 14–01–0001–682

UNITED STATES DEPARTMENT OF THE INTERIOR • Walter J. Hickel, Secretary
Carl L. Klein, Assistant Secretary for Water Quality and Research

For sale by the Superintendent of Documents, U.S. Government Printing Office, Washington, D.C. 20402 - Price $2.

As the Nation's principal conservation agency, the Department of the Interior has basic responsibilities for water, fish, wildlife, mineral, land, park, and recreational resources. Indian Territorial affairs are other major concerns of America's "Department of Natural Resources".

The Department works to assure the wisest choice in managing all our resources so each will make its full contribution to a better United States—now and in the future.

FOREWORD

This is one of a continuing series of reports designed to present accounts of progress in saline water conversion and the economics of its application. Such data are expected to contribute to the long-range development of economical processes applicable to low-cost demineralization of sea and other saline water.

Except for minor editing, the data herein are as contained in a report submitted by the contractor. The data and conclusions given in the report are essentially those of the contractor and are not necessarily endorsed by the Department of the Interior.

TABLE OF CONTENTS

LIST OF FIGURES

LIST OF FIGURES (Cont'd.)

LIST OF FIGURES (Con'd.)

LIST OF TABLES

1. Conclusions

Data is reported from a single tube pilot plant with 10 ft copper fluted tubes of 2 and 3 in. diameter. Detailed analytical studies will be included in a later report. Discussion of the experimental results is included in Sections 5, 6 and 7. Some of the major conclusions are as follows:

-- The brine and fresh water pressure drop data for the 3 in. tube and the fresh water pressure drop for the 2 in. tube are correlated reasonably well by a simple relationship (Equation 5.1). Liquid flowrate had little effect on the pressure drop.

-- Entrainment rates with brine at the higher heat fluxes and liquid flowrates used for this study were high, sometimes in excess of 100 lb/hr.

-- There is no evidence of flooding of the fluted condensing surface as would be indicated by a drop in condensing film heat transfer coefficient at the higher heat fluxes.

-- The condensing film heat transfer coefficient is 3 to 5 times higher than the evaporating film heat transfer coefficient.

-- Both the condensing film and vaporizing film heat transfer coefficients show a trend for an increase with an increase in temperature.

-- Sea water (concentration factor of one) gives higher evaporating film heat transfer coefficients than fresh water. Brine with a concentration factor of 2.5 to 3.2 gives lower evaporating film heat transfer coefficients than fresh water. One exception to this is the 1000 lb/hr rate in the 2 in. fluted tube. At this condition a very significant increase in evaporating film heat transfer coefficient is obtained within a certain heat flux range.

-- The Colburn-Hougen method (2.2) successfully predicts the effect on heat transfer of a noncondensable gas in condensing steam for the 3 in. by 10 ft fluted tube.

-- Some improvement in the heat transfer coefficient was obtained at a 500 lb/hr flowrate in the 3 in. fluted tube with inserts in the middle of the tube. The spiral baffle gave a 9 percent increase in overall heat transfer coefficient.

2. Introduction

The objective of this study was to obtain data suitable for engineering design purposes for the fluted tube in downflow VTE operation and to explore the effect of certain variables upon performance. Not only was heat transfer data taken but also data on pressure drop and entrainment. Three in. and two in. nominal diameter tubes with a 9 ft 10 in. fluted section were tested. Variables studied were liquid flowrate, salinity and temperature.

The effect of the presence of air in condensing steam on heat transfer with the fluted tube was also studied. The presence of air or any noncondensable gas in condensing steam reduces heat transfer by:

-- Reducing the bulk temperature of the steam, thereby reducing the temperature driving force available for heat transfer.

-- Providing a diffusional resistance to transport of the steam to the liquid interface which further reduces the available temperature driving force.

Air leakage into distillation effects operating under vacuum cannot be completely eliminated with present technology. Therefore, knowledge of the effect on heat transfer of air in the condensing steam is needed. An earlier segment of this study (2.1) determined the effect of noncondensables with condensation at one point on a vertical smooth tube. The relation of Colburn and Hougen (2.2) for predicting the effect of noncondensables gave good agreement with the experimental data. In the work reported here heat transfer for the fluted tube with air present in the condensing steam was checked over the widest range of conditions feasible with the present equipment. A comparison of the experimental results with the prediction of Colburn and Hougen is given.

Experiments to determine the effect on heat transfer of induced shear and turbulence on the evaporating side of the fluted tube are also reported here. The resistance to heat transfer in a doubly fluted tube was shown to be much higher on the evaporating side than on the condensing side. Further improvements in fluted tube heat transfer must be directed to reducing the resistance of the evaporating film.

(2.1) OSW R&D Report No. 287 (1967), Houston Research Institute.

(2.2) Colburn, A. P., and O. A. Hougen, Ind. Eng. Chem., 26, 1178-1182 (1934).

Three different methods of inducing shear and turbulence in the evaporating film were used in a 3 in. diameter by 10 ft doubly fluted tube:

1. Cylindrical 2 in. diameter baffle in approximate upper 1/3 of tube.

2. Balls of 2.15 in. diameter installed 5 in. apart in approximate upper 1/3 of tube.

3. Sephton spiral baffle over the full tube length.

Installation of the first two in the upper part of the tube serves to increase the velocity and shear where they are normally the lowest.

3. Experimental Equipment

Several different configurations of the fluted tube have been produced. The one used in this study is generally known as Profile 9. It was tested in both the 3 in. and 2 in. nominal diameter sizes. A photo of the 3 in. fluted tube tested is shown in Figure 3.1, and Figure 3.2 shows the approximate characteristic tube dimensions in cross-section based on information from Oak Ridge National Laboratory (ORNL) (3.1). Both tubes have a 9 ft 10 in. long fluted section with a smooth portion at each end and are made of ASTM 375 copper. The 2 in. tube was prepared from a 3 in. tube at ORNL by cutting out a 1 in. strip, reshaping it and welding it back together. The 3 in. tube, as received, had a moderately adherent layer of corrosion product resulting from previous testing at ORNL. This was removed by a thorough scrubbing both inside and out until the tube had the appearance shown in Figure 1. The 2 in. tube had apparently not been tested previously.

A flow diagram of the apparatus in which the two tubes were tested is shown in Figure 3.5 with mechanical details in Figures 3.7 and 3.8. Unevaporated water from the VTE (vertical tube evaporator) drops to the holdup tank. Makeup water is added at a rate sufficient to maintain a relatively constant salinity. Brine recirculation rate is measured with a rotameter. Steam or hot water flowing to the feed water heater is automatically controlled to maintain the desired feed water temperature. The water is evenly distributed around the periphery of the inside of the tube with a Shutte and Koerting model 1/2 SK 622F spray nozzle with a hollow cone pattern. Most of the water falls down the inner wall of the tube in an annular film. Some of the water, however, is torn from the wall by the shearing action of the steam which is generated. At the bottom of the tube, the entrainment sampling cone (shown in Figure 3.5 in lowered position) collects the steam and entrained liquid. A carefully machined deflector attached to the end of the tube draws the annular liquid film away from the sampling cone and directs it to the holdup tank. Clearance between the entrainment sampling cone and deflector must be great enough so that the tops of the waves in the liquid film are not clipped off and enter the sampling cone with the steam. To further assure that all the liquid is deflected, a small amount of steam is by-passed through the clearance between the deflector and sampling cone, bypassing the cyclone separator. The steam and entrained liquid from the sampling cone pass through the cyclone separator where the entrainment is removed and falls into the entrainment tanks for measurement.

(3.1) Alexander, L. G., J. D. Joyner, H. W. Hoffman, Advanced VTE Heat-Transfer Surfaces, OSW Symposium on Enhanced Tubes for Distillation Plants, Washington, D. C., March 1969

The steam produced in the operation goes to the condenser and vacuum system. A two-stage steam jet ejector is used to pull a vacuum on the system. Vacuum is controlled at any desired level by bleeding air into the line ahead of the vacuum system.

Steam flow rate to the four in. diameter shell is automatically controlled to maintain the desired shellside pressure. The steam is desuperheated with prescribed amounts of water in a desuperheater. This is a small vessel containing two sections of wire mesh into which the water required to desuperheat the steam is metered. The wire mesh prevents the water from passing out of the desuperheater without being evaporated.

Steam condensate at the bottom of the shell flows through a steam trap, is then cooled in a heat exchanger and collected in a condensate tank. This tank has a two position level control which actuates a pump to automatically pump out the condensate for weighing whenever it reaches a certain level. A manually controlled vent at the bottom of the shell is required to prevent the buildup of noncondensable gases. A careful testing procedure during installation finds the major leaks and allows them to be eliminated or minimized. However, it is impossible to completely eliminate all leakage. Noncondensables are also present with the incoming steam. These will in time build up on the shellside and seriously impede heat transfer if they are not vented.

Extensive temperature, pressure and flow rate measurements are taken on each run to permit the calculation of heat transfer rates from material and energy balances independently on both the shell side and tubeside. Manometers with water or mercury are used for pressure drop and vacuum measurements because of their accuracy and reliability. The absolute pressure and pressure drop measuring system is shown in Figure 3.3.

A special thermocouple system shown in Figure 3.4 was installed to determine temperature differences for calculation of experimental individual heat transfer coefficients. Thermocouples for this purpose have a stainless steel sheath with ceramic packing. Six thermocouples were installed in the wall along the length of the tube. Their location in the wall is shown in a profile view in Figure 3.2. Slots of 1.5 in. length were milled into the tube for each thermocouple so that the conduction error associated with this type of installation would be minimized. The thermocouples were soldered in place with a low melting solder, Eutec* Rod 157-B. In the 3 in.

---

* Eutectic Welding Alloys Corporation

diameter tube half of the thermocouples were 0.04 in. and half were 0.02 in. Figure 3.2 shows how each of these are located but only one thermocouple was used at each position. For the 2 in. tube all the imbedded thermocouples were 0.04 in. diameter.

Locations of all of the special thermocouples are shown in Figure 3.4. In addition to the thermocouples imbedded in the wall, 0.062 in. diameter thermocouples were used for measuring the temperature of the steam and the vapor produced on the tube side. Those thermocouples installed on the tube side were brought out through the lower end of the tube rather than through the wall in order to avoid disturbing the liquid flowing down the wall. Special limits of error were requested on all the sheathed thermocouples. Thermocouples for the three in. fluted tube were calibrated according to ASTM Standard E 220-64 Method C. For the two in. tube the thermocouples were calibrated by the manufacturer.

The thermocouples performed very well. The only problem was an occasional partial short, probably from moisture or dust, at the end of the thermocouple sheath where the transition to lead wire was made. This occurred only with the 0.02 and 0.04 in. thermocouples. After the problem was identified, the shorts were corrected, if they persisted, as soon as the job could be scheduled. This usually involved cutting back some of the stainless steel sheath and exposing additional thermocouple wire which was then connected to the lead wire.

The thermal conductivity of the copper tube wall was so high that the temperature drop across it in the worst case was only about 0.2°F. Therefore, the surface temperature could reasonably be assumed the same as the temperatures indicated by the thermocouples imbedded in the wall of the tube. The temperature across the evaporating and condensing films could then be determined. However, there was no way of obtaining heat flux at various points along the length of the tube. Therefore, individual heat transfer coefficients averaged over the length of the heated section were obtained based on mean thermal driving forces and the heat flux calculated from the material and energy balance. The thermocouple hook-up and switching circuit is shown in Figure 3.6. Temperature differentials are of primary importance in determining the experimental heat transfer coefficient. For this reason, a thermocouple switching and measuring circuit was designed so that various thermocouple pairs could be connected in series opposition. Since the thermocouples were of the grounded junction type and it was not practical to electrically insulate them from one another, an isolating comparator circuit, described by Dauphinee (3.2) and modified by Vanbo Pak (3.3), was included in the

---

(3.2) Dauphinee, T. M., Canadian Journal of Physics, 33, 275 (1955)

(3.3) Vanbo Pak, IZMERITEL NAYA TEKHNIKA, No. 6, 23, June 1962

circuit. The thermocouple reference junction used was 150°F Pace-Wiancko Model BRJR13-12TT.

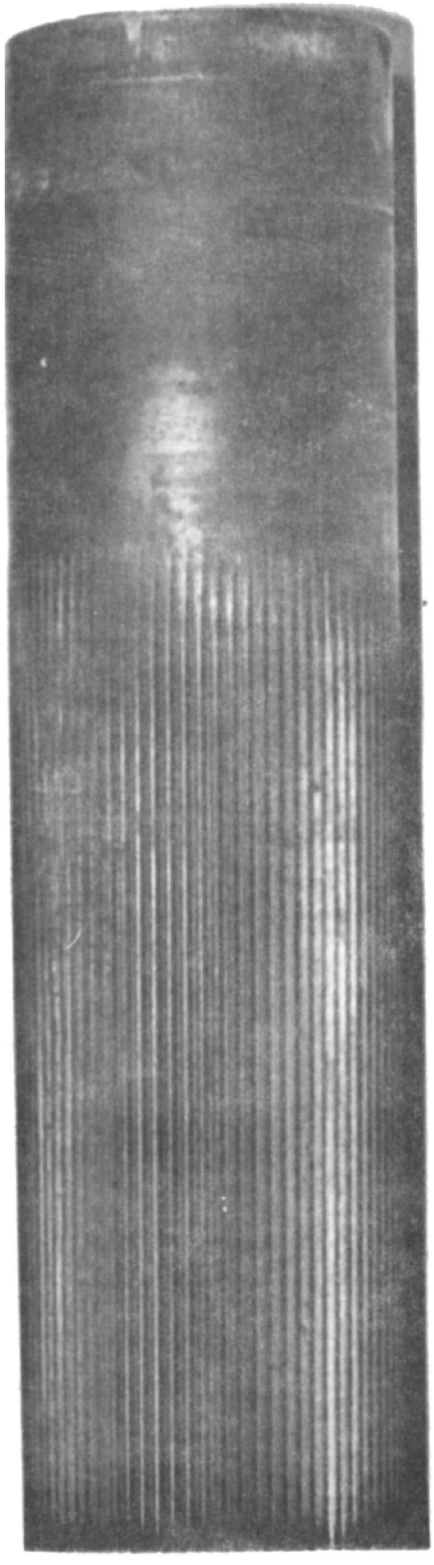

FIGURE 3.1 Three in. diameter fluted tube.

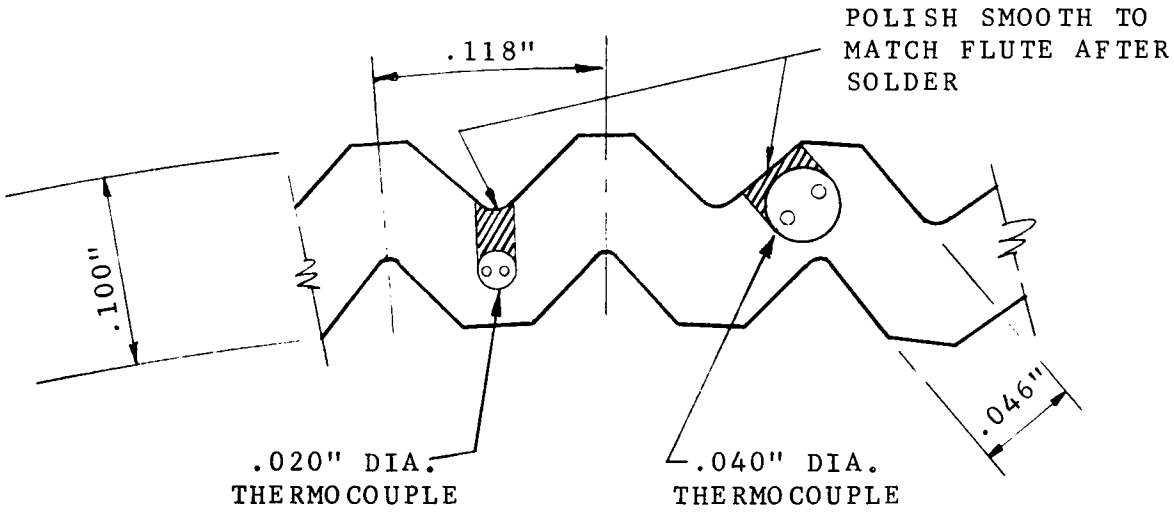

FIGURE 3.2. Profile of fluted tube showing method of installing wall thermocouples.

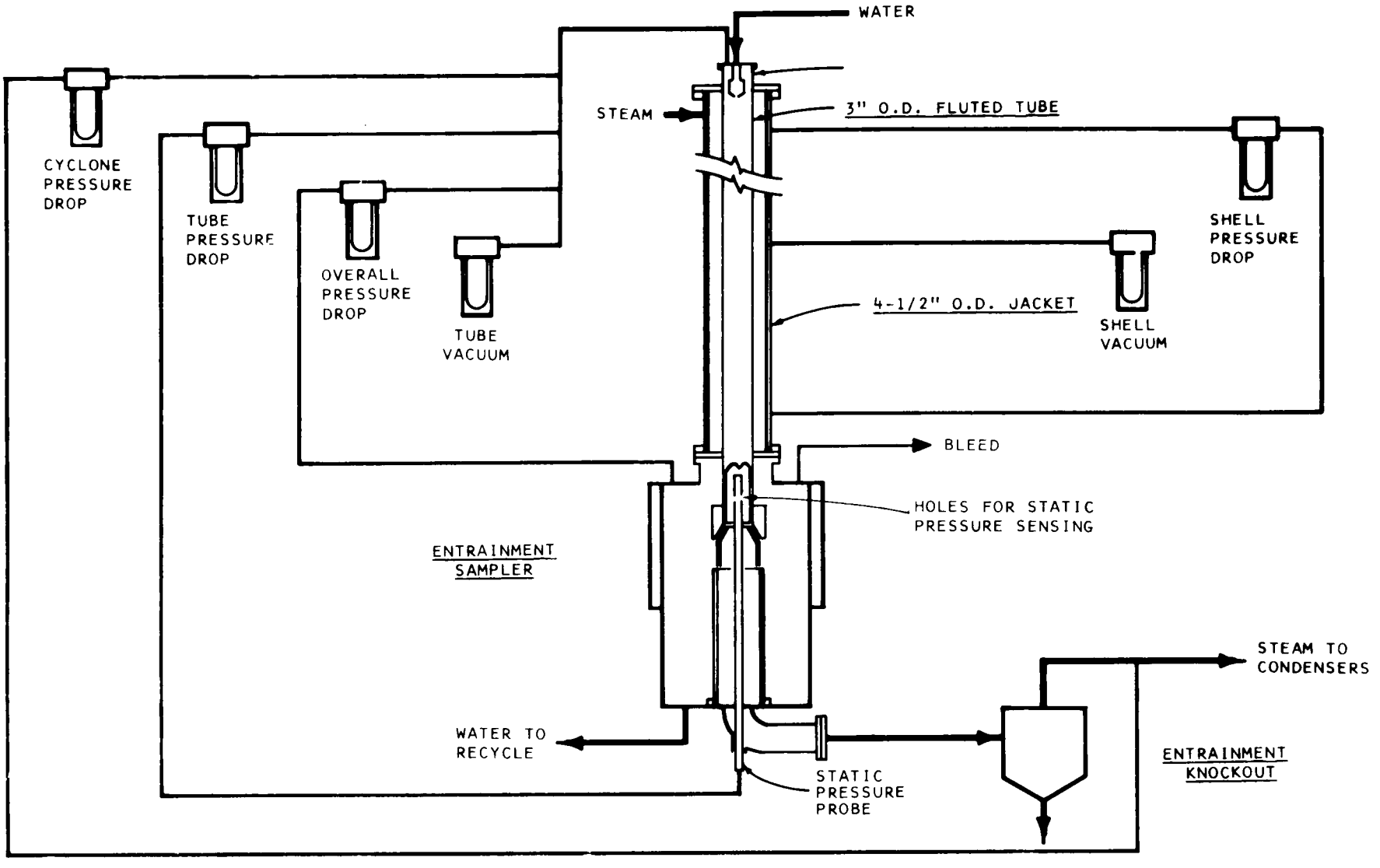

FIGURE 3.3. Manometer system for measuring pressure and pressure drop.

FIGURE 3.4. Location of special thermocouples.

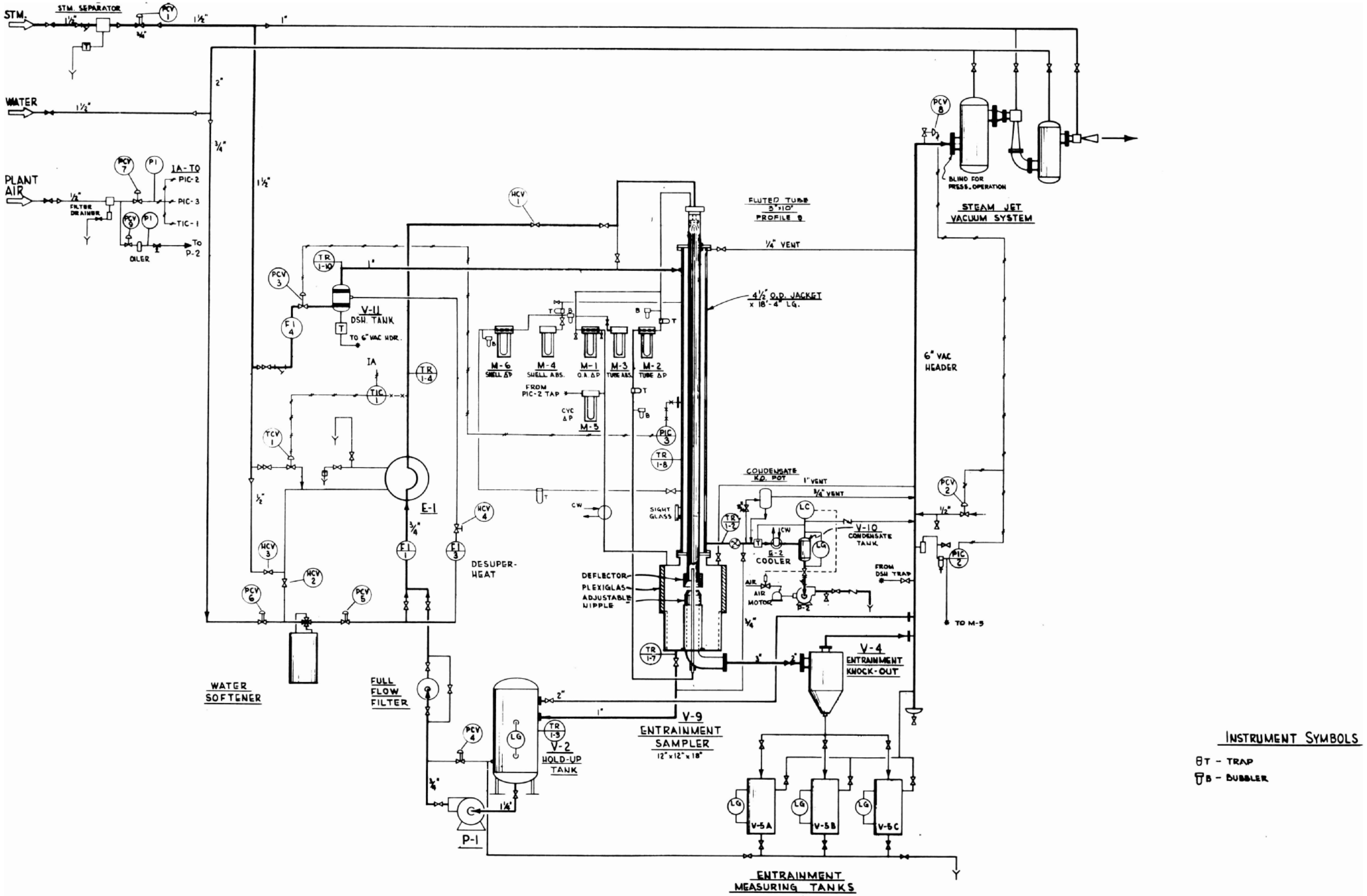

FIGURE 3.5. Mechanical Flowsheet of Test Equipment.

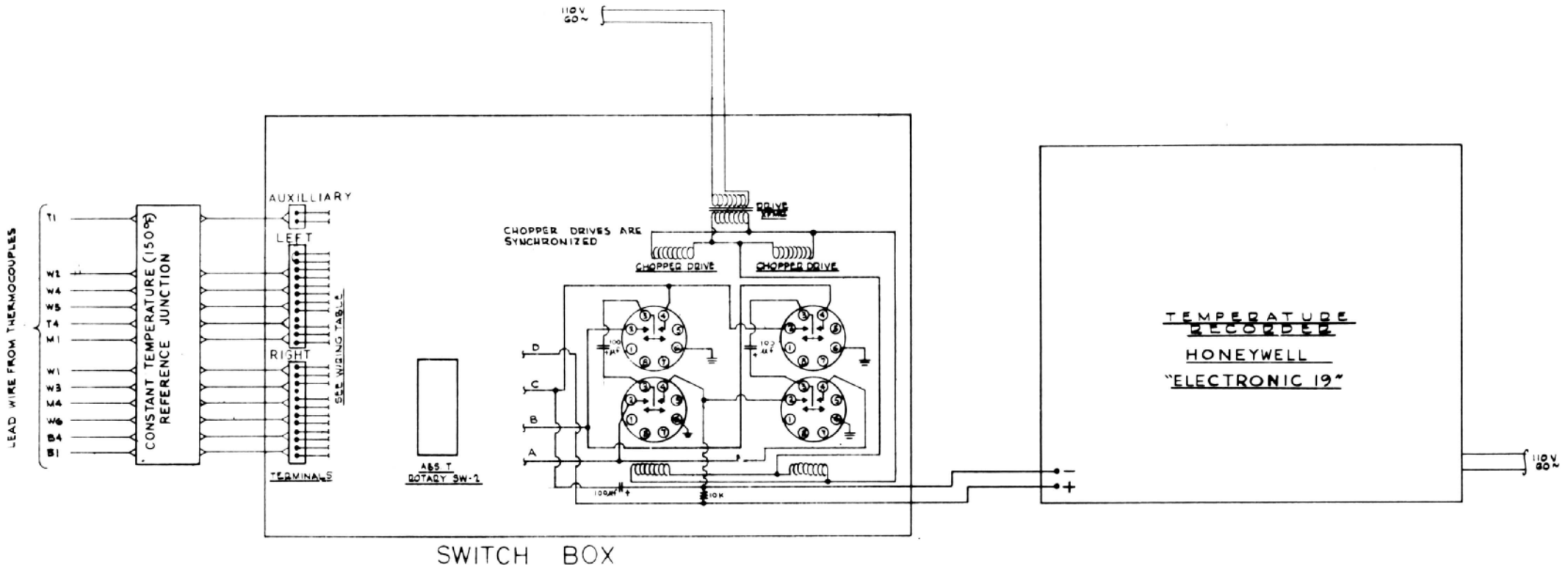

ROTARY SW-2

SWITCH POSITION	I	II	III	IV	V	VI	VII	VIII	IX	X	XI	XII
POLE A	T1+	T1+	T1+	T1+	T1+	T1+	T1+	T1+	T1+	T1+	T1+	T1+
POLE B	T1-	T1-	T1-	T1-	T1-	T1-	T1-	T1-	T1-	T1-	T1-	T1-
POLE C	SHORT	W2-	W3-	W4-	W5-	W6-	W -	M1-	B1-	T4-	M4-	B4-
POLE D	SHORT	W2+	W3+	W4+	W5+	W6+	W +	M1+	B1+	T4+	M4+	B4+

BOX (REFERENCE T.C.) ALWAYS < TUBE

FIGURE 3.6. Hookup and switching of special thermocouple system.

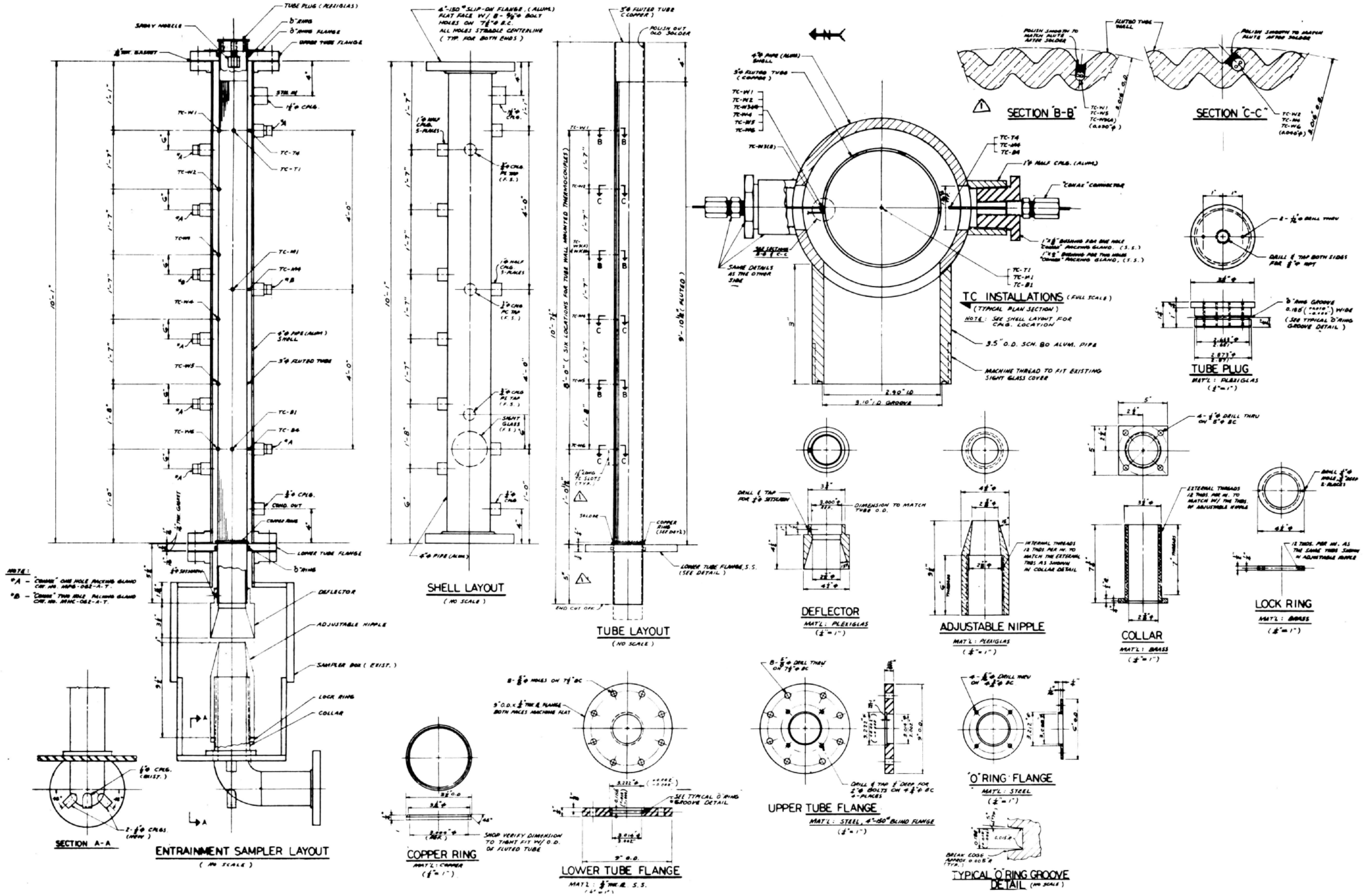

FIGURE 3.7. Mechanical details for three in. fluted tube installation.

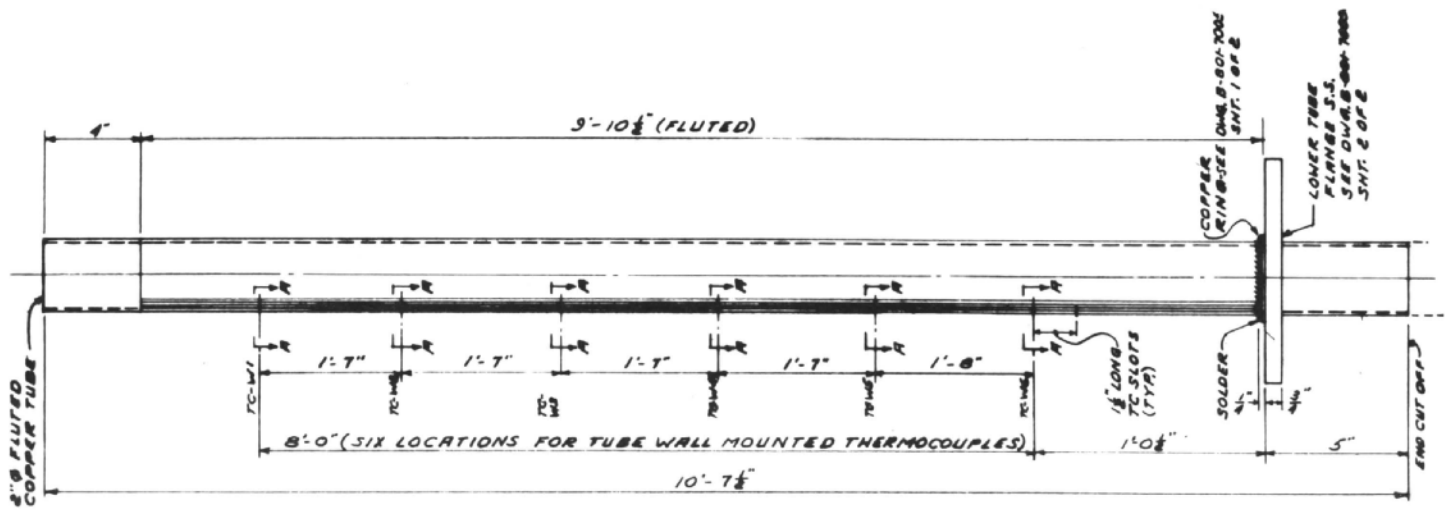

SECTION "A-A"

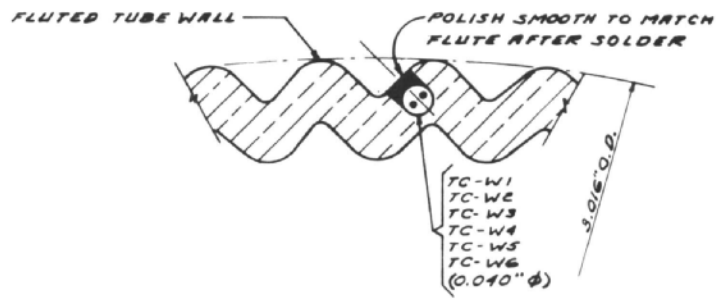

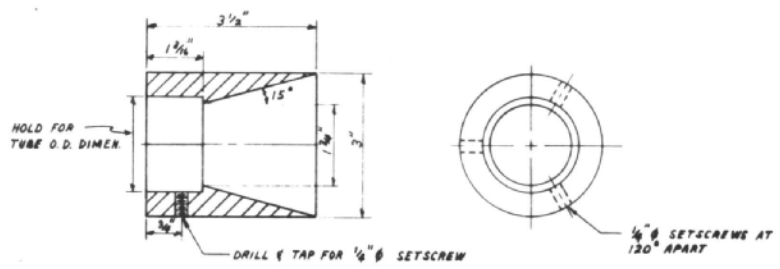

DEFLECTOR - PLEXIGLAS
(½" = 1")

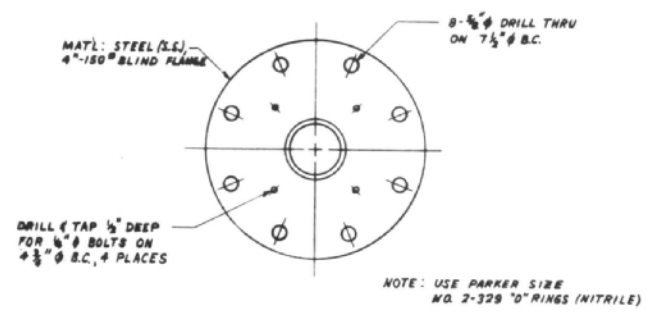

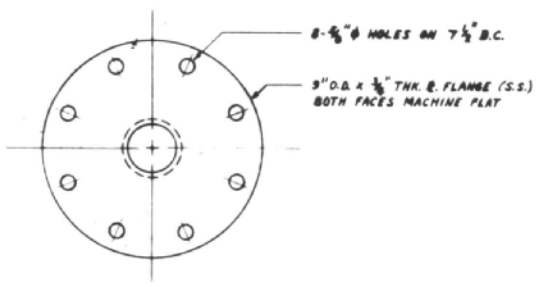

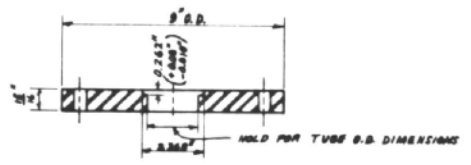

UPPER TUBE FLANGE
(⅛" = 1")

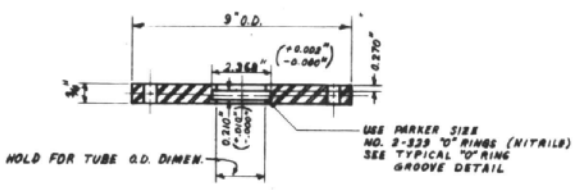

LOWER TUBE FLANGE
(⅛" = 1")

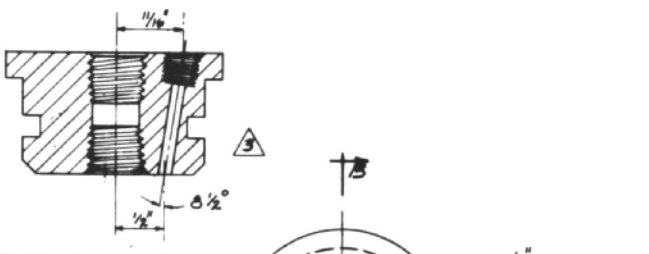

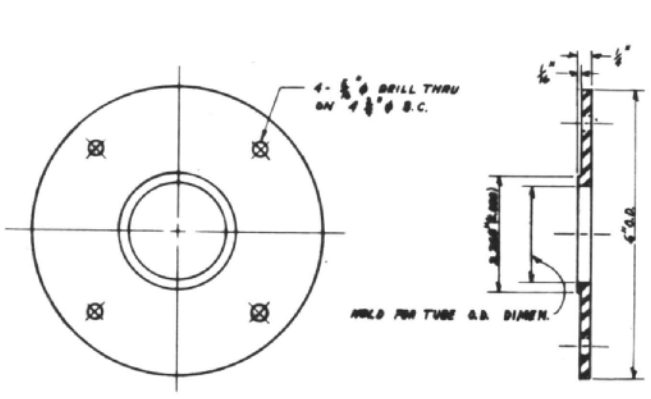

"O" RING FLANGE
MAT'L: STEEL (S.S.)
(½ = 1")

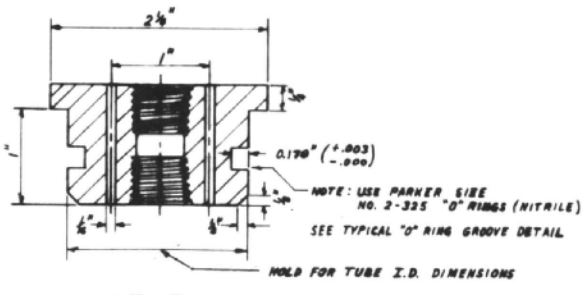

TUBE PLUG
MAT'L: BRASS
(FULL SCALE)

SECTION A-A

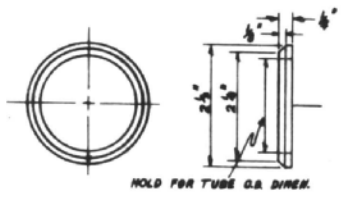

COPPER RING
MAT'L: COPPER
(½" = 1")

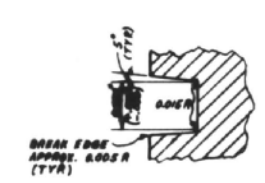

TYPICAL "O" RING GROOVE DETAIL
(NO SCALE)

FIGURE 3.8. Modifications required for two in. fluted tube installation.

4. Procedure

The range of operating conditions covered in this study is shown in Table 4.1. Three levels of tube side vacuum were explored; 0, 18 and 26 in. Hg vacuum. Temperature driving force ranged from 2 to 18°F. Experiments were run on a standard 3 in. fluted tube as well as on the special 2 in. fluted tube. Between the two tubes the liquid flow rate ranged from a low of 250 to a high of 1000 lb/hr. As indicated in the table, the Reynolds number of the evaporating liquid in the tube based on nominal tube diameter varied from about 900 to 5400. Reynolds number is calculated from

$$Re_L = \frac{4W_L}{\pi D \mu_L} \qquad (4.1)$$

where Re_L = Reynolds number of liquid film on vaporizing side

W_L = liquid flow rate, lb/hr

π = dimensionless constant, 3.1416

D = nominal tube diameter, ft.

μ_L = viscosity of liquid film, lb/(ft) (hr)

The fresh water runs used tap water which was softened before charging to the equipment in a household type softener. Sea water for testing was obtained from the Freeport Test Bed or prepared from a commercially available artificial sea salt. The unevaporated water was recirculated in the system. With brine recirculation, makeup water was added continuously during a run to replace the evaporated water and keep a uniform brine concentration. The amount of water added was accurately weighed so that its contribution to the material balance could be determined. The recirculating brine was continuously filtered using a ten micron cartridge filter.

The pH and alkalinity of the recirculating brine tended to drift upward during the runs. The pH was determined frequently during the operation and acid was added when necessary to maintain scale-free operation. In spite of this, an alkaline scale was deposited on the inside surface on two occasions when solubility limits were exceeded. This was removed in each case by a short period of recirculation of a sulfamic acid solution containing a corrosion inhibitor.

Data taking at a given condition was not begun until the system had reached a steady operating condition. The time

TABLE 4.1

RANGE OF OPERATING CONDITIONS

Tubeside Vacuum, in. Hg		
0 (1 atm)	18	26
Concentration Factor		
0.0	0.0	0.0
0.8	0.8	0.8
1.5	1.9	2.8

Range of Differential Temperatures
2 to 18°F

Water Flowrates			
Rate for 3" Tube Lb/Hr	Rate for 2" Tube Lb/Hr	Nominal Peripheral Rate Lb/(hr)(in.)	Re_L
250	---	27	900
500	330	53	↓
1000	670	106	↓
---	1000	159	5400

required to line out the equipment was normally 30 to 60 minutes unless some abnormal problem was encountered, such as equipment malfunction or a load change which required readjustment of the proportional band or reset rate on one of the controllers. Usually four complete sets of data were taken at intervals of 8 to 15 minutes. Data recorded consisted of temperatures, thermocouple EMF outputs, rotameter readings, tank levels, pressures, differential pressures and weight of condensate and makeup water. Tank levels and condensate weighings were converted to flowrates and the mean values for these and each of the other recorded variables were calculated. The averaged values were then transferred to punched cards for computer analysis. The computer program included calculation of thermocouple calibration corrections, average individual heat transfer coefficients, material balance and energy balance.

In order to complete the material and energy balance for each run, values for the heat loss from both the tubeside and shellside were required. These were determined experimentally for a range of differences between the equipment temperature and ambient temperature. A saml1 amount of steam was passed through both the shellside and tubeside with the pressure equalized between the two. Changes in level of the condensate tank, holdup tank, and entrainment tanks were recorded for a period of about two hours. The changes in levels, resulting from heat loss and condensation of the steam, were converted into equivalent heat loss terms for the appropriate portions of the equipment.

5. Test Results for Two and Three In. Fluted Tubes

The test results for the three in. tube are summarized in Tables 5.1 and 5.2 and results for the two in. tube are listed in Tables 5.3 and 5.4. Data which was unavailable because of equipment malfunction, e.g., short-circuit in thermocouple connection, or for any other reason are left blank.

The test results are presented graphically in Figures 5.1 to 5.28 with the accompanying discussion in Sections 5.1 to 5.5.

The various headings for Tables 5.1 to 5.4 are further described as follows:

Run Number

Each of the identifying run numbers in the table includes a sequential integer number.

Tubeside

Water Rate: Feed water rate to top of tube as measured by rotameter (FI1 in Figure 3.5).

Feed water Temperature: Measurement from thermocouple TR1-4 in line before control valve used to regulate flow to tube.

Overall Pressure Drop: Pressure drop between tube inlet and entrainment sampler (See Figure 3.3).

Tube Pressure Drop: Pressure drop between tube inlet and static pressure probe (See Figure 3.3).

Entrainment: Amount of water entrained in steam at the tube exit.

Water Evaporated: Steam at tube exit calculated from material and energy balance.

Heat Transfer:

Based on shellside material and energy balance.

Heat Balance Check:

Comparison of heat transfer based on shellside to that based on tubeside.

Log-Mean ΔT: Overall thermal driving force determined from readings of thermocouples T1, T4, B1 and B4 in Figure 3.4.

TABLE 5.1

SUMMARY OF RUNS WITH FRESH WATER FOR 3 IN. BY 10 FT FLUTED TUBE

Run No.	TUBESIDE Water Rate Lb/Hr	Feed Water Temp,°F	Overall Pressure Drop In.Water	Tube Pressure Drop In.Water	Entrainment Lb/Hr	Water Evaporated Lb/Hr	Heat Transfer M BTU/Hr	Heat Balance Check %	Log-Mean ΔT °F	TEMPERATURES, °F (See Figure 3.4 for locations) T4	M4	B4	W1	W2	W3	W4	W5	W6	T1	M1	B1	HEAT TRANSFER COEFFICIENT BTU/HR - FT^2 - °F U(1)	h_o(2)	h_i(3)
VIII26-208	500	127.0	.30	.20	4.6	71.0	71.0	-3.8	7.2	131.2	131.5	131.1	131.4	129.9			129.7	129.5	124.0	123.9	123.7	1267	5812	1234
VIII26-209	750	126.0	.30	.30	7.1	67.1	69.2	.1	7.8	130.9	131.0	130.9	131.1	130.0			129.7	129.7	123.2	123.2	123.0	1143	7534	1055
VIII26-210	250	128.0	.30	.20	12.1	83.2	80.5	-6.9	6.6	130.1	130.1	130.1	130.5	129.0			128.7	128.7	123.6	123.5	123.3	1571	8254	1510
VIII26-211	250	128.0	.20	.15	12.1	48.4	48.3	2.6	3.4	125.4	125.3	125.2	125.3	124.4			124.5	124.4	122.0	121.9	121.8	1823	6634	1893
VIII26-212	500	124.0	.10	.10	3.6	44.8	47.2	-.4	5.4	126.9	126.8	126.8	126.9	126.1			125.8	125.7	121.5	121.5	121.4	1128	6154	1977
VIII26-213	250	126.0	.60	.55	14.4	114.6	115.1	-2.9	11.7	133.0	133.0	133.0		130.2			129.6	129.4	121.5	121.3	121.0	1271	4380	1342
VIII26-214	500	126.0	.50	.30	4.3	96.7	99.9	1.0	13.2	135.1	134.8	134.8		133.1			132.7	132.1	122.0	121.8	121.5	977	5489	929
VIII26-215	500	126.0	.20	.10	5.3	52.2	51.5	-4.3	7.3	130.1	130.0	130.0		129.3			129.1	128.7	122.8	122.8	122.6	909	6208	839
VIII26-216	250	126.0	.35		13.2	73.0	75.0	-1.3	6.7	130.6	130.6	130.5		129.0			128.6	128.2	124.0	123.9	123.7	1442	4761	1549
VIII26-217	750	127.0	.20	.15	8.6	56.4	55.7	-1.3	8.0	130.7	130.6	130.6		129.8			129.6	129.4	122.8	122.8	122.6	906	6439	833
VIII26-218	500	126.0	.40	.33	4.6	83.7	89.8	3.6	12.0	135.5	135.3	135.1		133.8			132.6	129.9	123.5	123.5	123.2	972		
VIII26-219	250	126.0	.50	.40	10.1	93.9	100.7	2.8	10.7	134.6	134.4	134.1		132.9			131.7	129.7	123.9	123.7	123.4	1218		
VIII18-220	500	170.0	.07	.05	5.3	15.6	22.0	17.1	2.2	170.8	170.6	169.8		169.0			169.1	168.9	168.1	168.1	168.0	1201		
VIII18-221	250	170.0	.08	.05	9.8	22.1	21.6	-18.6	2.1	170.5	170.2	169.5		169.1			169.0	168.7	167.9	167.9	167.9	1342		
VIII18-222	500	171.0	.10	.10	4.6	52.7	53.7	-2.5	6.0	174.8	174.6	174.4		173.5			172.9	172.0	168.6	168.7	168.6	1163	3785	1254
VIII18-223	750	170.0	.10	.10	6.7	48.1	48.9	-2.6	5.8	175.0	174.6	174.2		173.6			173.1	172.4	168.8	168.8	168.8	1094	4249	1115
VIII18-224	250	172.0	.20	.17	9.1	59.6	61.7	-2.2	5.2	173.8	173.7	173.3		172.7			171.9	170.8	168.4	168.5	168.4	1543	4419	1724
VIII18-225	500	168.0	.20	.20	4.2	89.9	95.0	1.7	9.8	178.1	177.9	177.7		176.3			175.1	174.0	168.1	168.2	168.1	1282	4361	1317
VIII18-227	250	173.0	.30	.30	4.7	113.3	120.4	3.3	11.1	179.4	179.1	179.0		176.4			175.3	175.1	168.1	168.1	168.1	1408	4251	1552
VIII26-228	500	126.0	.30	.25	4.3	62.3	71.7	11.1	7.2	129.5	129.5	129.5		128.4			127.8	127.7	122.4	122.4	122.2	1288	5839	1274
VIII 0-229	250	213.5	.30	.10	6.5	23.8	33.5	15.7	1.9	213.4	213.4	213.4	213.3	213.1			212.9	213.3	211.4	211.5	211.5	2226	11670	2174
VIII 0-230	500	213.0	.10	.10	7.9	25.4	33.1	9.4	2.2	213.5	213.5	213.5	213.4	213.1			213.0	213.3	211.2	211.3	211.3	1909	10424	1844
VIII 0-231	750	214.0	.15	.10	15.1	59.9	65.7	6.4	4.9	216.6	216.5	216.5	216.4	215.9			215.6	215.9	211.6	211.7	211.6	1732	10068	1623
VIII 0-232	500	215.5	.20	.15	10.3	66.8	70.6	3.1	4.9	216.8	216.8	216.8	216.7	216.1			215.8	216.0	211.8	211.9	211.9	1850	10495	1756
VIII 0-234	500	214.0	.30	.25	8.4	133.6	143.0	5.9	9.7	221.6	221.6	221.5	221.5	219.9			218.9	218.9	211.8	211.9	211.9	1904	7452	1943
VIII26-235	500	125.0	.15	.10	4.3	29.0	30.7	-.3	3.5	127.4	127.2	126.8	127.2	126.7			126.0	125.7	123.6	123.7	123.6	1130	3977	1174
VIII26-236	250	126.0	.10	.05	11.7	34.7	37.2	1.8	2.8	126.3	126.2	125.8	126.2	125.6			124.9	124.7	123.3	123.3	123.2	1715	4738	1917
VIII26-237	250	124.0	.30	.20	11.0	66.1	68.0	-1.7	6.0	129.2	129.1	129.1	129.0	128.1			127.4	127.5	123.2	123.2	123.0	1463	5949	1480
VIII26-238	250	124.0	.35	.35	8.6	101.9	105.8	-.4	10.3	134.4	134.3	134.3	134.4	132.6		132.4	132.2	132.4	124.2	124.1	123.8	1325	6853	1278
VIII 0-239	250	214.0	.25	.20	9.3	73.5	75.2	-2.8	5.6	218.1	218.0	218.0	217.8	217.2	217.4	216.9	216.6	216.7	212.4	212.5	212.4	1729	8278	1686
VIII 0-240	250	215.0	.25	.22	4.5	124.0	126.7	.1	9.8	221.9	221.9	221.9	221.7	220.1	220.5	219.5	219.0	219.3	212.0	212.1	212.1	1665	6865	1678
VIII26-241	500	124.0	.25	.20	2.8	52.2	52.3	-5.0	6.6	130.8	130.8	130.4	130.7	129.7	129.8	129.4	128.9	128.3	124.0	124.0	123.9	1021	4528	1003
VIII26-249	500	126.0	.40	.20	4.3	91.5	95.2	.9	11.3	135.2	135.1	135.1	135.1	133.6	133.9		132.6	131.8	124.0	124.0	123.7	1094	5699	1052
VIII26-250	250	127.0	.42	.20	8.0	101.0	110.4	5.0	10.4	134.8	134.8	134.8	134.6	133.2	133.7	132.9	132.3	131.9	124.6	124.5	124.2	1373	6858	1341
VIII 0-262	500	217.0	.10	.10	31.7	47.6	48.5	-1.8	4.4	215.6	215.5	215.1	215.1	215.1	215.1	215.1	214.9	215.2	211.2	211.3	211.2	1430(4)	10930	1303(4)
VIII 0-264	500	217.0	.10	.10	20.1	23.1	19.9	-27.9	2.1	213.9	213.9	213.8	213.8	213.6	213.6	213.6	213.6	213.7	211.8	211.9	211.8	1252(4)	8684	1167(4)
VIII 0-268	500	217.5	.15	.10	32.7	80.8	80.9	-1.1	6.8	218.9	218.8	218.8	218.7	217.7	217.7	217.8	217.6	217.9	212.0	212.1	212.0	1538(4)	8883	1455(4)
X 26-266	1000	126.0	.40	.25	13.8	72.2	75.8	6.5	7.6	130.0	130.0	130.1	129.7	129.1	129.2	128.8	128.6	128.7	122.6	122.5	122.3	1294	7780	1218
X 26-267	1000	123.0		.80	31.7	114.3	118.6	-.0	12.5	137.3	137.4	137.6	137.6	135.4	135.8	135.1	134.4	134.6	125.2	125.0	124.6	1223	6189	1183
X 26-268	500	126.0	.55	.45	3.7	100.3	110.7	7.8	10.4	133.9	133.8	133.8	133.7	132.2	132.6	132.0	131.4	131.4	123.6	123.5	123.1	1371	6931	1326
X 26-269	1000	130.0	.55	.40	24.0	156.0	162.8	6.8	17.1	139.4	139.4	139.5	140.0	137.3	137.8	136.8	135.8	136.1	122.9	122.6	121.7	1228	7730	1149
X 18-270	1000	181.0			14.7	117.3	126.0	6.6	10.9	180.0	180.0	180.1	179.7	178.4	178.9	178.2	177.7	177.7	169.2	169.2	169.1	1502	8224	1431
X 18-271	500	190.0			5.3	125.7	128.1	5.2	11.2	177.1	177.1	177.1	176.9	175.5	175.9	175.1	174.5	174.6	166.0	166.0	165.9	1483	7747	1424
X 18-272	500	172.0			5.3	122.7	120.9	-2.4	10.9	179.7	179.7	179.7	179.5	178.1	178.3	177.8	177.3	177.3	168.8	168.8	168.8	1431	7476	1374
X 0-273	1000	213.0			19.1	129.9	141.0	8.7	9.7	221.8	221.7	221.7	221.6	220.3	220.7	220.0	219.5	219.7	212.0	212.1	212.0	1872	9916	1794
X 0-274	500	214.0			7.2	138.8	150.7	8.1	9.3	221.0	221.0	221.0	220.9	219.4	219.7	218.9	218.3	218.4	211.6	211.7	211.7	2090	8994	2088
X 18-288	500	169.0	.30	.30	3.1	91.4	98.1	6.2	11.7	180.4	180.4	180.3	180.1	178.9	179.2	178.5	178.1	178.2	168.7	168.7	168.6	1083	6473	1016
X 18-291	500	170.0	.05	.05	4.9	45.4	48.7	5.8	5.0	173.1	173.1	173.1	172.9	172.5	172.6	172.4	172.3	172.4	168.2	168.2	168.1	1261	7762	1101
X 18-295	500	172.0	.30	.20	3.1	115.2	121.0	5.3	11.5	179.4	179.4	179.4	179.2	177.8	177.5	177.4	177.1	177.3	167.9	167.9	167.8	1356	7421	1292
X 26-296	500	126.0	.20	.20	3.6	48.8	52.8	7.0	6.2	129.4	129.4	129.4	129.2	128.6	128.4	128.5	128.4	128.5	123.3	123.3	123.1	1104	6594	1039
X 26-298	500	125.0	.25	.30	3.9	74.7	82.3	7.2	9.4	131.8	131.7	131.8	132.0	131.0	130.8	130.8	130.6	130.7	122.5	122.5	122.3	1138	10646	1015
X 26-304	500	126.0	.05	.80	3.7	109.8	116.8	4.8	14.5	135.7	136.8	135.7	135.5	134.2	133.8	133.7	133.2	133.2	121.4	121.4	121.0	1043	6611	969
X 0-305	500	217.0	.24	.05	4.1	108.1	106.1	.7	8.8	220.0	219.8	219.8	219.6	218.4	218.3	218.3	217.7	217.9	211.1	211.2	211.1	1566	7338	1538
X 0-307	500	208.0	.28	5.60	4.8	74.5	83.2	7.7	6.5	217.7	217.6	217.7	217.6	216.8	216.5	216.6	216.3	216.4	211.2	211.2	211.2	1651	8011	1586
X 26-309	500	126.0	.50	.44	0.0	101.7	105.8	2.1	12.1	135.9	136.8	135.8	136.0	134.2	134.1	134.1	134.1	133.9	123.9	123.8	123.5	1129	7521	1043
X 26-312	500	124.0	.68	.59	8.0	109.2	113.4	2.0	13.6	135.3	135.2	135.1	134.9	133.1	133.0	133.3	133.0	133.0	121.9	121.7	121.3	1079	6413	1014
X 0-313	500	214.0	.10	.10	6.2	53.4	56.1	4.7	4.4	215.6	215.6	215.6	215.5	215.0	215.0	215.0	214.8	214.8	211.2	211.3	211.3	1659	9199	1585
X 26-318	500	126.0	.21	.17	3.6	52.4	53.3	2.4	6.6	127.7	127.7	127.7	127.5	126.8	126.7	126.6	126.6	126.6	121.2	121.2	121.0	1046	6286	984
X 0-320	500	217.0	.10	.05	31.0	44.2	47.5	8.1	3.2	214.9	214.8	214.8	214.8	214.3	214.3	214.4	214.2	214.3	211.6	211.7	211.6	1914	10932	1820
X 18-332	500	173.0	.10	0.00	2.1	61.5	65.4	6.3	5.3	174.3	174.2	174.2	174.1		173.5	173.5	173.4	173.4	168.9	169.0	168.9	1593	10123	1492
X 18-333	1000	173.0	.00	0.00	7.0	51.6	53.8	8.1	5.0	174.2	174.2	174.2	174.0		173.5	173.5	173.4	173.4	169.1	169.2	169.2	1307	8966	1302
X 18-334	500	173.0	.20	0.00	1.3	107.2	112.4	4.9	9.8	178.7	178.7	178.7	178.8		177.7	177.6	177.3	177.4	168.9	169.0	168.9	1484	12205	1340
X 18-335	1000	174.0	.25	0.00	8.7	109.3	111.3	5.1	10.5	179.4	179.3	179.4	179.3		178.1	178.1	177.9	177.8	168.8	169.0	168.8	1368	9651	1258

(1) Area for calculating U based on nominal tube diameter of 3.00 in.
(2) Area for calculating h_o based on developed outside heat transfer area estimated to be 1.00 sq ft/ft of length.
(3) Area for calculating h_i based on developed inside heat transfer area estimated to be 0.967 sq ft/ft of length.
(4) Inside of tube scaled.

TABLE 5.2

SUMMARY OF RUNS WITH BRINE FOR 3 IN. BY 10 FT FLUTED TUBE

	Run No.	TUBESIDE: Water Rate Lb/Hr	Feed Water Temp, °F	Chlorinity G/Kg	Overall Pressure Drop In.Water	Tube Pressure Drop In.Water	Entrainment Lb/Hr	Water Evaporated Lb/Hr	Heat Transfer M BTU/Hr	Heat Balance Check %	Log-Mean ΔT °F	TEMPERATURES, °F (See Figure 3.4 for locations): T4	M4	B4	W1	W2	W3	W4	W5	W6	T1	M1	B1	HEAT TRANSFER COEFFICIENT BTU/(HR)(SQ FT)(°F): U(1)	h_o(2)	h_i(3)
IX	26-242	500	127.0	53.9	.10	.10	5.7	16.4	23.2	23.3	3.3	129.7	129.5	129.0	129.5	129.1	129.0	128.7	128.4	128.2	126.1	126.1	126.0	904	4098	877
IX	26-243	250	126.0	60.4	.10	.10	24.0	22.8	24.0	-4.9	3.4	128.7	128.5	128.1	128.6	128.2	128.2	127.9	127.5	127.4	125.1	125.1	125.0	921	5066	867
IX	26-244	500	126.0	56.3	.25	.15	6.5	43.8	47.2	-.1	6.6	132.0	131.9	131.6	131.8		131.2	130.8	130.7	130.4	125.3	125.3	125.2	930	6038	850
IX	26-245	750	126.0	58.8	.20	.20	3.8	45.5	47.3	1.4	6.3	131.5	131.4	131.2	131.4	130.8	130.8	130.5	130.3	130.0	125.1	125.1	125.0	965	6515	849
IX	26-246	250	125.5	59.8	.15	.10	28.7	43.4	46.8	-3.5	6.7	131.9	131.7	131.4	131.6	131.1	131.2	130.8	130.6	130.5	125.0	125.0	124.8	897	6911	813
IX	26-247	500	126.0	57.3	.25	.20	5.7	44.3	48.8	.6	10.5	136.7	136.7	136.5	136.5			136.1	135.9	135.8	126.1	126.2	126.1	845	12860	725
IX	26-251	1000	129.0	54.5	.40	.30	18.3	52.6	55.7	17.2	7.0	133.0	132.9	132.8	132.9	132.2	132.3	132.2	131.8	131.5	126.0	125.9	125.8	1023	7408	935
IX	26-252	500	130.0	60.6	.50	.35	13.2	104.0	113.0	4.7	17.4	145.1	145.0	145.0	145.0			143.7	143.5	143.4	127.8	127.8	127.5	842	11322	730
IX	26-253	250	128.0	49.6	.30	.20	39.5	71.2	78.3	-4.6	16.2	142.2	142.1	142.8	142.2			140.4	139.8	139.8	126.0	125.9	125.8	624(4)	6495	549(4)
IX	26-254	1000	130.0	59.6	.70	.55	31.4	117.6	121.9	6.9	15.5	142.5	142.4	142.4	142.6			141.1	140.4	140.3	127.2	127.1	126.7	1019(4)	10290	901(4)
IX	26-255	250	132.0	59.3	.40	.30	45.8	85.5	91.2	-.1	25.9	152.4	152.4	152.4	152.0			151.8	150.6	150.0	126.6	126.5	126.5	456(4)	7210	390(4)
IX	0-256	500	220.0	45.7	.15	.10	4.1	16.3	16.3	-18.2	2.8	215.5	215.5	215.5	215.4	215.2	215.3	215.3	215.2	215.3	213.5	213.6	213.6	1072(4)	7792	988(4)
IX	0-257	500	221.0	47.3	.10	.05	3.9	31.8	46.5	28.3	5.6	219.0	219.0	218.9	218.9	218.4	218.6	218.4	218.3	218.5	213.3	213.4	213.4	1076(4)	10143	956(4)
IX	0-258	250	220.0	53.3	.15	.10	4.1	46.6	48.7	2.1	6.6	221.0	220.9	220.9	220.8		220.4	220.3	220.3	220.5	214.3	214.5	214.5	961(4)	10510	848(4)
IX	0-259	500	218.0	63.2	.20	.15	3.9	108.8	110.9	-.7	16.3	231.0	231.0	231.0	231.0			230.1	230.1	230.3	214.7	214.8	214.8	803(4)	17787	748(4)
IX	0-260	250	221.0	62.9	.10	.10	4.4	23.2	25.5	-8.7	4.1	218.9	218.8	218.8	218.7		218.5	218.5	218.5	218.6	214.7	214.8	214.8	801(4)	10960	699(4)
IX	0-261	1000	218.0	53.4	.05	0.00	170.0	41.9	40.8	-3.5	4.1	218.8	218.8	218.8	218.7		218.4	218.4	218.2	218.3	214.7	214.8	214.7	1291(4)	11714	1158(4)
XI	26-276	1000	128.0	14.5	.27	.20	8.0	59.0	57.4	4.6	5.5	126.3	126.2	126.2	126.0	125.3	125.6	125.4	125.3	125.3	120.9	120.8	120.6	1352	7728	1278
XI	26-277	500	126.0	14.5	.21		11.6	71.0	69.7	-2.1	5.5	129.9	129.9	129.9	129.8	129.0	129.2	128.9	128.8	128.9	124.5	124.5	124.3	1645	8074	1575
XI	26-278	500	123.0	14.5	.60	.40	11.6	127.5	122.8	-7.5	9.3	132.5	132.4	132.4	132.4	130.9	131.3	130.8	130.3	130.4	123.4	123.2	122.9	1705	8950	1638
XI	26-279	1000	125.0	14.5	1.00	.47	54.5	106.8	115.7	3.3	10.0	133.2	133.2	133.2	133.0	131.8	132.3	131.9	131.3	131.2	123.6	123.3	122.8	1502	9176	1407
XI	18-280	1000	174.0	14.5	.70		83.6	128.9	129.0	-2.7	9.9	178.4	178.4	178.4	178.3	176.7	177.3	176.8	176.3	176.4	168.6	168.6	168.5	1693	9017	1618
XI	18-281	500	172.0	14.5	.40		2.7	121.2	122.0	-.7	11.0	179.3	179.3	179.3	179.1	177.4	177.9	177.7	177.6	177.8	168.3	168.4	168.3	1428	8730	1339
XI	0-282	500	212.0	15.5	.25		5.3	152.9	158.2	2.5	10.6	223.8	223.9	223.9	223.5	221.7	222.4	221.8	221.2	221.4	213.2	213.3	213.2	1927	8839	1894
XI	26-283	500	123.0	15.5	.80	.60	12.4	156.1	163.0	-1.9	16.3	140.2	140.1	140.1	139.9	137.8	138.5	137.8	137.1	137.0	124.4	124.1	123.4	1298	7714	1228
XI	26-284	1000	127.0	15.5	.90		35.7	158.5	165.0	-3.6	17.1	141.3	141.4	141.3	141.2	139.0	139.8	139.0	138.2	137.9	124.8	124.5	123.7	1250	7692	1169
XI	0-285	1000	213.0	15.5	.40		286.0	141.0	155.4	14.6	9.5	222.3	222.3	222.3	222.1	220.3	221.0	220.6	220.8	220.1	212.8	212.8	212.8	2113	9604	2000

(1) Area for calculating U based on nominal tube diameter of 3.00 in.
(2) Area for calculating h_o based on developed outside heat transfer area estimated to be 1.00 sq ft/ft of length.
(3) Area for calculating h_i based on developed inside heat transfer area estimated to be 0.967 sq ft/ft of length.
(4) Inside of tube scaled.

TABLE 5.3

SUMMARY OF RUNS WITH FRESH WATER FOR 2 IN. BY 10 FT FLUTED TUBE

Run No.	TUBESIDE Water Rate Lb/Hr	Feed Water Temp, °F	Overall Pressure Drop In. Water	Tube Pressure Drop In. Water	Entrainment Lb/Hr	Water Evaporated Lb/Hr	Heat Transfer M BTU/Hr	Heat Balance Check %	Log-Mean ΔT °F	TEMPERATURES, °F (See Figure 3.4 for locations) T4	M4	B4	W1	W2	W3	W4	W5	W6	T1	M1	B1	HEAT TRANSFER COEFFICIENT BTU/(HR)(SQ FT)(°F) U(1)	h_o(2)	h_i(3)
XIV 26-347	330	126.0			7.2	45.9	45.3	2.3	5.7	124.6	124.2	124.2		123.0	123.0	122.7	122.9	122.7	119.2	118.9	118.3	1543	4568	1745
XIV 26-348	670	126.0	.50		7.2	37.2	35.8	3.8	5.8	127.5	127.3	127.4		126.4	126.5	126.3	126.3	126.3	121.9	121.7	121.3	1179	5151	1183
XIV 26-349	330	126.0	1.90	1.25	11.2	80.3	86.1	4.9	11.0	137.2	136.9	136.5	133.7	134.4	134.3	133.7	134.2	134.2	126.6	126.2	125.1	1506	4740	1649
XIV 26-350	670	126.0	1.20	.38	8.4	60.9	65.5	6.6	11.2	136.8	136.7	136.8	134.7	135.3	135.2	134.8	134.8	134.5	126.1	125.8	125.1	1125	5335	1109
XIV 26-351	330	124.5	2.00	1.10	9.5	79.1	83.5	3.3	15.8	140.9	140.1	139.6	136.7	137.8	137.5	136.9	137.2	137.2	125.2	124.7	123.7	1018	4185	1034
XIV 26-352	670	124.0	2.80	2.10	10.3	92.6	99.6	6.9	17.2	141.3	141.3	141.3	138.3	138.7	139.1	138.4	138.6	138.0	125.2	124.6	123.0	1117	5487	1092
XIV 26-356	1000	125.0	.96	1.02	9.6	52.1	50.3	1.9	10.1	130.8	130.5	130.5	128.2	128.1	128.6	128.2	128.3	128.2	121.1	120.8	120.1	960	3253	1030
XIV 26-357	1000	120.0	.36	.36	9.4	30.9	32.2	1.7	6.0	127.4	127.3	127.3	126.4	126.3	126.5	126.4	126.4	126.3	121.6	121.5	121.1	1030	4947	1011
XIV 26-358	670	123.0	1.85	1.75	8.9	78.8	83.2	2.8	15.1	139.9	139.9	139.6	137.5	137.0	137.7	137.1	137.3	136.7	125.3	125.0	124.0	1059	4857	1044
XIV 26-359	1000	124.0	3.22	3.06	25.4	97.1	103.7	4.7	17.7	143.0	142.8	142.7	139.9	139.5	140.3	139.5	139.5	138.4	126.3	125.8	123.9	1128	4783	1144
XIV 26-360	1000	124.0	4.90	4.56	30.7	105.3	105.4	3.1	17.8	139.0	139.7	138.6	136.1	135.5	136.1	135.3	135.5		122.7	121.9	119.2	1139	4678	1143
XIV 18-370	670	174.0	.70		8.6	75.7	75.0	3.3	10.6	178.2	178.2	178.2	176.4	176.3	176.8		176.7	176.3	167.6	167.7	167.6	1358	6854	1317
XIV 18-371	1000	174.0	.60		12.3	70.6	63.8	.2	9.7	176.1	176.0	176.0	174.7	174.4	174.9	174.5	174.7	174.7	166.3	166.5	166.3	1261	6927	1206
XIV 0-372	670	212.0	1.10		27.9	92.3	94.2	3.1	9.3	220.3	220.3	220.4	218.4	218.2	219.0	218.5		218.6	210.8	211.5	211.4	1959	7817	2015
XIV 26-373	330	124.0	.50	.52	13.7	39.2	41.6	6.3	5.9	128.4	128.3	128.3	127.3	127.1	127.4			127.0	122.7	122.5	122.2	1359	5497	1379
XIV 26-374	1000	123.0	.41	.35	34.0	31.0	29.4	1.7	5.6	127.5	127.5	127.5	126.6	126.5	126.7			126.3	122.1	122.0	121.7	1017	4486	1010
XIV 0-379	1000	212.0	.30		14.4	68.8	71.2	5.0	8.9	219.6	219.5	219.6	218.4	218.0	218.8	218.3	218.3	218.4	210.3	210.9	210.9	1536	9017	1457

TABLE 5.4

SUMMARY OF RUNS WITH BRINE FOR 2 IN. BY 10 FT FLUTED TUBE

Run No.	TUBESIDE Water Rate Lb/Hr	Feed Water Temp, °F	Chlorinity G/Kg	Overall Pressure Drop In. Water	Tube Pressure Drop In. Water	Entrainment Lb/Hr	Water Evaporated Lb/Hr	Heat Transfer M BTU/Hr	Heat Balance Check %	Log-Mean ΔT °F	TEMPERATURES, °F (See Figure 3.4 for locations) T4	M4	B4	W1	W2	W3	W4	W5	W6	T1	M1	B1	HEAT TRANSFER COEFFICIENT BTU/HR - FT^2 - °F U(1)	h_o(2)	h_i(3)
XV 26-353	670	125.0	47.5	.60		9.4	30.4	31.8	-9.9	6.1	130.5	130.4	130.4	129.1	129.4	129.6	129.0	129.5		124.6	124.5	124.2	1010	4235	1016
XV 26-354	670	125.0	51.3	.65		10.4	30.0	29.8	-14.0	6.0	129.8	129.7	129.7	128.4	128.7	128.9		128.7		124.0	123.9	123.6	963	4180	964
XV 26-355	670	126.0	51.0	1.16		12.6	52.0	51.0	-8.3	10.2	133.8	133.2	133.3	131.6	131.7	131.9	131.6	131.8	131.6	123.8	123.5	122.9	965	4435	964
XV 26-361	670	125.5	50.0	5.30	5.90	25.0	108.5	100.7	-24.8	16.9		142.7	142.7	140.0	139.9	140.5	139.5	139.9		128.1	127.5	125.7	1145	4362	1227
XV 26-362	1000	126.0	54.0	1.36	.90	21.2	40.9	32.4	-16.4	6.0	128.1	127.9	128.0	126.8	126.9	126.6	126.9	126.9		122.4	122.1	121.6	1041	4135	1065
XV 26-363	1000	126.5	54.0	7.40	5.70	64.8	89.1	86.6	-2.3	12.3	135.3	135.5	135.2	133.0	133.4	133.3	132.3	132.5		125.0	123.8	120.7	1357	5338	1394
XV 26-364	1000	128.0	52.0	13.20		168.0	213.0	113.5	-81.2	17.7	147.4	147.3	147.3	145.3	143.3	143.4	142.4	142.7	139.0	135.3	132.7	122.4	1235	3695	1417
XV 26-365	670	130.0	51.0	.80		9.1	38.2	34.8	7.9	6.5	126.9	126.5	126.5	125.6	125.6	125.8	124.6	125.7	125.4	120.5	120.3	119.9	1031	4391	1046
XV 26-366	670	134.0	51.0	3.90		12.7	103.5	103.0	9.3	19.0	141.7	142.1	141.6	139.0	138.9	139.1	138.5	138.8	137.9	124.0	123.1	121.2	1044	5088	1011
XV 26-367	1000	126.0	48.0	2.93		65.6	61.6	64.6	4.5	7.2	132.5	132.4	132.4	130.7	130.6	130.9	130.4	130.8	130.4	126.6	125.8	123.8	1733	5411	1936
XV 18-368	1000	179.0	38.0	4.20		49.5	101.8	97.0	8.6	10.5	179.5	179.5	179.5	177.3	177.2	177.8	177.1	177.5	176.8	169.3	169.3	168.7	1785	6713	1856
XV 18-369	670	178.0	37.0	1.40		23.8	76.9	74.6	2.9	9.7	179.6	179.6	179.6	177.7	177.8	178.5	178.3	178.2	178.0	169.8	170.0	170.0	1477	7356	1436
XV 26-375	1000	126.0	50.8	.76		37.8	24.7	24.0	4.0	4.7	129.7	129.6	129.6	128.7	128.8	129.0	128.8		128.7	125.2	125.2	124.7	992	4631	991
XV 26-376	1000	125.0	51.0			85.7	74.9	78.7	8.7	10.4	138.4	137.8	137.6	135.7	135.6	136.1	135.4		135.3	127.9	127.0	127.3	1455	5095	1506
XV 26-377	1000	120.0	56.5			130.5	76.0	74.6	-1.8	10.9	138.4	138.4	138.4	136.2	136.1	136.0	134.6		133.4	128.5	126.7	126.4	1315	3366	1489
XV 26-378	1000	125.0	60.0	1.20		40.2	32.3	34.1	8.1	6.2	132.6	132.5	132.5	131.3	131.5	131.6	131.2		131.3	126.6	126.4	126.0	1052	4365	1068
XV 4-380	1000	205.0	27.0	1.80		75.1	95.1	95.0	6.4	11.2	215.7	215.7	215.7	213.6	213.5	214.4	213.6		213.9	204.3	204.7	204.7	1636	7630	1606
XV 5-381	670	205.0	23.0	.98		49.0	76.0	74.3	-9.8	9.9	214.3	214.2	214.2	212.5	212.4	213.3	212.9		213.1	204.1	204.5	204.6	1445	8174	1373

(1) Area for calculating U based on nominal tube diameter of 3.00 in.
(2) Area for calculating h_o based on developed outside heat transfer area estimated to be 0.67 sq ft/ft of length.
(3) Area for calculating h_i based on developed inside heat transfer area estimated to be 0.648 sq ft/ft of length.

5.1 Pressure Drop

Pressure drop measurements for the fluted tube are shown in Figures 5.1 to 5.6. The values shown here are overall pressure drops taken as shown in Figure 3.3.

Pressure drop from manometer readings for the 3 in. tube at 26 in. Hg tubeside vacuum are shown in Figure 5.1a. The pressure drop is quite low for the three in. tube even at this high vacuum condition. The liquid flowrate has very little effect on the pressure drop in contrast to the smooth tube where the pressure drop increases with increasing liquid flowrate. Salinity also has very little effect on the pressure drop for the three in. tube. The data are seen to correlate fairly well by the equation

$$\Delta P = K \frac{W_s^{1.8}}{\rho_s^{0.7}} \qquad (5.1)$$

where ΔP = pressure drop, in. water
K = 3.6×10^{-6} for 3 in. fluted tube
W_s = total water vaporized, lb/hr
ρ_s = steam density, lb/cu ft

The pressure drop in the 3 in. tube at 26 in. Hg vacuum was determined in a completely independent manner in Figure 5.1b. Here the pressure drop is calculated from the difference in temperature between thermocouples T1 and B1 (see Figure 3.4) using the properties of saturated steam. The data determined in this manner are seen to be slightly higher than in Figure 5.1a but more consistent and with less scatter. This indicates that the stray points in Figure 5.1a at the higher steam rates are the result of measurement inaccuracies and less reliance should be placed on them.

The pressure drop data for the 18 in. Hg vacuum and one atmosphere cases with the 3 in. tube are shown in Figures 5.2 and 5.3, respectively. As would be expected, the pressure drop decreases with increasing pressure and resulting higher vapor density. The curve corresponding to Equation 5.1 is plotted for comparison. Some deviation from this line is seen at one atmosphere. However, the pressure drop here is less than 0.2 in. water in most instances and the accuracy of the points is not good at such low levels.

Overall pressure drop data for the two in. fluted tube at 26 in. Hg vacuum are shown in Figure 5.4. Here the fresh water data are again shown to follow Equation 5.1 with fair agreement if K

is given the value of 2.0×10^{-5}. In contrast to the 3 in. tube, however, the ΔP with brine for the 2 in. tube is consistently higher than for fresh water. The largest deviation is with a brine flowrate of 1000 lb/hr or a peripheral flowrate of 159 lb/(hr)(in). This is a higher peripheral flowrate than was tested in the three in. tube. Pressure drop for the three in. tube at the higher flowrate (1500 lb/hr) should be obtained. Higher heat transfer coefficients with the two in. tube (See Section 5.4.2) show possible economic benefit from operating at this condition.

5.2 Entrainment

Entrainment data for the 3 in. tube are shown in Figures 5.7 to 5.10 and for the 2 in. tube in Figures 5.11 to 5.13. Figure 5.7 shows an unmistakable increase in entrainment with brine at 500 lb/hr in the three in. tube as opposed to fresh water. This was generally observed in both the 3 in. and 2 in. tubes for the range of flowrates and vacuums tested. The increase in entrainment over that with fresh water is greatest where a high brine recirculation rate is combined with a high evaporation rate. Although the points for this condition on the graphs are few, other runs with high vapor and brine rates were aborted because the entrainment rate exceeded the entrainment measuring capability of the equipment.

A trend for decreased entrainment was seen in going from 26 in. Hg to 18 in. Hg vacuum for both the 2 and 3 in. tubes at peripheral flowrates greater than 53 lb/(hr)(in). However, no major difference in entrainment between 18 in. Hg vacuum and 1 atmosphere was found.

Increasing the liquid recirculation rate was found to generally increase entrainment. One exception to this was entrainment for the 250 lb/hr flowrate for the 3 in. tube which fell between the entrainment data for the 500 and 1000 lb/hr flowrates. No explanation for this was apparent. Entrainment for the 330 and 670 lb/hr flowrate in the 2 in. tube showed little difference but the 1000 lb/hr flowrate was noticeably higher.

In general, the entrainment data for the 2 in. tube were higher than for the 3 in. tube. However, the nominal peripheral liquid flowrate was also generally higher. A comparison between the 2 tubes for a peripheral flowrate of 106 lb/(hr)(in.) at 26 in. Hg vacuum shows a higher entrainment rate for the 3 in. tube.

A further exploration of entrainment with brine using equipment with the present entrainment measurement limitations removed

is needed. This would better define the regions of high entrainment and help to determine factors affecting entrainment. A system for observing the surface of the vaporizing film is also desirable to help determine the mechanism resulting in the higher entrainment for brine as opposed to fresh water.

5.3 Condensing Film Heat Transfer Coefficients

The condensing film heat transfer coefficients for the 2 in. and 3 in. tubes at 26 in. Hg vacuum are shown in Figures 5.14 and 5.15 respectively as a function of total condensate rate. Symbols are used to indicate the brine concentration and flowrate on the tubeside. Tubeside flowrate has no noticeable effect on the condensing film coefficient. However, the condensing coefficient for the 3 in. tube in Figure 5.15 with brine on the tubeside shows a tendency to be higher. The reason for this is not clear and this trend was not confirmed with the 2 in. tube data shown in Figure 5.14. Examination of Figures 5.14 and 5.15 shows no indication of flooding of the fluted condensing surface as might have been indicated by a drop-off of condensing coefficient at high condensate rates.

Figures 5.16 and 5.17 show the variation of the condensing coefficient with steam temperature for the 3 in. and 2 in. tubes respectively. A significant increase with temperature is seen for both tubes as would be expected because of the increasing liquid film Prandtl number. This effect was also noticed with the circular unenhanced tube (2.1). The coefficients for the 3 in. tube are higher than those for the 2 in. tube, averaging 13 percent more. This could be due to one or more of the following:

- -- Difference in surface condition between the two tubes.
- -- More reliable thermocouple calibration for the three in. tube.
- -- Higher interfacial shear for the three in. tube. (A four in. heat exchanger shell was used for both tubes so the annular cross-section was much smaller for the three in. tube).

5.4 Vaporizing Film Heat Transfer Coefficients

5.4.1 Three In. Tube

The tubeside vaporizing heat transfer coefficients for the 3 in. tube are plotted in Figures 5.18 to 5.22. Examination shows a general trend for a decrease with increasing vapor rate. This trend is most pronounced for the 250 lb/hr flowrate with fresh water shown in Figure 5.18.

Evaporating coefficients for brine with a concentration factor in the range of 2.5 to 3.2 were shown to be lower than for fresh water. However, heat transfer coefficients with normal sea water were higher than for fresh water. The effect of brine concentration seems to decrease as liquid flowrate is increased.

Values obtained when the inside surface of the tube was scaled as indicated in Tables 5.1 and 5.2 have not been plotted here. The three in. tube was acid cleaned twice using an inhibited sulfamic acid solution. Each time the evaporating coefficient for several runs after that was noticeably higher. These runs after descaling are plotted and contribute somewhat to the scatter of the data. The fresh water data in Figure 5.20 are just after acid cleaning of the tube and are probably somewhat high for that reason, although they still fall below the normal sea water runs.

The conclusions about brine concentration for the 3 in. tube are based largely on the 26 in. Hg vacuum data as few unscaled points are available at the higher pressures. A definite increase in the evaporating coefficient with temperature was observed for the fresh water runs in the three in. tube.

5.4.2 Two In. Tube

Vaporizing heat transfer coefficients for the 2 in. tube are plotted in Figures 5.23 to 5.26. Data in Figure 5.24 for the 670 lb/hr flowrate show reasonable agreement with the coefficient for the 3 in. tube at the same peripheral flowrate. Data at the corresponding peripheral flowrate for the 3 in. tube shown in Figure 5.20 were slightly higher but this is attributed to just having acid cleaned the tube. The fresh water data for the 330 lb/hr flowrate are higher on the average than the corresponding data for the same peripheral flowrate for the 3 in. tube. No explanation for this discrepancy could be determined unless it is that the higher interfacial shear in the two in. tube was particularly effective for enhancing the heat transfer coefficient at this peripheral flowrate and not at the higher rates. Some evidence of enhancement in the three in. tube at this peripheral flowrate is reported in Section 7 where additional shear was induced.

At the 1000 lb/hr flowrate in the 2 in. tube shown in Figure 5.23, a very significant phenomenon was observed with the brine runs with concentration factor in the range of 2.5 to 3.2. A very steep increase in heat transfer coefficient is observed in going from 50 to 60 lb/hr of water evaporated. This coefficient drops off as the water vaporized is increased further but is still very significant in the range of 80 lb/hr water vaporized. This peripheral flowrate is 50 percent higher than the highest flowrate tested for the 3 in. tube. Whether this effect is peculiar to the 2 in. tube or would also be present in the 3 in. tube is not known. It is unfortunate that there were not provisions for

observing the surface of the vaporizing film so that differences in appearance of the vaporizing liquid which might give clues to the mechanism could be obtained. The pressure drop and entrainment were quite significantly higher for these runs than for corresponding fresh water runs. Spot checks at 18 in. Hg vacuum and at one atm, shown in Figures 5.25 to 5.26, also showed that the coefficient with brine at the 1000 lb/hr rate was higher than for fresh water although the brine concentration was also decreased to avoid scaling at the higher temperatures.

Additional data should be obtained to determine how reproducible this effect is, whether it is present in the three in. tube and whether additional improvement is obtained at even higher flowrates.

5.5 Overall Heat Transfer Coefficients

Overall heat transfer coefficients at 26 in. Hg vacuum for the 2 and 3 in. fluted tubes are plotted against overall temperature difference in Figures 5.27 and 5.28 respectively. The trends here are the same as for the vaporizing film heat transfer coefficient since this accounts for the major resistance to heat transfer in the fluted tube.

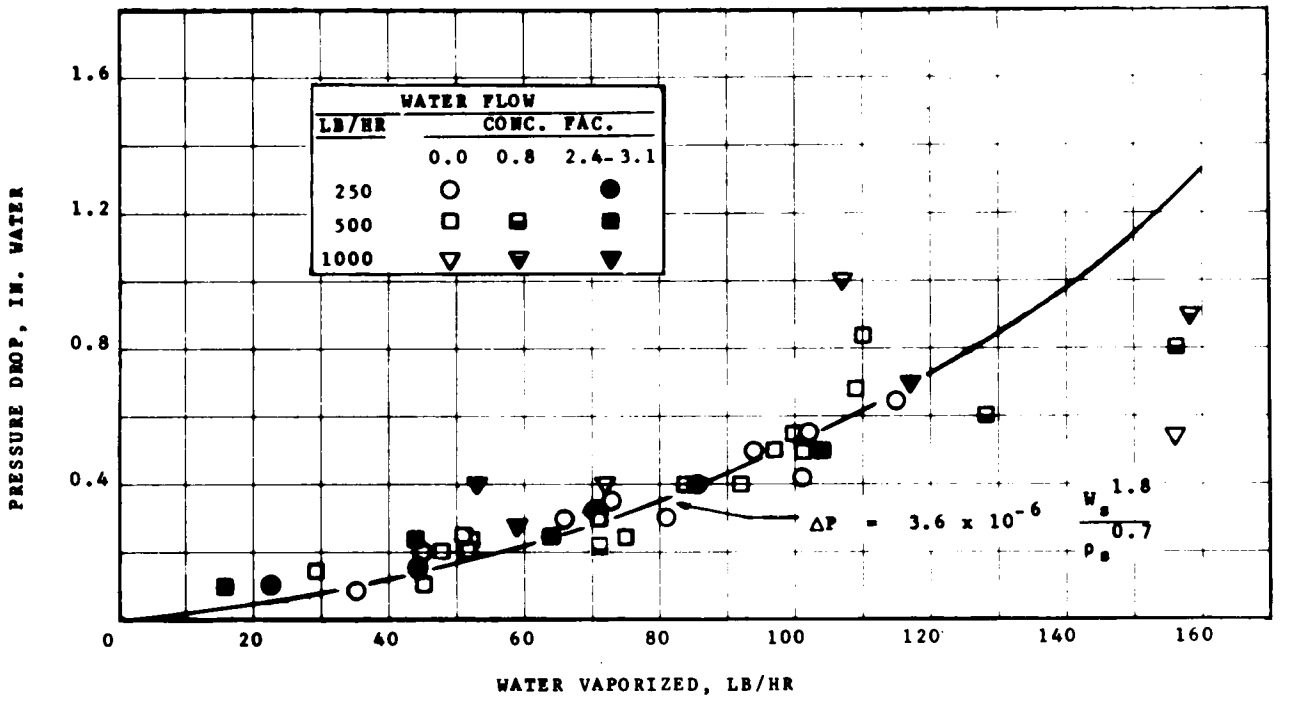

FIGURE 5.1a. Pressure drop in the 3 in. fluted tube at 26 in. Hg vacuum.

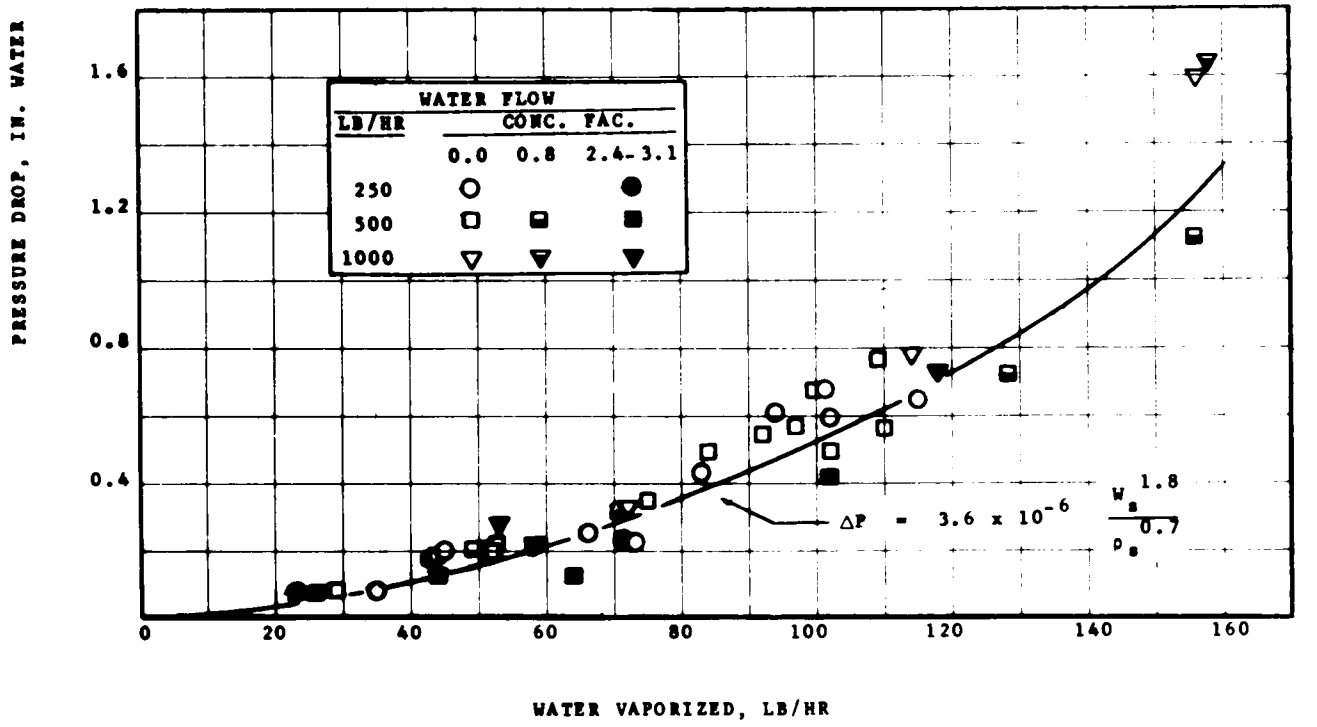

FIGURE 5.1b. Pressure drop in the 3 in. fluted tube at 26 in. Hg vacuum, calculated from temperature measurements.

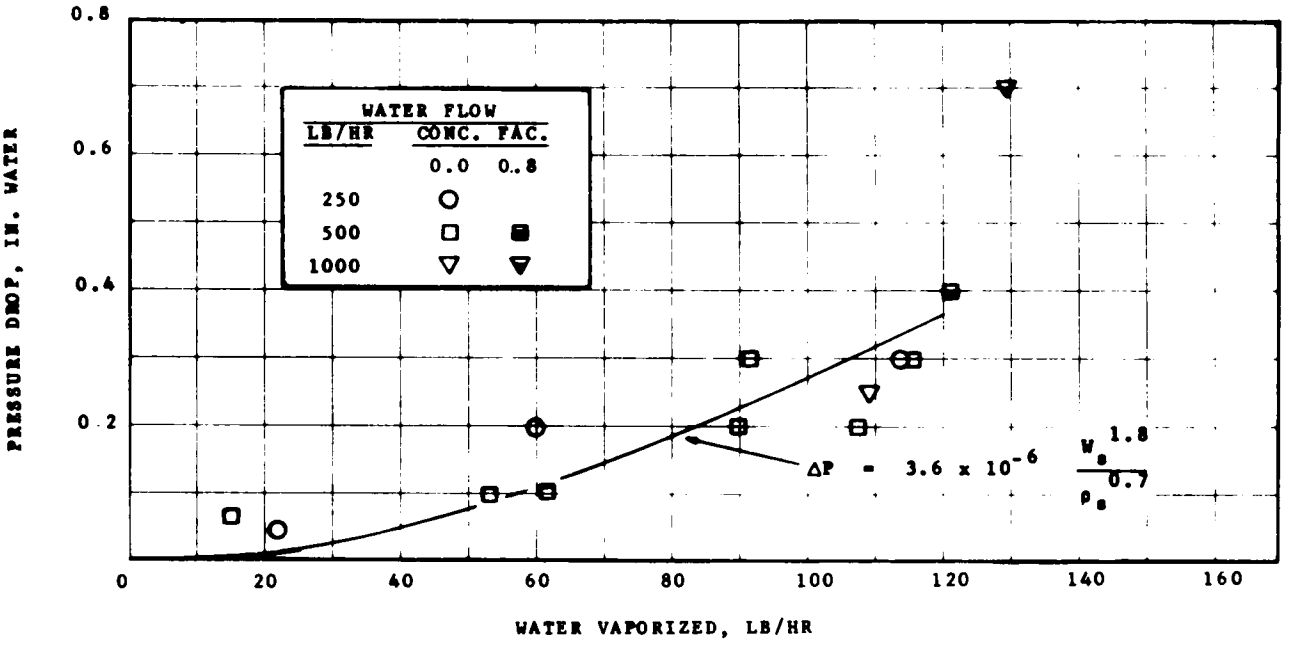

FIGURE 5.2. Pressure drop in the 3 in. fluted tube at 18 in. Hg vacuum.

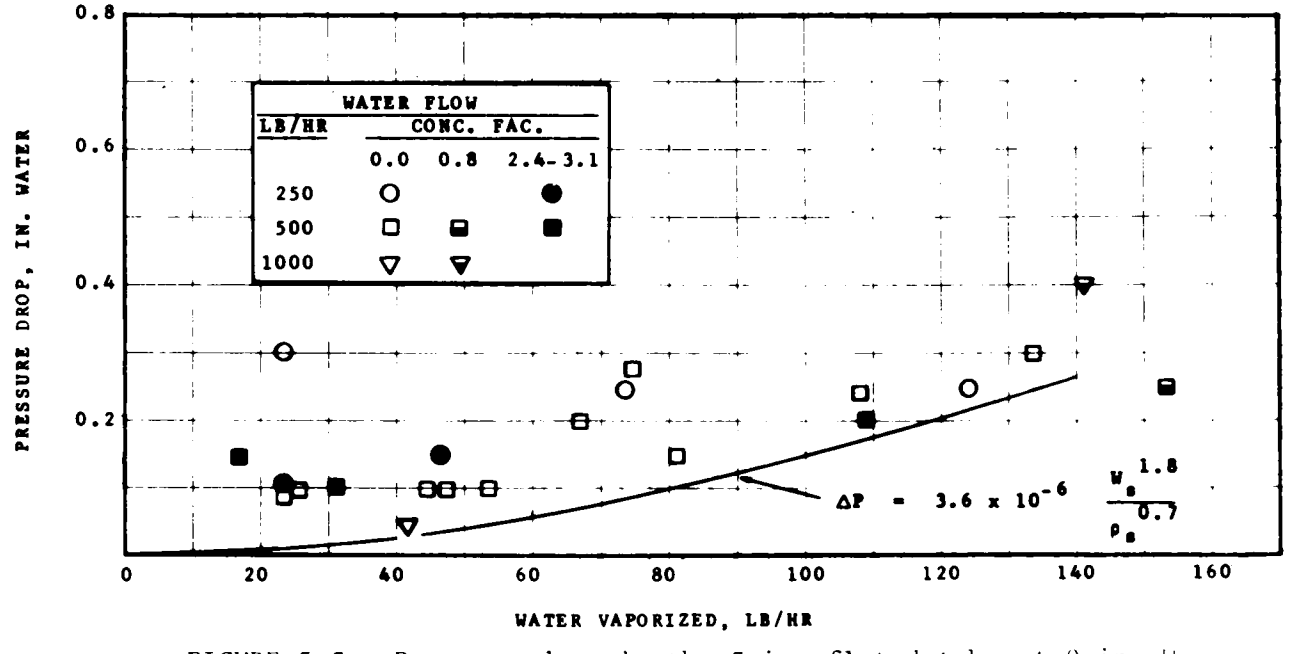

FIGURE 5.3. Pressure drop in the 3 in. fluted tube at 0 in. Hg vacuum.

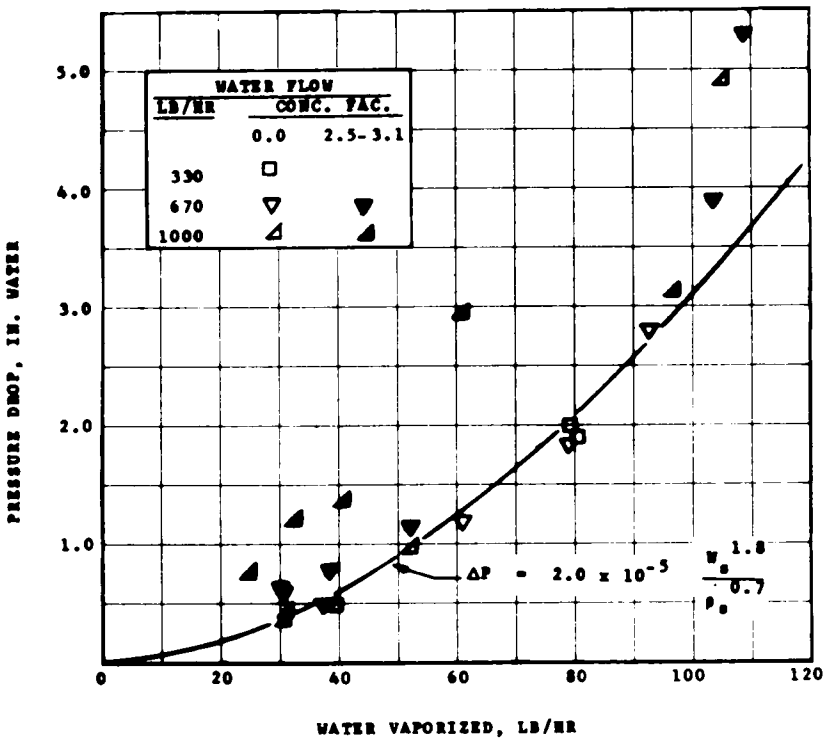

FIGURE 5.4. Pressure drop in the 2 in. fluted tube at 26 in. Hg vacuum.

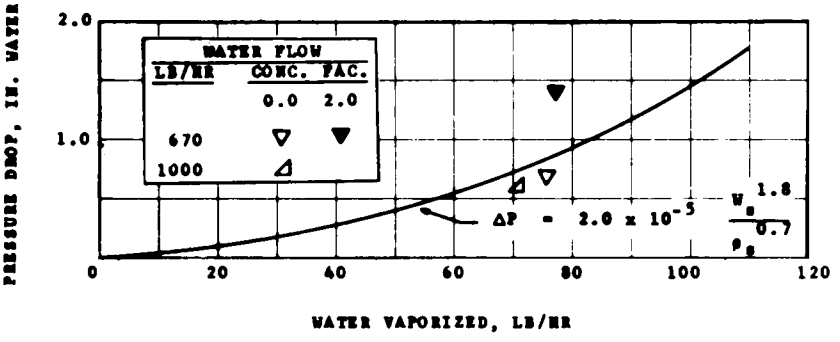

FIGURE 5.5. Pressure drop in the 2 in. fluted tube at 18 in. Hg vacuum.

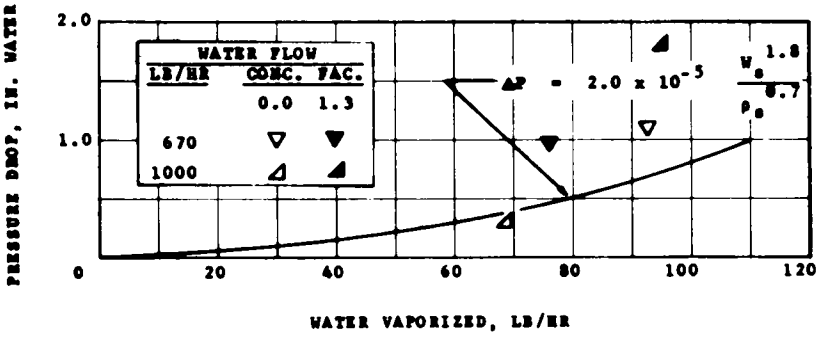

FIGURE 5.6. Pressure drop in the 2 in. fluted tube at 0 in. Hg vacuum.

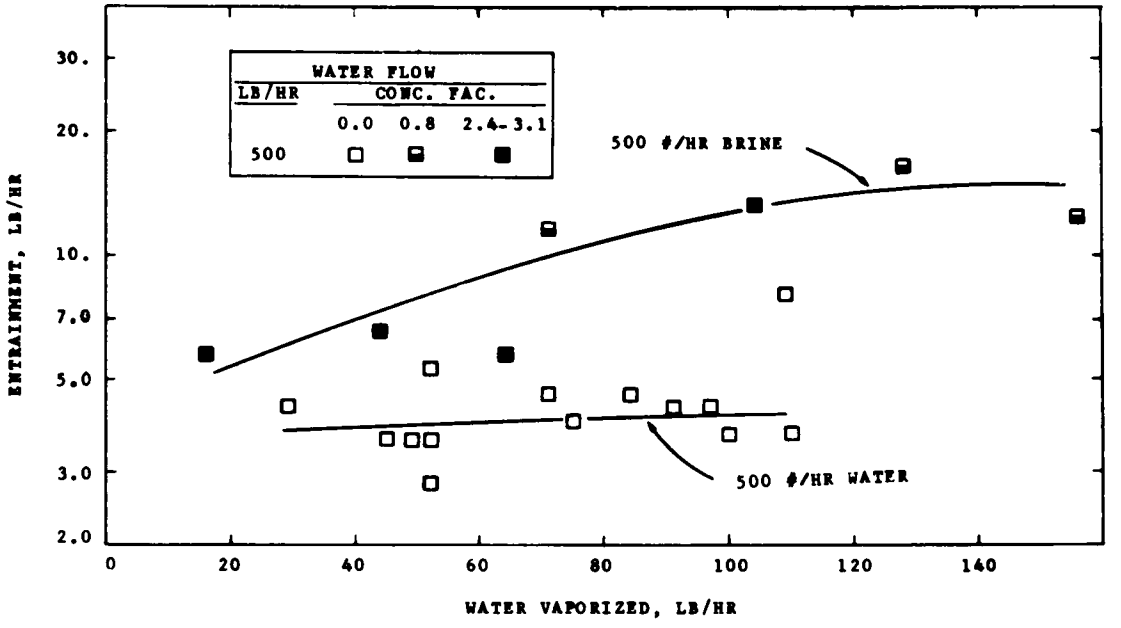

FIGURE 5.7. Entrainment rate in the 3 in. fluted tube at 26 in. Hg vacuum.

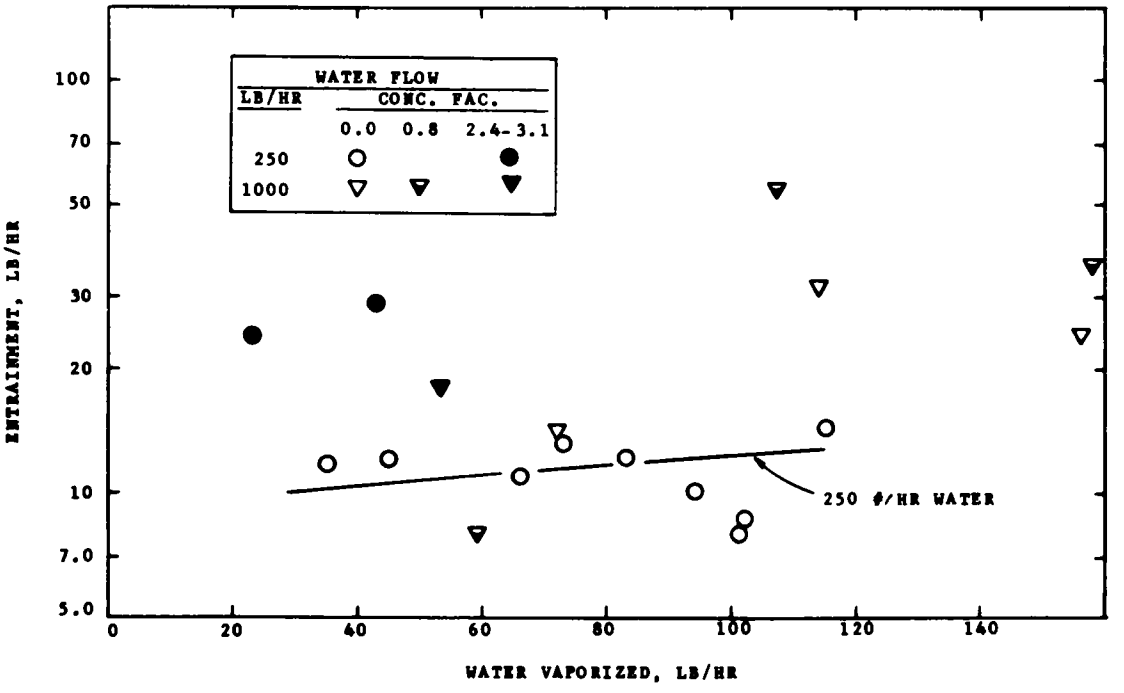

FIGURE 5.8. Entrainment rate in the 3 in. fluted tube at 26 in. Hg vacuum.

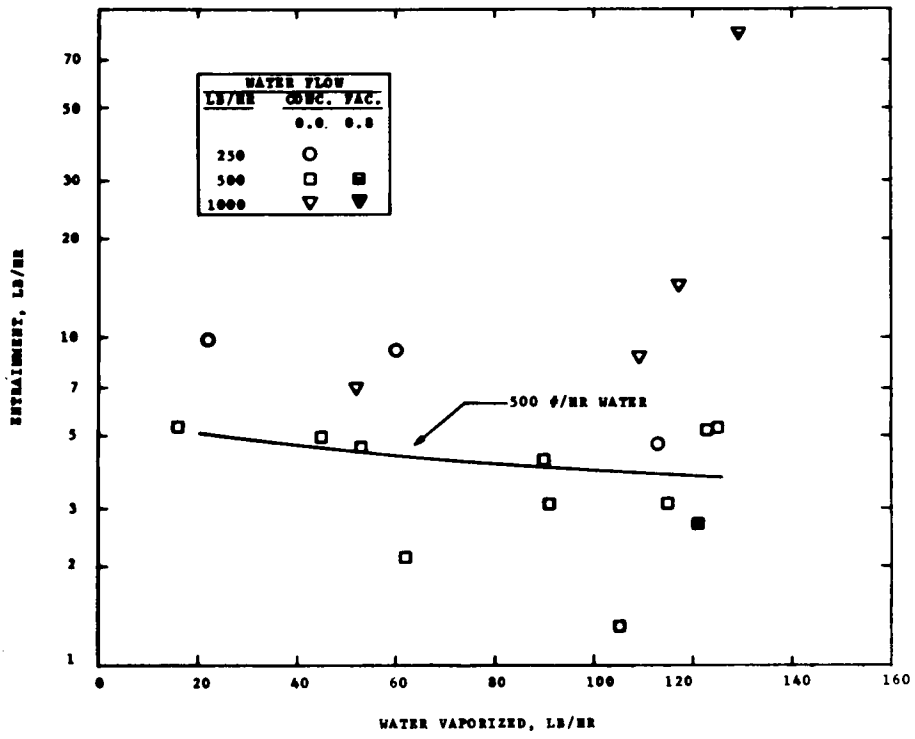

FIGURE 5.9. Entrainment rate in the 3 in. fluted tube at 18 in. Hg vacuum.

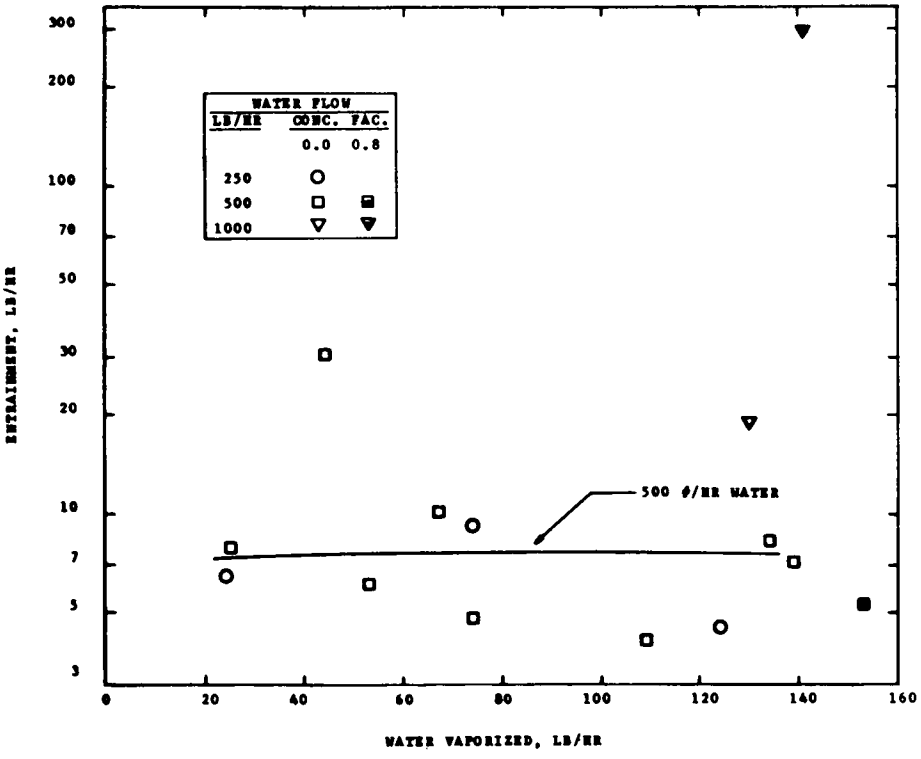

FIGURE 5.10. Entrainment rate in the 3 in. fluted tube at 0 in. Hg vacuum.

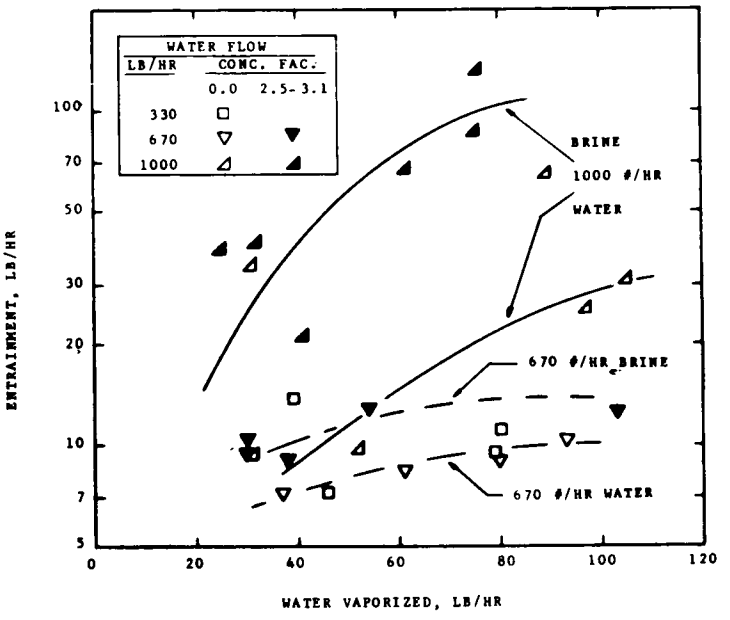

FIGURE 5.11. Entrainment rate in the 2 in. fluted tube at 26 in. Hg vacuum.

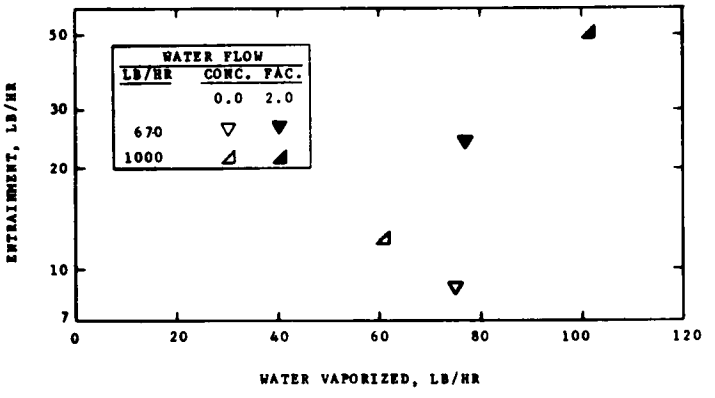

FIGURE 5.12. Entrainment rate in the 2 in. fluted tube at 18 in. Hg vacuum.

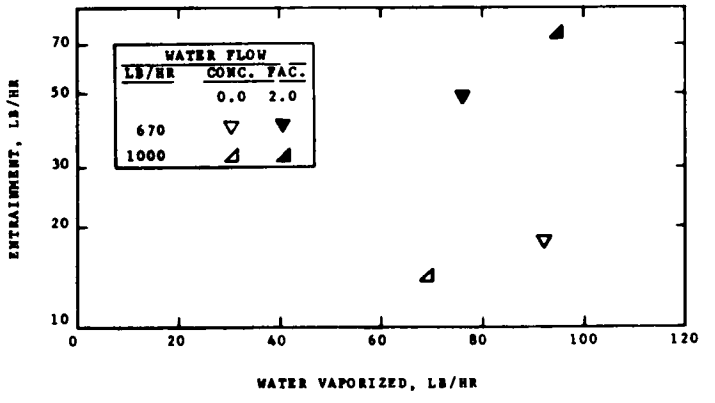

FIGURE 5.13. Entrainment rate in the 2 in. fluted tube at 0 in. Hg vacuum.

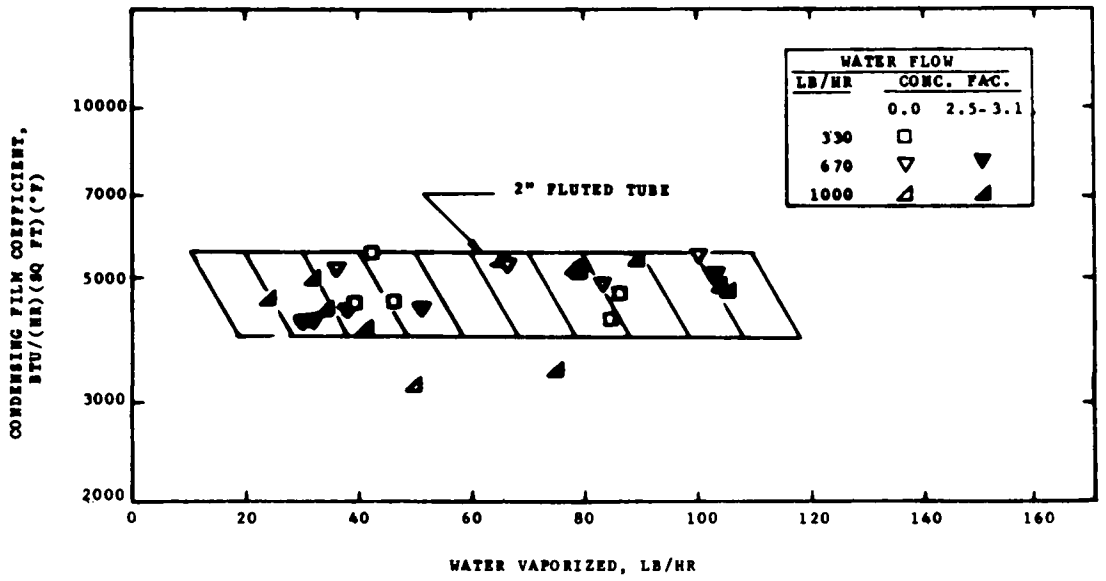

FIGURE 5.14. Condensing film heat transfer coefficient for the 2 in. fluted tube at 26 in. Hg vacuum. Coefficient based on mean temperature difference and developed heat transfer area of 0.67 sq ft/ft of length.

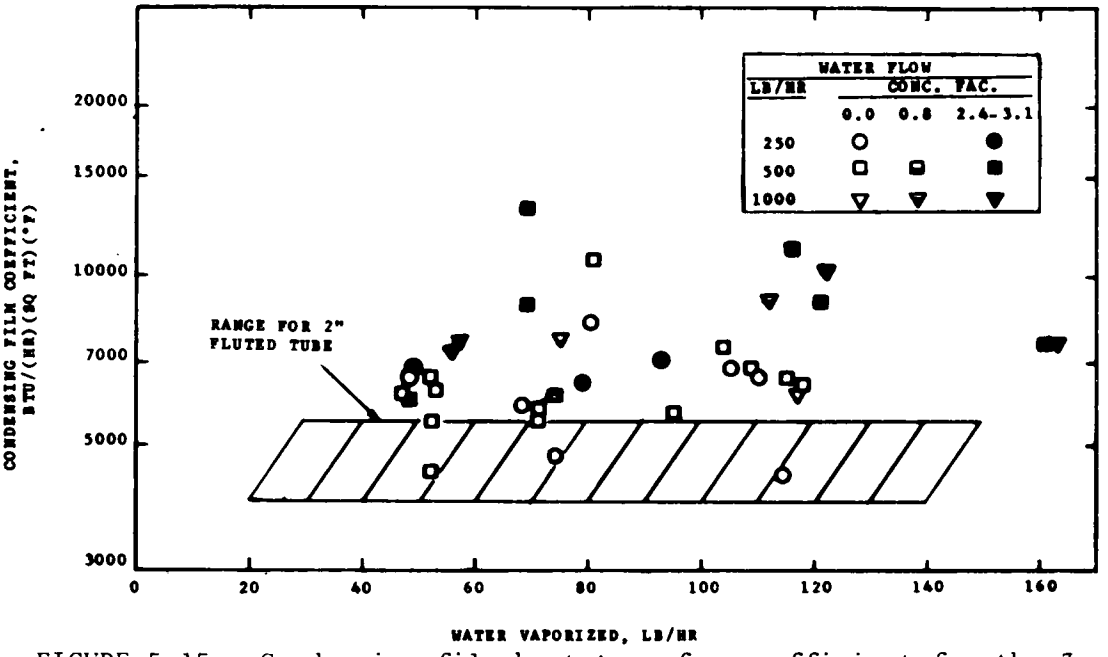

FIGURE 5.15. Condensing film heat transfer coefficient for the 3 in. fluted tube at 26 in. Hg vacuum. Coefficient based on mean temperature difference and developed heat transfer area of 1.00 sq ft/ft of length.

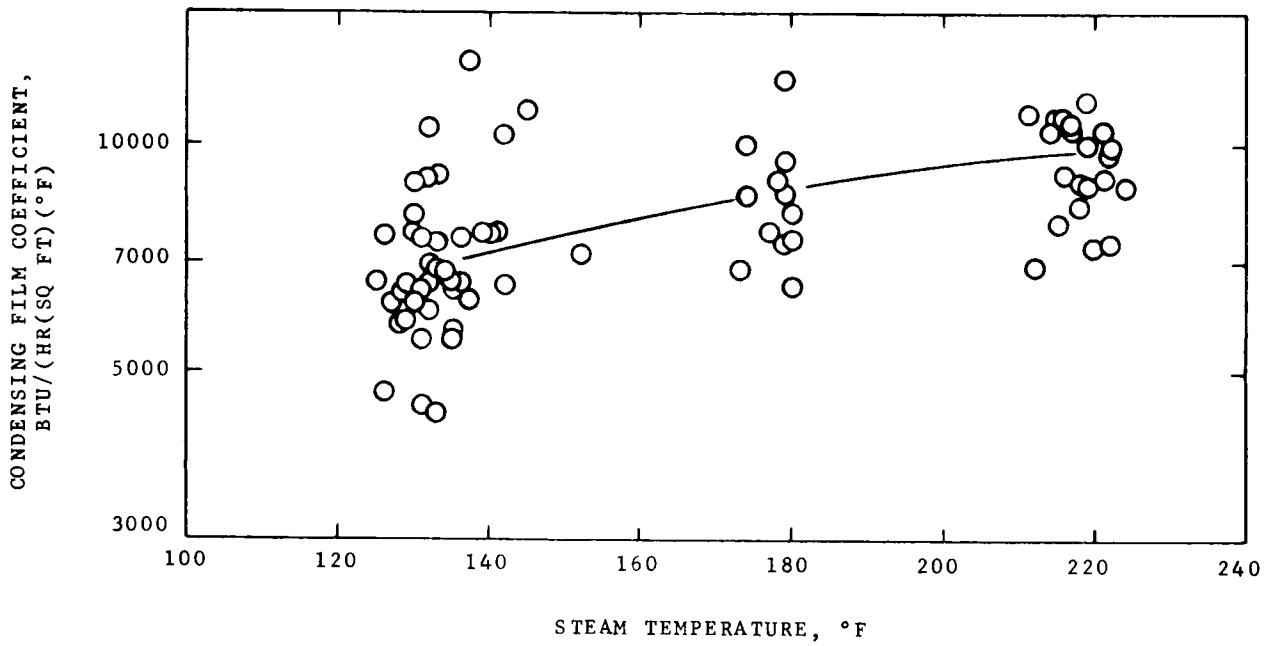

FIGURE 5.16. Condensing film heat transfer coefficient for 3 in. fluted tube. Coefficient based on mean temperature difference and developed heat transfer area of 1.00 sq.ft/ft of length.

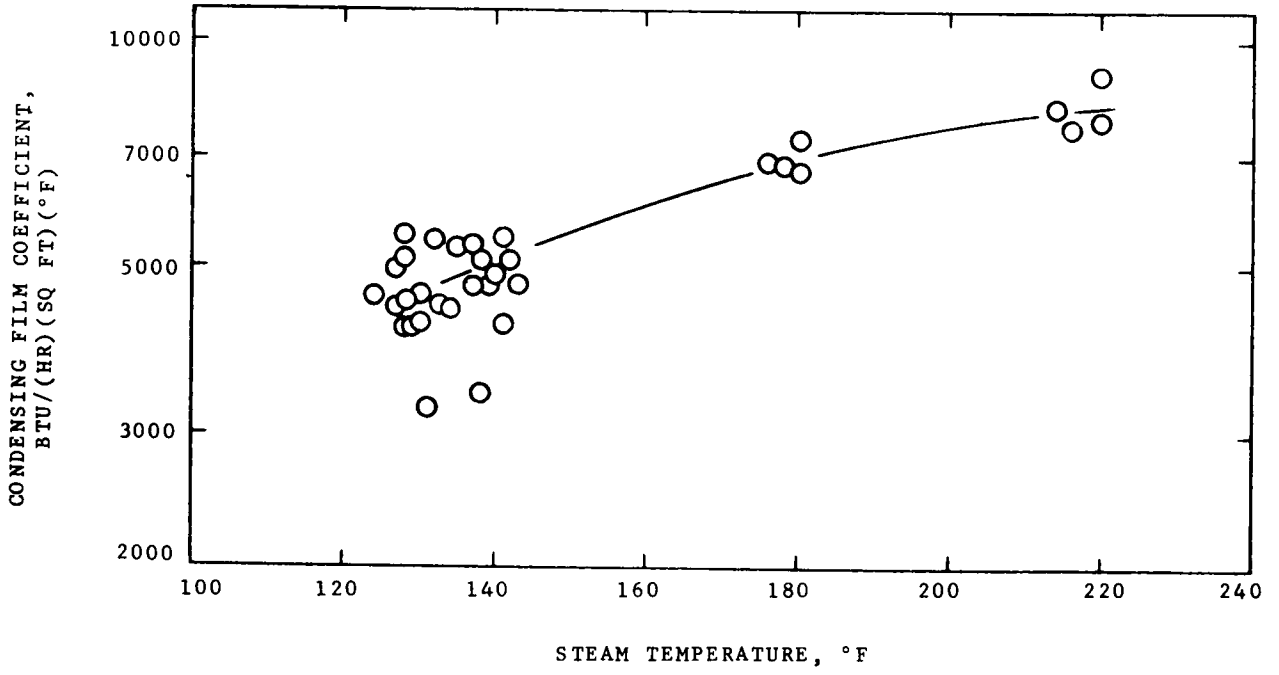

FIGURE 5.17. Condensing film heat transfer coefficient for 2 in. fluted tube. Coefficient based on mean temperature difference and developed heat transfer area of 0.67 sq ft/ft of length.

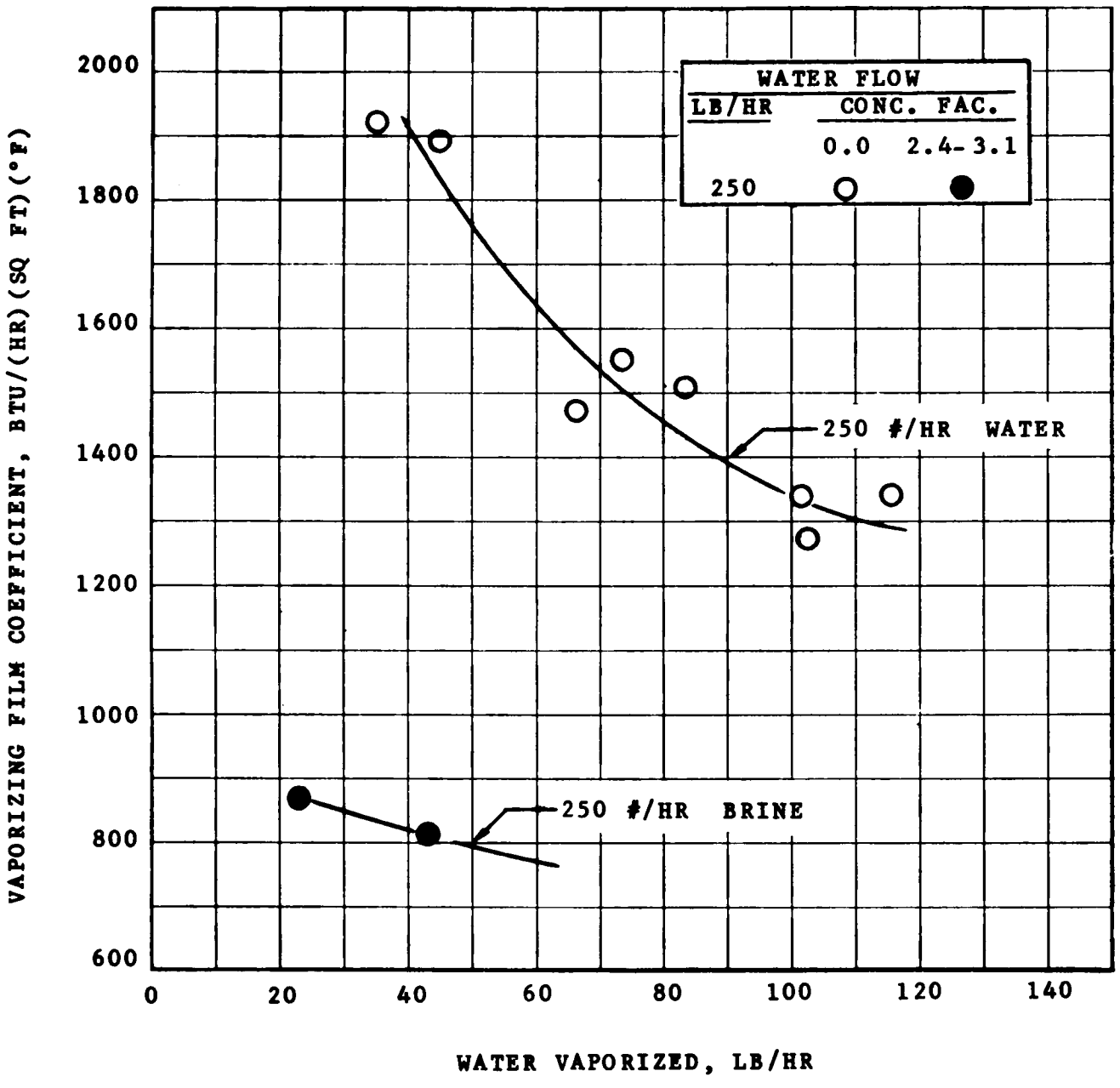

FIGURE 5.18. Vaporizing film heat transfer coefficient for the 3 in. fluted tube at 26 in. Hg vacuum. Coefficient based on mean temperature difference and developed heat transfer area of 0.967 sq ft/ft of length.

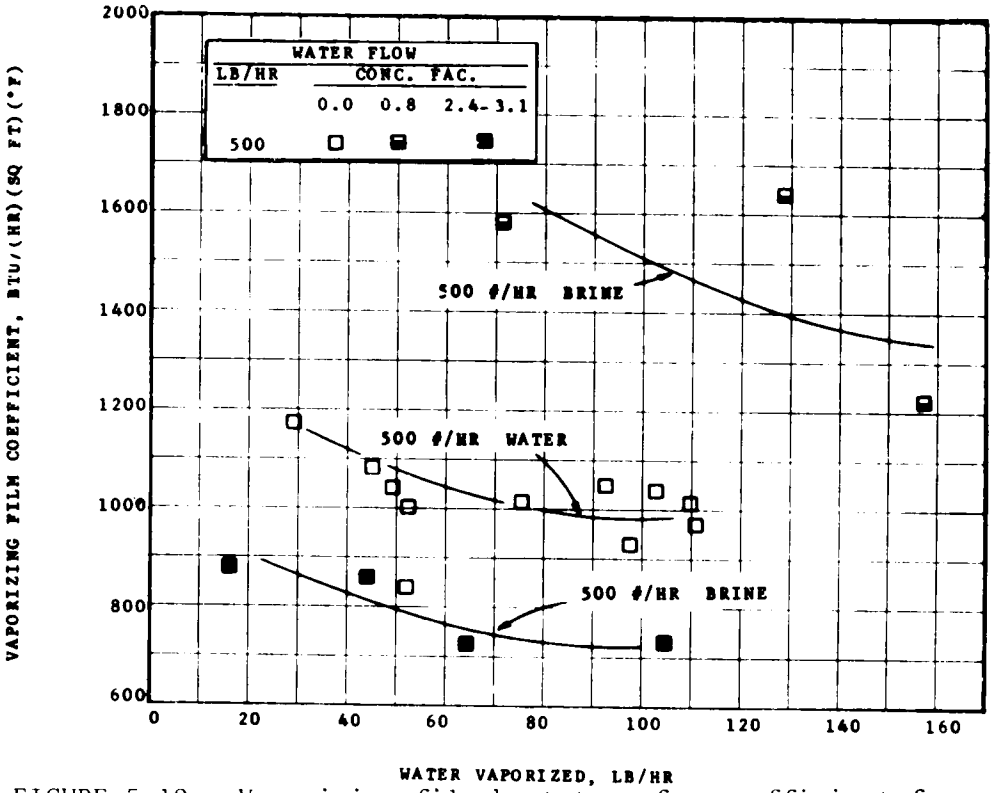

FIGURE 5.19. Vaporizing film heat transfer coefficient for the 3 in. fluted tube at 26 in. Hg vacuum. Coefficient based on mean temperature difference and developed heat transfer area of 0.967 sq ft/ft of length.

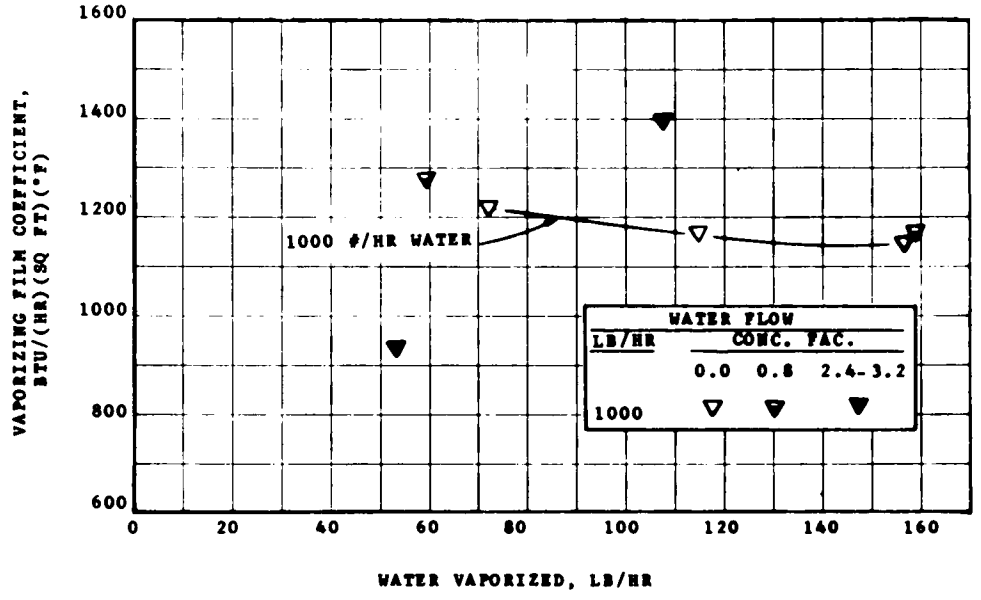

FIGURE 5.20. Vaporizing film heat transfer coefficient for the 3 in. fluted tube at 26 in. Hg vacuum. Coefficient based on mean temperature difference and developed heat transfer area of 0.967 sq ft/ft of length.

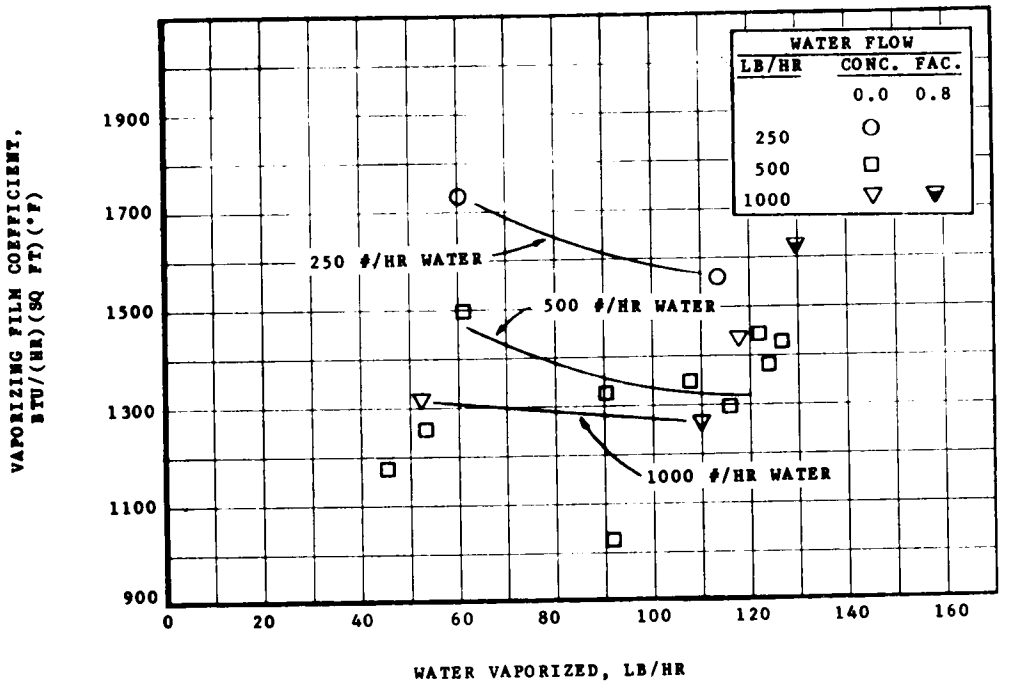

FIGURE 5.21. Vaporizing film heat transfer coefficient for the 3 in. fluted tube at 18 in. Hg vacuum. Coefficient based on mean temperature difference and developed heat transfer area of 0.967 sq ft/ft of length.

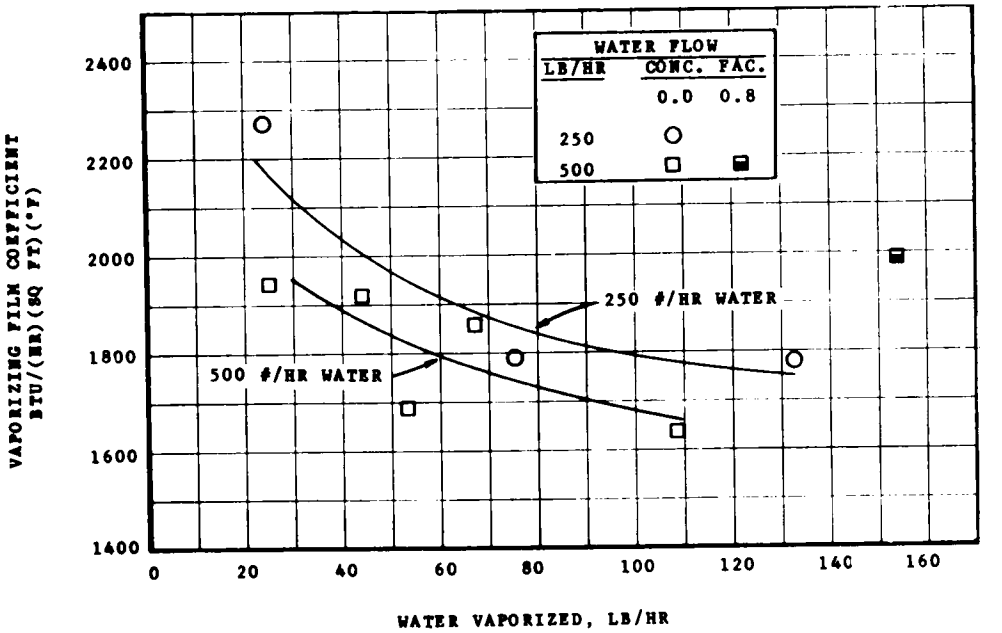

FIGURE 5.22. Vaporizing film heat transfer coefficient for the 3 in. fluted tube at 0 in. Hg vacuum. Coefficient based on mean temperature difference and developed heat transfer area of 0.967 sq ft/ft of length.

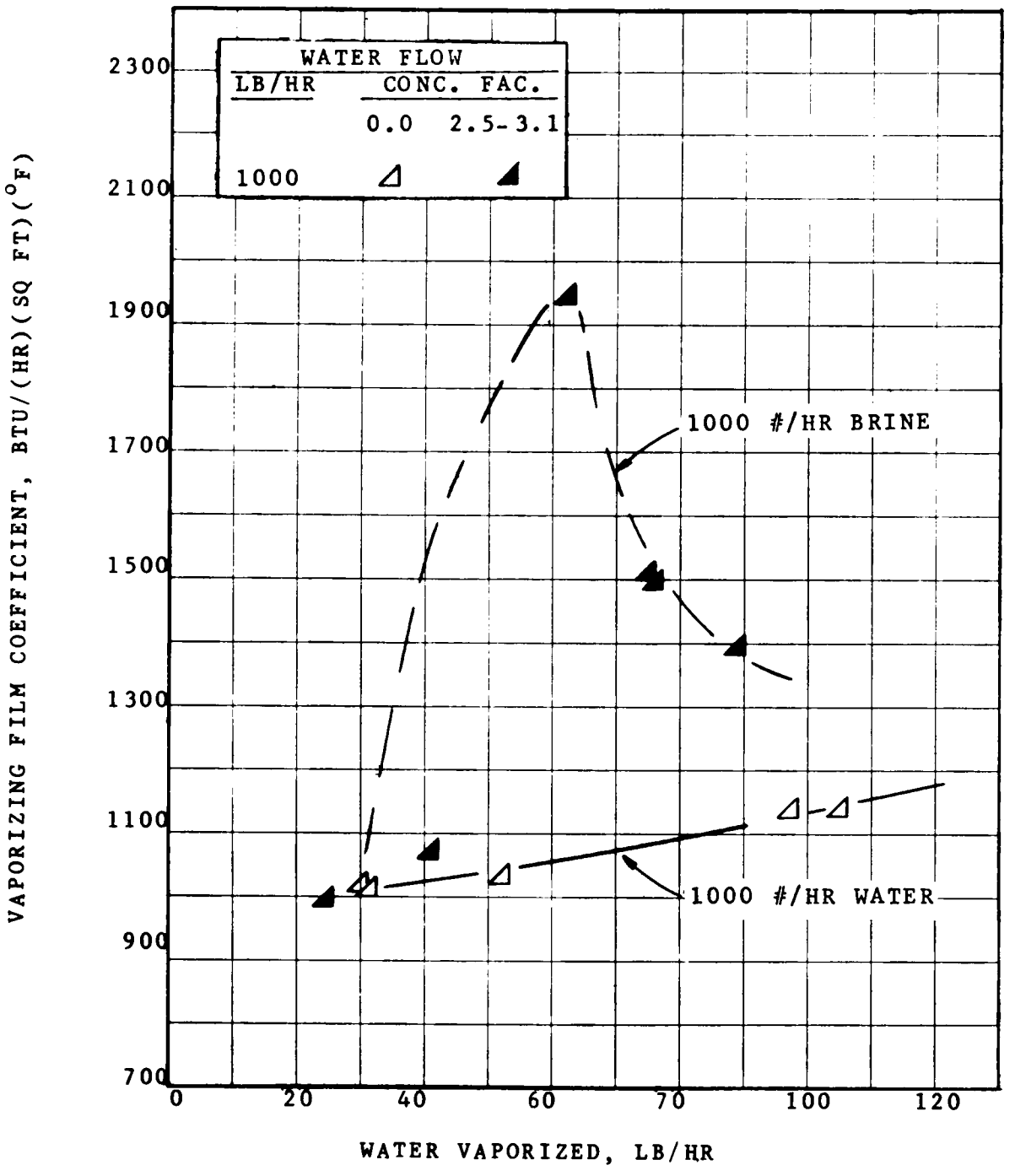

FIGURE 5.23. Vaporizing film heat transfer coefficient for 2 in. fluted tube at 26 in. Hg vacuum. Coefficient based on mean temperature difference and developed heat transfer area of 0.6 sq ft/ft of length.

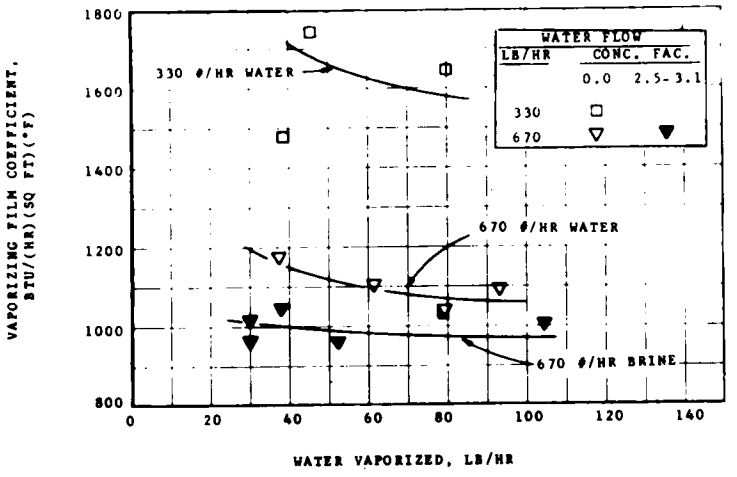

FIGURE 5.24. Vaporizing film heat transfer coefficient for the 2 in. fluted tube at 26 in. Hg vacuum. Coefficient based on mean temperature difference and developed heat transfer area of 0.648 sq ft/ft of length.

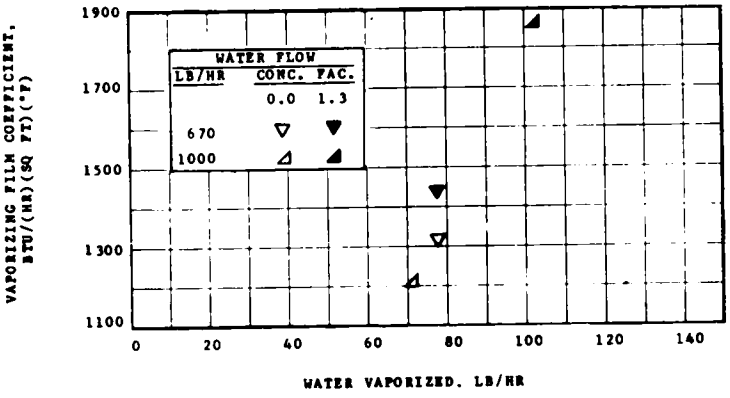

FIGURE 5.25. Vaporizing film heat transfer coefficient for the 2 in. fluted tube at 18 in. Hg vacuum. Coefficient based on mean temperature difference and developed heat transfer area of 0.648 sq ft/ft of length.

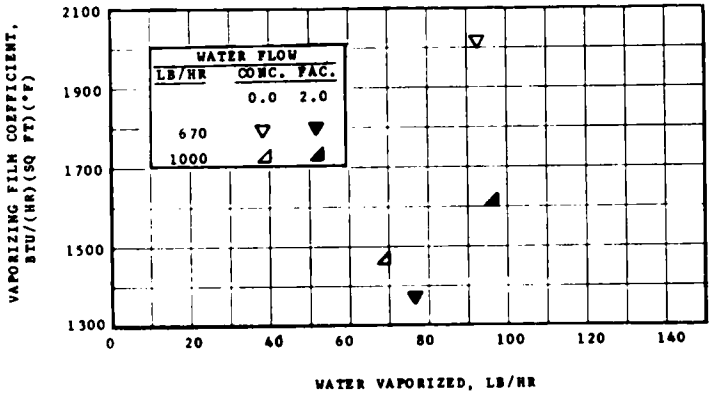

FIGURE 5.26. Vaporizing film heat transfer coefficient for the 2 in. fluted tube at 0 in. Hg vacuum. Coefficient based on mean temperature difference and developed heat transfer area of 0.648 sq ft/ft of length.

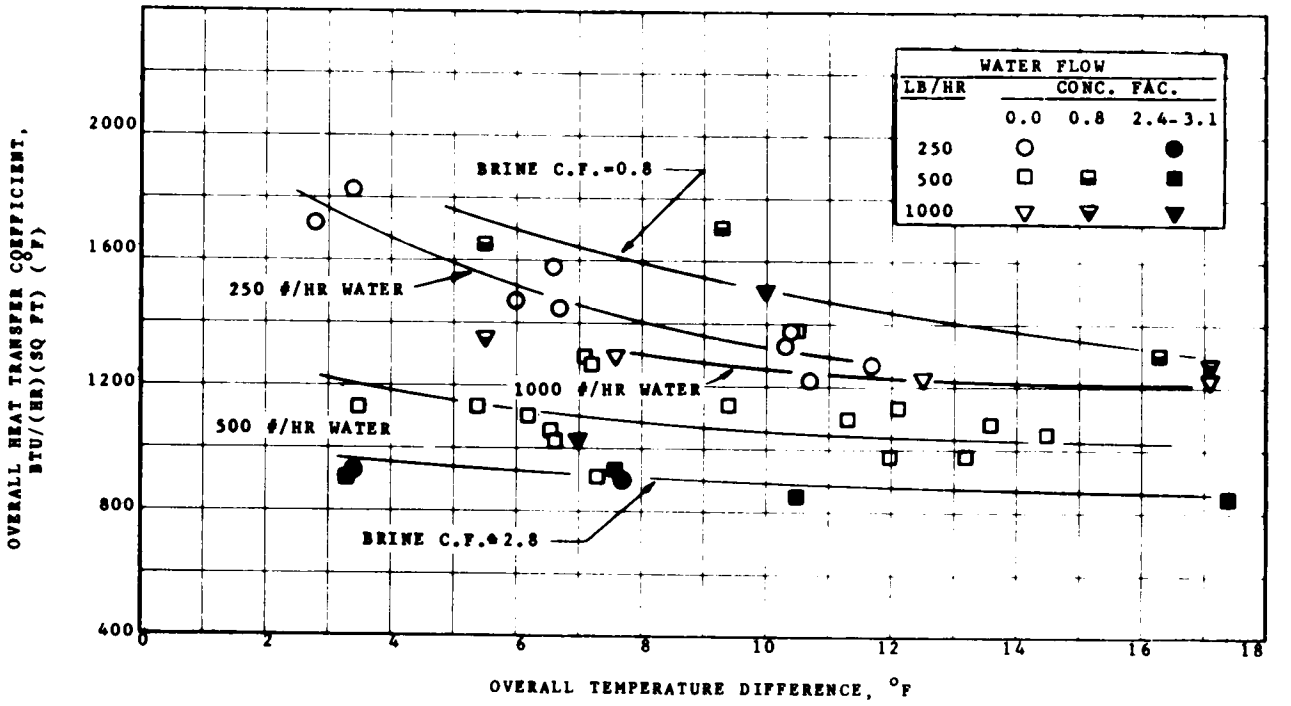

FIGURE 5.27. Overall heat transfer coefficient for the 3 in. fluted tube at 26 in. Hg vacuum. Coefficient based on mean temperature difference and developed heat transfer area of 1.00 sq ft/ft of length.

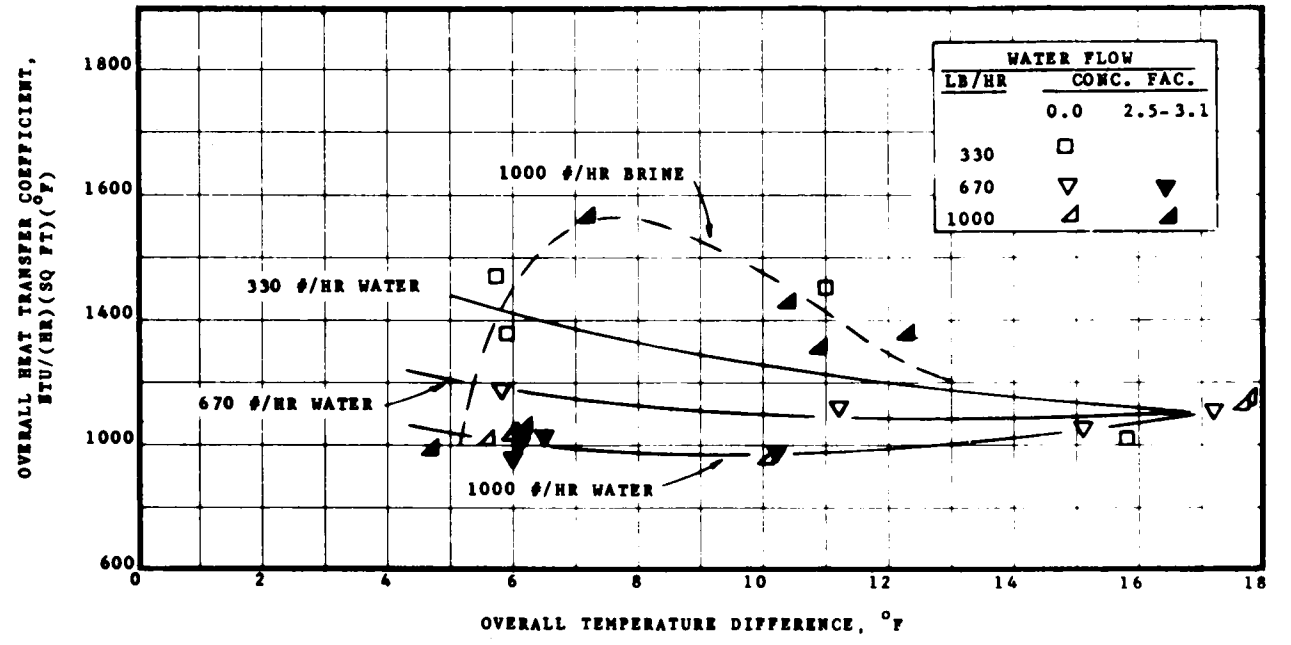

FIGURE 5.28. Overall heat transfer coefficient for the 2 in. fluted tube at 26 in. Hg vacuum. Coefficient based on mean temperature difference and developed heat transfer area of 0.670 sq ft/ft of length.

6. Air in Condensing Steam -- Effect on Heat Transfer in the Fluted Tube

The reduction in heat transfer caused by the presence of a noncondensable gas, even in small quantities, in condensing steam has long been known. The vapor must diffuse through the noncondensable gas to reach the vapor-liquid interface where it gives up its latent heat. This provides an additional resistance which lowers the vapor-liquid interfacial temperature and thus the driving force available for heat transfer. Sensible heat is also transferred since, with a noncondensable gas present, there is a temperature gradient between the bulk of the fluid and the surface of the condensate film. A relation for predicting the effect of a noncondensable gas was proposed by Colburn and Hougen in 1934 (2.2). Good agreement between this relation and experiment was found for condensation on the outside surface of a smooth tube (2.1). Application of the Colburn-Hougen relation to the fluted tube where condensation does not occur uniformly over the tube but primarily on the ridges has not been previously tested. The objective of this work was to determine for a range of conditions with the fluted tube what the effect of air in steam is and to determine if the Colburn-Hougen relation is adequate for prediction of heat transfer. The equation proposed by Colburn and Hougen is

$$q = U(t_i - t_L) = h_G(t_b - t_i) + \lambda K_G(p_b - p_i) \qquad (6.1)$$

where q = heat flux, Btu/ (hr)(sq ft)
U = overall heat transfer coefficient, Btu/(hr)(sq ft)(°F)
h_G = local coefficient for transfer of sensible heat through gas film, Btu/(hr)(sq ft)(°F)
K_G = mass transfer coefficient through gas film, lb of vapor condensed/(hr)(sq ft)(°F)(atm)
t_i = temperature of liquid-gas interface, °F
t_b = bulk temperature of gas stream on shellside, °F
t_L = bulk temperature of steam on tubeside, °F
p_b = bulk partial pressure of the shellside steam, atm
p_i = vapor pressure of the liquid at temperature t_i, atm
λ = latent heat of condensation of steam, Btu/lb

Basically we see that the latent heat given up at the interface by the diffusing molecules plus the sensible heat transferred from the vapor is equated to the heat transferred away from the interface. The interfacial temperature t_i is an unknown quantity which must be solved for by trial and error. The vapor and liquid are assumed to be in equilibrium at the interface so that for any assumed t_i the corresponding vapor pressure p_i can be determined. t_i varies over the length of a heat exchanger since the noncondensable gas concentration and value of K_G also vary with length. Therefore some type of graphical or numerical

technique must be used to apply this equation to the determination of the total heat transfer area.

In 1937, it was pointed out by Ackermann (6.1) and independently by Colburn and Drew (6.2) that the sensible heat carried by the diffusing molecules was not accounted for in Equation 6.1. A correction factor was derived to be applied to the sensible heat term $h_G (t_b - t_i)$. This factor is now generally known as the Ackermann correction. The correction is generally ignored because it is small unless the noncondensable gas concentration is much higher than encountered in this study.

Smith (6.3), in 1942, showed that consideration of subcooling of the condensate film below the interfacial saturation temperature was sometimes significant. Equation 6.1 does not account for this and Smith proposed an additional term to correct for it. This was found to make as much as 10 or 15 percent difference in the calculated condenser surface area for an organic vapor with low latent heat. Calculations showed that it was insignificant for the case at hand.

For the experimental runs, air was metered through a rotameter and introduced into the shell of the exchanger with the steam. The air was removed through the vent at the bottom of the shell along with any uncondensed steam. Concentration of air was controlled by varying the amount of air fed in with the steam along with regulation of the vent rate. The average air concentration (mean of inlet and outlet) was varied in the range up to 7 percent by volume except for one run (No. 317) which was 15.7 percent. The condensing steam temperature was varied from 134°F to 224°F and overall temperature driving force was varied from 4°F to 20°F. The data for the runs with noncondensables present is shown in Table 6.1. Base runs without air present were made at conditions corresponding to the air runs to provide a basis for determining how much effect the air had. The base runs used here are the runs in Table 5.1 with consecutive numbers between 288 and 320.

A method for determination of air concentration in the steam at the inlet and outlet of the heat exchanger was needed. A simple and inexpensive apparatus devised by Classen (6.4) was used by Meisenburg, et al (6.5) to measure air in steam at concentrations which included the range planned for our tests. A

6.1 Ackermann, G., Forschungsheft, No. 382, 1, (1937).

6.2 Colburn, A. P., and T.B. Drew, Trans, AICHE, 33, 197, (1937).

6.3 Smith, J. C., Ind. Eng. Chem., 34, 1248, (1942).

6.4 Claasen, Chem. Zeit., 13, 133 (1934)

6.5 Meisenburg, S. J., R. M. Boarts and W. L. Badger, Trans. Am. Inst. Chem. Engrs. 31, 622-635 (1935)

TABLE 6.1

SUMMARY OF RUNS WITH AIR IN CONDENSING STEAM
FOR 3 IN. BY 10 FT FLUTED TUBE

	TUBESIDE		SHELLSIDE	TUBESIDE																				
Run No.	Water Rate Lb/Hr	Feed Water Temp,°F	Air Rate Lb/Hr	Overall Pressure Drop In.Water	Tube Pressure Drop In.Water	Entrainment Lb/Hr	Water Evaporated Lb/Hr	Heat Transfer M BTU/Hr	Heat Balance Check %	Log Mean ΔT °F	T4	M4	B4	W1	W2	W3	W4	W5	W6	T1	M1	B1	h_i (3) BTU/(HR)(SQ FT)(°F)
XII 18-289	500	168.0	2.73	.16	.20	4.2	73.9	79.0	4.9	10.5	180.0	179.6	178.4	180.1	176.9	176.0	174.3	173.2	172.3	168.7	168.8	168.7	1237
XII 18-290	500	167.8	1.33	.25	.25	3.1	74.5	78.1	3.0	9.0	177.9	177.7	177.0	178.0	176.2	175.6	174.3	173.3	172.5	168.4	168.5	168.4	1254
XII 18-293	500	170.0	.33	.15	.15	2.8	76.8	79.1	2.6	8.4	176.5	176.5	176.4	176.5	175.3		174.6	174.1	173.6	168.1	168.1	168.1	1230
XII 18-294	500	171.0	2.02	.30	.20	3.5	121.0	126.2	4.5	14.8	183.8	183.7	183.0	183.4	180.8		178.0	176.5	174.9	168.6	168.6	168.5	1295
XII 26-299	500	125.0	2.60	.30	.25	6.2	85.8	93.3	5.4	13.2	137.9	137.4	136.2	138.1	135.1		131.8	130.0	128.6	124.0	123.9	123.8	1099
XII 26-300	500	126.0	1.33	.40	.30	6.7	90.8	96.8	4.7	13.0	136.9	136.7	136.1	136.8	134.6		132.7	131.3	129.7	123.6	123.5	123.3	1054
XII 26-302	500	128.0	.33	.60	.50	8.9	88.4	93.8	5.7	11.2	133.9	133.8	133.8	134.1	132.1		131.8	131.0	130.4	122.8	122.6	122.4	1062
XII 26-303	500	126.0	1.77	.85	.90	3.8	125.7	132.3	3.4	19.3	143.8	143.7	142.8	143.6	140.7		137.4	135.1	132.8	124.3	124.1	123.6	990
XII 0-308	500	211.0	1.68	.33		6.5	93.8	89.3	-6.0	8.7	220.5	220.4	219.9	220.5	218.5		217.2	216.3	215.4	211.5	211.5	211.5	1524
XII 26-311	500	124.0	1.78	1.10	.90	9.6	137.9	141.8	.5	19.5	143.1	143.2	142.0	142.9	139.8		136.9	134.6	131.5	123.5	123.1	122.6	1045
XII 0-314	500	214.0	1.33	.15	.10	27.9	64.1	63.2	-2.9	6.0	218.9	218.7	218.3	218.7	217.3		216.3	215.5	215.1	212.6	212.7	212.6	1663
XII 0-315	500	214.0	.40	.20		37.9	69.6	69.2	-1.8	5.5	217.4	217.3	217.2	217.2	216.3		215.9	215.3	215.1	211.8	211.8	211.8	1747
XII 0-316	500	214.0	2.65	.20		60.9	68.1	67.7	-2.6	7.3	219.8	219.4	218.5	219.9	217.1		215.4	214.3	214.0	211.9	211.9	211.8	1658
XII 26-317	500	126.0	.73	.10	.15	3.6	48.2	47.7	-1.3	7.0	129.1	128.9	128.4	128.9	127.7		126.6	125.9	125.2	121.8	121.8	121.7	976
XII 0-319	500	216.0	.73	.10		6.1	35.4	36.7	4.6	3.7	215.4	215.2	214.7	215.3	214.4		213.8	213.3	213.1	211.3	211.4	211.3	1446
XII 0-321	500	215.0	2.20	.10	.10	10.7	78.1	80.5	4.2	9.4	224.4	223.1	219.7	224.8	219.6		215.9	214.2	213.7	212.5	212.5	212.4	1629
XII 26-322	500	126.0	2.67	.35	.35	5.3	85.7	90.4	4.3	13.1	136.6	136.5	135.0	136.6	133.3		130.0	127.9	126.3	122.8	122.7	122.5	1146

(3) Area for calculating h_i based on developed inside heat transfer area estimated to be 0.967 sq ft/ft of length.

close examination showed this method to be of limited accuracy. The steam from a sample is condensed and the relative amounts of water and air are determined from the levels of two 500 ml burets. The quantity of water, sometimes as little as a few ml must be determined by difference from these readings. A major revision to improve the accuracy was necessary. With the revised system, condensed steam is collected in a 50 ml buret so that the volume can be accurately measured. A diagram of the revised apparatus and the method of using it is included in Appendix I.

For each experimental run the Colburn-Hougen relation was used to predict how much heat transfer area was required to transfer the same amount of heat under the same conditions. The overall heat transfer coefficient, U, was determined from the corresponding base runs and was assumed to be constant over the length of the heat exchanger. The Colburn-Hougen equation was then used to find the vapor-liquid interfacial temperature so that the true temperature driving force could be estimated. The values of K_G and h_G were determined by the methods recommended by McAdams (6.6). The equivalent diameter was calculated based on four times the cross-sectional area of the annulus divided by the heated perimeter of the fluted tube. The value of the Schmidt number used for the determination of K_G was taken as 0.55.

The calculation was performed incrementally using a digital computer starting at the top of the heat exchanger and working down. Increments of 0.655 ft were used except for the last increment which was variable so that the heat transfer would match the corresponding experimental run. A flow chart, nomenclature and program listing for the calculation are shown in the Appendix.

The results of the comparison of the area predicted by the Colburn-Hougen equation with the actual area are shown in the following table:

TABLE 6.2

COMPARISON BETWEEN COLBURN-HOUGEN PREDICTION AND EXPERIMENTAL RESULTS

Number of Runs	17
Mean of Predicted Areas	9.85 sq ft
Actual Area (Based on Nominal Diameter)	9.83 sq ft
Mean Absolute Deviation	0.59 sq ft
Standard Deviation	0.42 sq ft

6.6 McAdams, W. H., "Heat Transmission", 3rd Ed., McGraw-Hill, New York (1954).

It is seen that the average predicted area is very close to the actual area. Another method of looking at the same results is shown in Figure 6.1 where the increase in heat transfer area caused by the presence of air over that which would have been required for corresponding runs without air is compared for experiment and as predicted by the Colburn-Hougen equation.

To further illustrate this concept, let A' be the area required to transfer the same amount of heat without air present as with air present but at the same conditions otherwise. A' will be less than the actual area of 9.83 sq ft. This area, A', corresponding to each of the runs with air present, can be calculated using the overall heat transfer coefficient from the corresponding base runs. The experimental area increase required to transfer the same amount of heat due to the presence of air is then

$$\text{Area increase, } \% = \frac{9.83-A'}{A'} \times 100 \qquad (6.3)$$

The predicted area increase was obtained by replacing 9.83 in Equation 6.3 with the value calculated by the Colburn-Hougen equation. The results are seen to be good over the full range for which results were obtained.

An example of the steam Reynolds number and air concentration variations along the length of the tube, a by-product of the Colburn-Hougen stepwise calculation procedure, is shown in Figure 6.2 for Run No. 300. It is noted that the Reynolds number drops into the laminar flow region near the bottom of the tube as was the case for a number of runs. If a large portion of the tube had been in laminar flow it is likely that the poor agreement between theory and experiment would have been obtained since the method used for calculation of K_G is suitable only for turbulent flow.

Figure 6.3 shows the decrease in heat transfer as a function of distance down the tube as predicted with the Colburn-Hougen equation for Run 300. It is noted that due to the increasing air concentration and lower steam velocity the heat flux at the bottom of the tube is only about 60 percent of that at the top for this particular run.

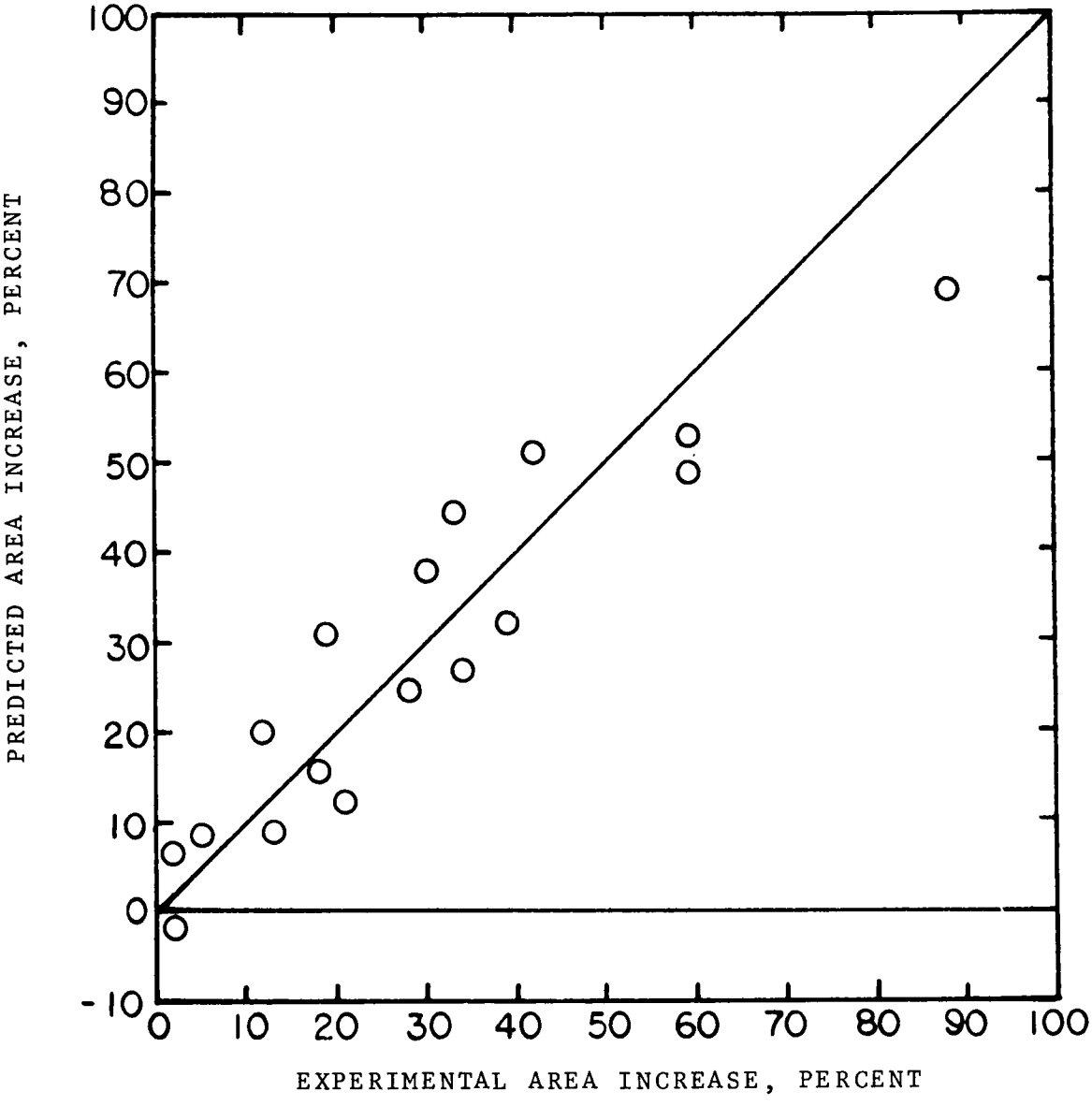

FIGURE 6.1. Additional area required for the 3 in. fluted tube due to the presence of noncondensable gas - a comparison of the Colburn-Hougen method with experiment.

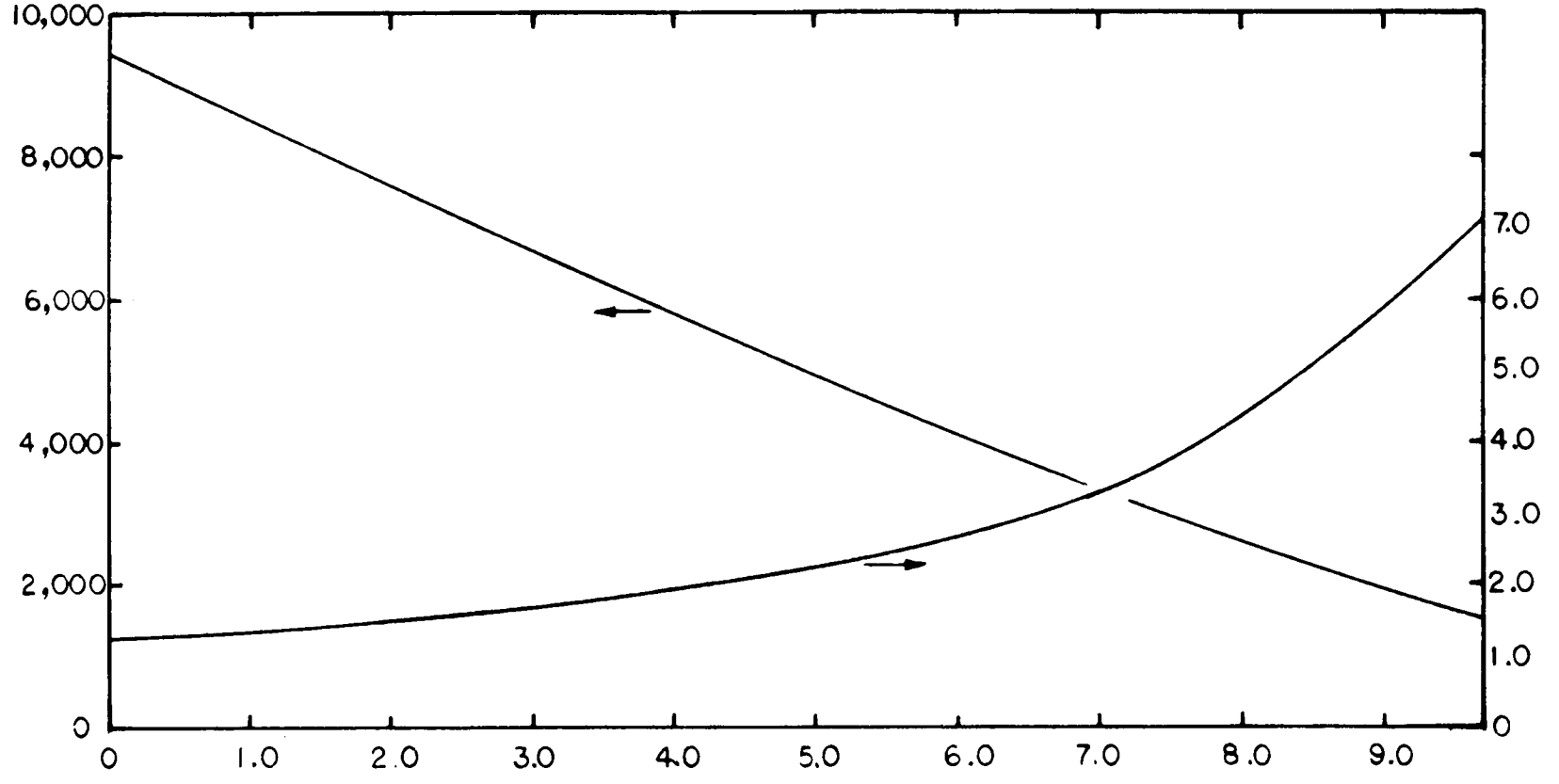

FIGURE 6.2. Profile of steam Reynolds number and air concentration - computer simulation at 26 in. Hg vacuum for 3 in. fluted tube.

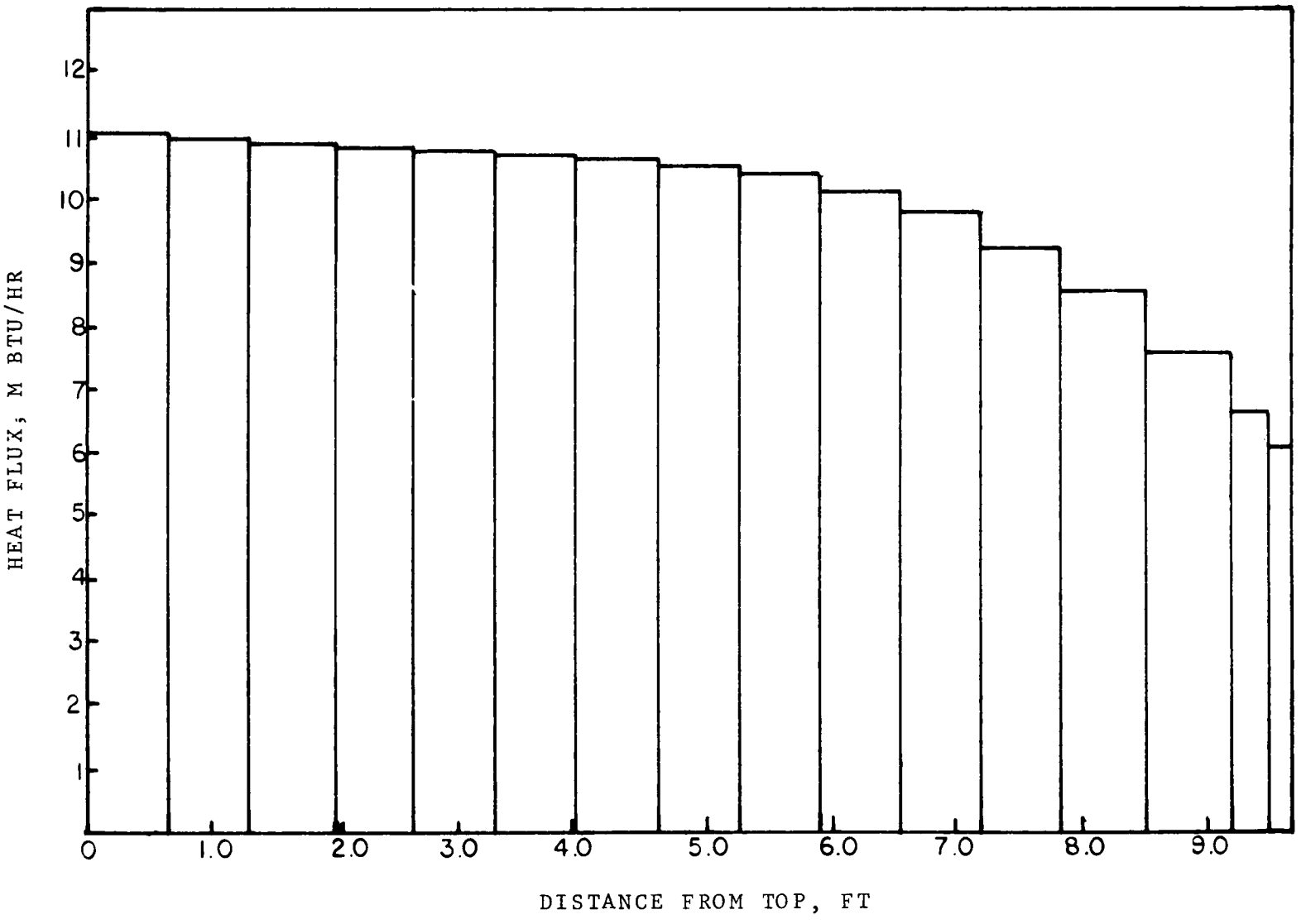

FIGURE 6.3. Profile of heat flux with noncondensable gas -- computer simulation at 26 in. Hg vacuum for 3 in. fluted tube.

7. Effect of Induced Shear on Evaporating Side of Three In. Fluted Tube

This series of tests was run to determine the improvement in heat transfer from inducing additional shear and turbulence on the evaporating side of the three in. fluted tube. A limited number of tests were made with three different types of inserts to determine if the improvement was enough to warrant further testing. A discussion of the different installations and the results are given in Sections 7.1 and 7.2.

7.1 Cylindrical Insert and Spherical Balls

Two of the devices tested for inducing additional shear and turbulence in the evaporating film are shown in Figures 7.1 and 7.2. The three in. by ten ft fluted tube described in Section 3 was used for the tests. The cylindrical baffle was prepared by brazing a plate over each end of a two in. diameter brass tube and installing hooks by which it could be suspended in the tube. Rubber balls, of 2.15 in. diameter, were used for inducing turbulence as shown in Figure 7.2. The balls were split at the center and fastened onto the thermocouples in the center of the tube. Spacers of 3/8 in. diameter plastic tubing were used to keep the 5 in. spacing between the balls. The baffle was attached with a 25 lb weight on the bottom as shown in Figure 7.1.

Fresh water was introduced at the top of the tube through a spray nozzle. Recirculation rates of 500 and 1000 lb/hr were used with overall temperature differences of approximately 5 and 10°F.

Some of the pertinent results of the runs in this series are shown in Table 7.1. Overall heat transfer coefficients with the cylinder insert and suspended balls are plotted in Figures 7.3 and 7.4, respectively. Base run coefficients with no induced interfacial shear are also plotted for easy comparison. The cylindrical insert showed an improvement of only about 3 percent at the 500 lb/hr flowrate. This is probably within the range of experimental error. The results with the spherical balls suspended in the upper portion of the tube showed an increase of 8 to 12 percent in heat transfer coefficient. At a flowrate of 1000 lb/hr, which is presently more realistic for actual plant operating conditions, there was no detectable improvement. The variation with flowrate was remarkably consistent. For each condition the coefficient with the lower water flowrate was always higher in this series of runs.

Pressure drop for the cylindrical insert and the suspended spheres is compared against the base run values in Figures 7.5

and 7.6. A significant increase in pressure drop was observed for the cases with induced shear. At high heat fluxes the pressure drop was roughly 2 to 3 times that of the corresponding base run.

Entrainment measurements, plotted in Figure 7.7 to 7.8, are seen to be much higher with the inserts. Qualitative observations had shown earlier that a portion of the water impinging upon the wall from the spray nozzle will bounce off the wall and fall down the center of the tube. Entrainment measurements indicate that without inserts much of this water is redeposited on the wall again before it reaches the bottom of the tube. The insert in the middle provides a surface down which this liquid can flow at least for the length of the insert with little chance of reaching the wall. This is probably a factor in the higher entrainment with inserts.

While some improvement in heat transfer was noticed with these inserts at the lower water rates, it must be remembered that this is at the expense of a significant increase in pressure drop and resultant reduction of temperature driving force. The improvement in heat transfer shown here for these particular baffles is not enough to justify their use when the costs of manufacture and installation are considered.

7.2 Spiral Baffle

Another method of inducing shear and turbulence on the evaporating side of the VTE is the spiral baffle. This has been tested extensively and a significant improvement in heat transfer has been shown for smooth circular tubes.

The spiral baffle was installed in the three in. by ten ft fluted tube as shown in Figure 7.9. Two wires attached to the bottom of the baffle pass through a packing gland at the bottom of the apparatus. A specially designed coil spring attached to the wires assured that the 75 lb tension was maintained on the baffle after the seal was tightened. This took care of changes in thermal expansion if the seal held the wire tight enough to prevent the force of the weight from being transmitted to the baffle. The 1/16 in. o.d. thermocouples were attached to the center of the baffle as shown in the diagram for measurement of the vapor temperature. With the baffle under tension, the thermocouples provided no visible distortion of the normal spiral pattern of the baffle.

Runs were carried out initially with fresh water. Improvement was less than the 5 to 15 percent reported for the fluted tube with similar conditions (7.1). Additional runs were then made with the conditions in Reference 7.1 more closely simulated.

7.1 Sephton, H. H., May 1968 Progress Report on OSW Contract No. 14-01-0001-1744.

This included the use of artificial sea water instead of fresh water and replacement of the spray nozzle with another type of distributor. Two spiral baffles were supplied from the University of California, Berkeley, by H. H. Sephton, for the test. The baffle used for the fresh water runs had a 10 in. pitch and two in. width. This baffle was damaged upon removal and could not be used again for the test with sea water. A baffle with 8.5 in. pitch and 1.75 in. width, which was found by Sephton to have comparable performance to the other baffle, was used for the runs with sea water.

The tests with fresh water were made at 18 in. tubeside vacuum with recirculation rates of 500 and 1000 lb/hr. Overall temperature differences of approximately 5 and 10 °F were used. The results are tabulated in Table 7.1 and the overall heat transfer coefficient, pressure drop and entrainment are plotted in Figures 7.10, 7.11, and 7.12, respectively, for both the fresh water and brine runs. The runs with sea water were made at the same condition except the higher flowrate was reduced to 800 lb/hr because this was the flowrate used in Reference 7.1. In addition, an annular flow distributor was used, as shown in Figure 7.13, to prevent splashing of the water from the spray nozzle onto the baffle. The corresponding base runs are also plotted in the same graphs for easy comparison. The improvement obtained with fresh water was only about three percent, for the 500 lb/hr water rate. No improvement could be detected at the 1000 lb/hr water flowrate.

For the sea water runs, the baffle gave an improved heat transfer coefficient of nine percent at a liquid flowrate of 500 lb/hr. This is within the 5 to 15 percent range reported by H. H. Sephton. At the 800 lb/hr flowrate, however, any improvement was too small to distinguish from the normal data scatter. The higher heat transfer coefficient with sea water (concentration factor of one) versus fresh water was again apparent as was noted in Section 5.

The pressure drop, shown in Figure 7.11, was higher with the spiral baffle but still lower than the cylindrical insert or the suspended spheres. Entrainment results are shown in Figure 7.12. The entrainment for the fresh water runs with the spiral baffle are considerably higher than the corresponding base runs. This is thought to be the result of the water from the spray nozzle splashing off the wall and onto the baffle where it runs down and is collected as entrainment. Use of the annular entrance device corrected this situation for the runs with sea water. Entrainment was actually lower with the baffle installed than the corresponding base runs. However, as was noted in Section 5, the base runs with sea water are higher than base runs with fresh water.

The percentage improvement in heat transfer for the 3 in. by 10 ft fluted tube attributed to use of the spiral baffle is considerably less than for the smooth tube. Use of an annular entrance device rather than a spray nozzle cuts down on the liquid which flows down the baffle. This possibly offers some improvement in heat transfer coefficient although this could not be separated from the effect of sea water in these tests. However, an improvement in heat transfer of only 9 percent would still make installation of the spiral baffle difficult to justify for the 3 in. by 10 ft fluted tube.

TABLE 7.1

SUMMARY OF HEAT TRANSFER RUNS
FOR 3 IN. X 10 FT FLUTED TUBE
WITH INDUCED SHEAR AND TURBULENCE

Run No.	Tubeside Vacuum In. Hg	Mean Temperature Difference °F	Chlorinity gm/Kg	Water Flow Rate Lb/Hr	Heat Transferred BTU/Hr	Total Water Evaporated Lb/Hr	Overall ΔP In. Water	Entrainment Lb/Hr	Overall U BTU/FT^2 HR °F
	CYLINDER INSERT								
337	17.87	5.6	0.	1000	57100	54.5	0.15	104	1085
338	18.01	5.3	0.	1000	57800	56.2	0.10	102	1089
339	18.13	10.2	0.	500	120500	114.7	0.49	12	1195
340	18.18	10.3	0.	1000	108700	105.4	0.71	79	1067
341	18.18	5.2	0.	500	66400	64.1	0.21	10	1299
342	18.13	5.0	0.	1000	55100	54.5	0.10	109	1122
	2.15" DIA. RUBBER BALLS								
343	18.05	5.0	0.	500	68100	65.1	0.25	4	1404
344	17.99	5.2	0.	1000	58300	54.5	0.17	184	1141
345	18.09	10.4	0.	500	130100	123.5	0.78	10	1265
346	18.16	10.4	0.	1000	116800	106.9	0.63	97	1051
	SEPHTON BAFFLE								
326	17.95	5.0	0.	500	62900	57.4	0.10	34	1278
327	17.92	4.9	0.	1000	51200	47.0	0.10	79	1059
328	17.99	6.7	0.	500	82300	77.3	0.20	35	1257
329	17.93	6.9	0.	1000	72800	69.7	0.10	90	1072
330	18.09	10.6	0.	500	124900	118.3	0.33	34	1205
331	18.08	10.5	0.	1000	107800	104.6	0.25	94	1048
391	18.30	6.0	20.	500	87600	86.9	0.35	14	1460
392	18.19	10.7	24.7	500	146000	145.0	0.63	21	1370
393	18.13	11.1	22.2	800	141000	125.0	1.10	79	1290
398	18.40	5.0	21.0	800	61600	59.5	0.30	55	1270
399	18.30	5.2	21.0	800	61800	68.1	0.30	38	1200

TABLE 7.1 (Continued)

Run No.	Tubeside Vacuum In. Hg	Mean Temperature Difference °F	Chlorinity gm/Kg	Water Flow Rate Lb/Hr	Heat Transferred BTU/Hr	Total Water Evaporated Lb/Hr	Overall ΔP In. Water	Entrainment Lb/Hr	Overall U BTU/FT^2 HR °F
	BASE RUNS								
332	18.05	5.4	0.	500	65400	61.5	0.10	2	1252
333	17.97	5.1	0.	1000	53800	51.6	0.0	7	1090
334	18.00	9.8	0.	500	112400	107.2	0.20	1	1167
335	18.02	10.6	0.	1000	111300	109.3	0.25	9	1075
401	18.38	5.3	24.	500	69600	74.4	0.20	16	1330
402	18.36	5.4	19.	800	67900	68.7	0.25	96	1270
403	18.23	10.9	26.	500	136000	134.0	0.40	51	1260
404	18.14	8.7	26.	800	110100	105.0	0.30	310	1285

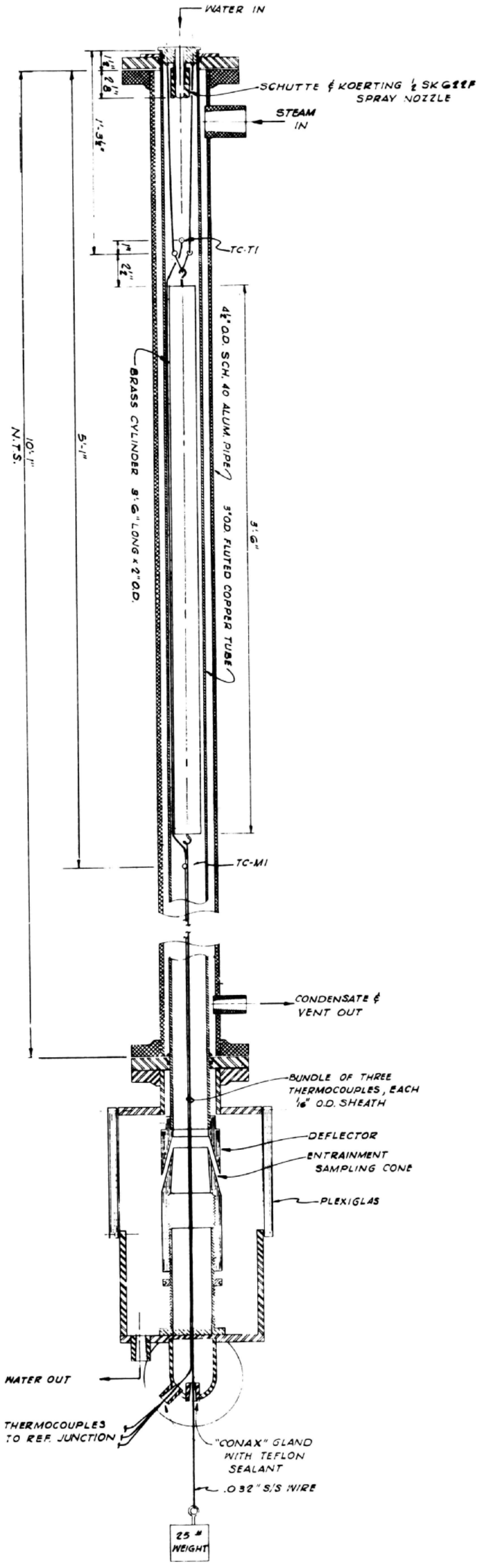

FIGURE 7.1 Cylindrical insert installed in 3 in. by 10 ft fluted tube

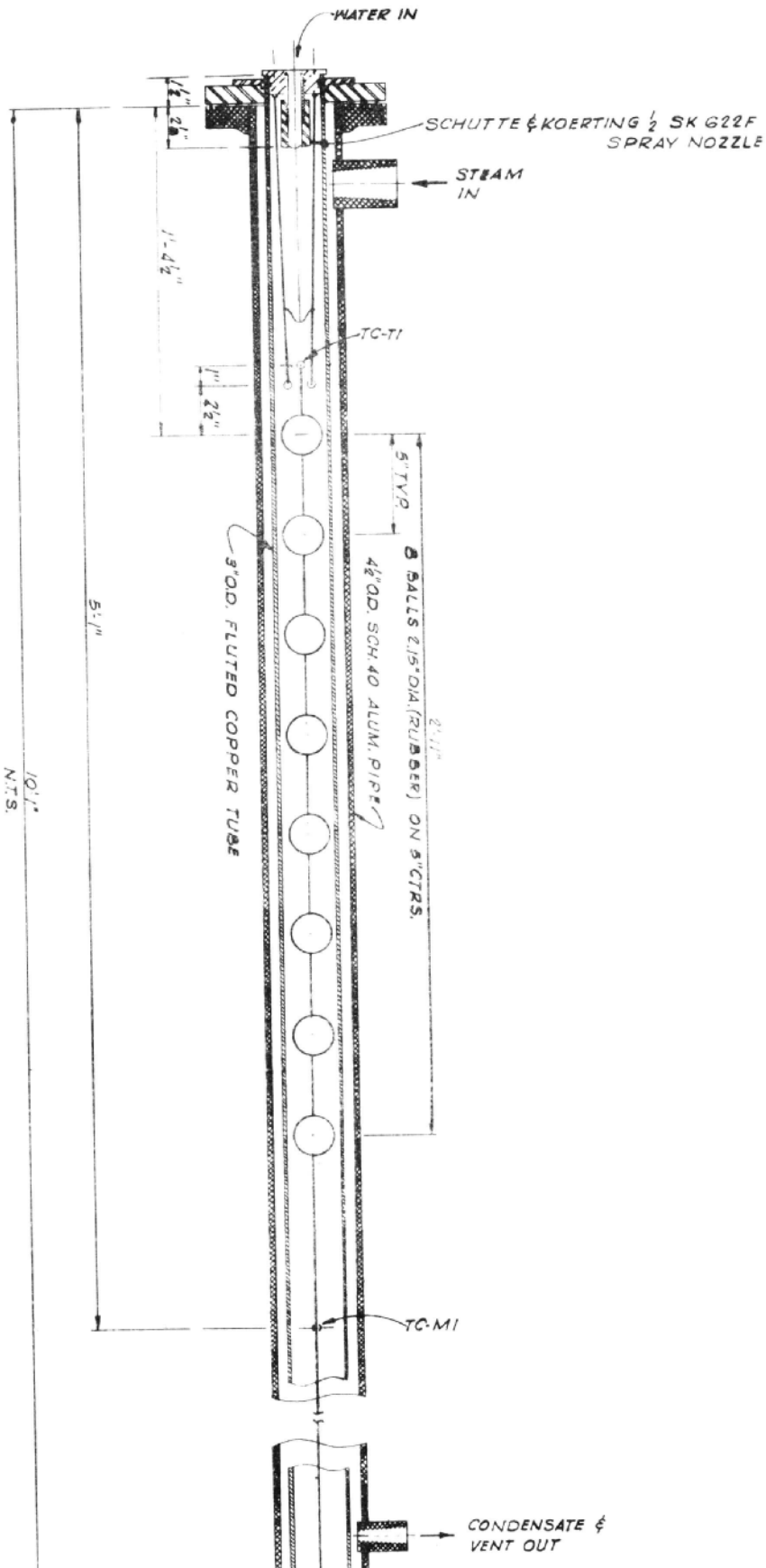

FIGURE 7.2 Balls 2.15 in. in diameter installed in 3 in. by 10 ft fluted tube

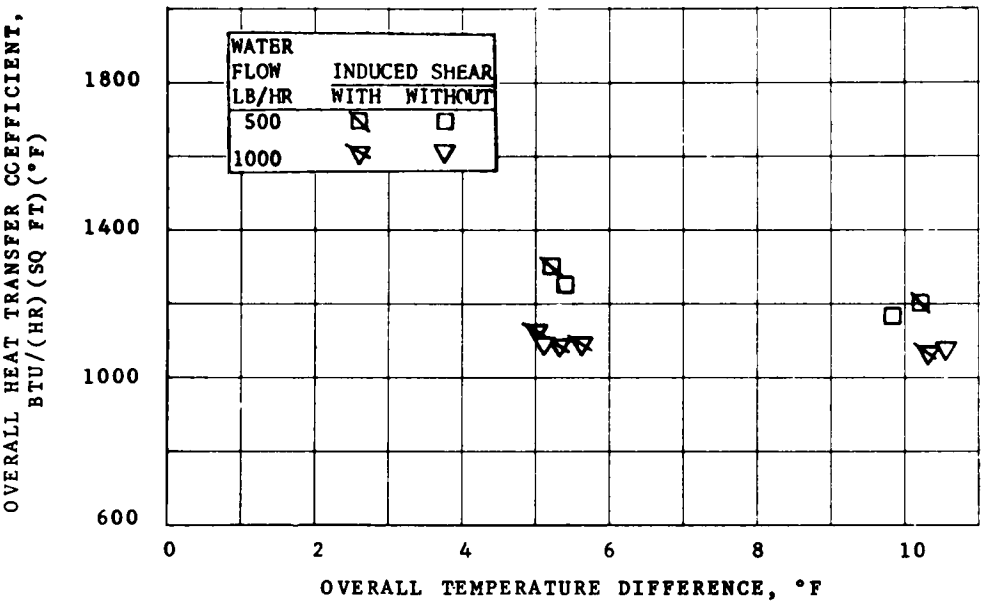

FIGURE 7.3. Comparison of heat transfer coefficient with and without 2 in. cylindrical insert (see Figure 7.1) at 18 in. Hg vacuum with fresh water. Coefficient based on mean temperature difference and developed heat transfer area of 1.00 sq ft/ft of length.

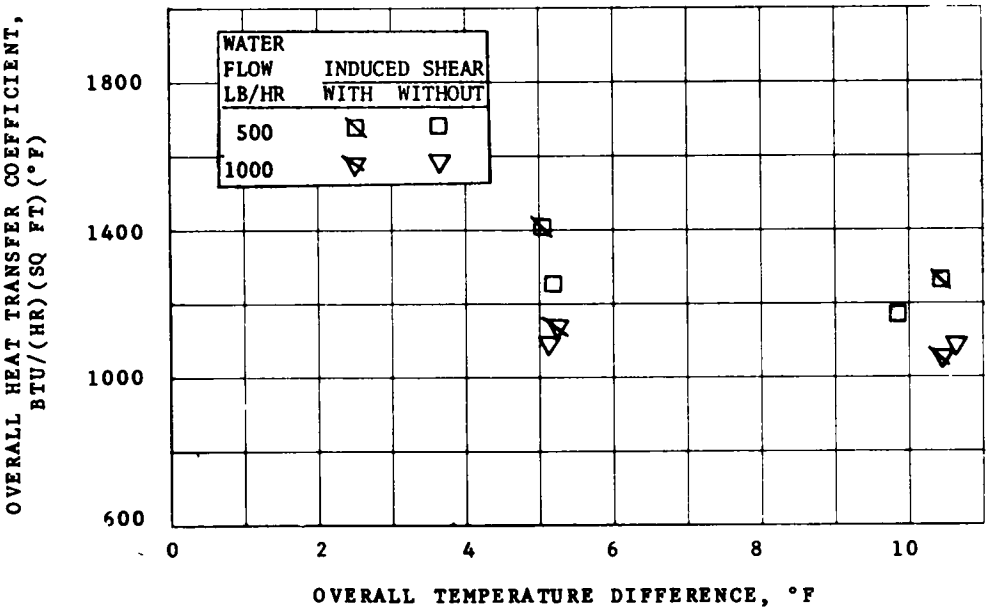

FIGURE 7.4. Comparison of heat transfer coefficient with and without 2.15 in. balls (see Figure 7.2) at 18 in. Hg vacuum with fresh water. Coefficient based on mean temperature difference and developed heat transfer area of 1.00 sq ft/ft of length.

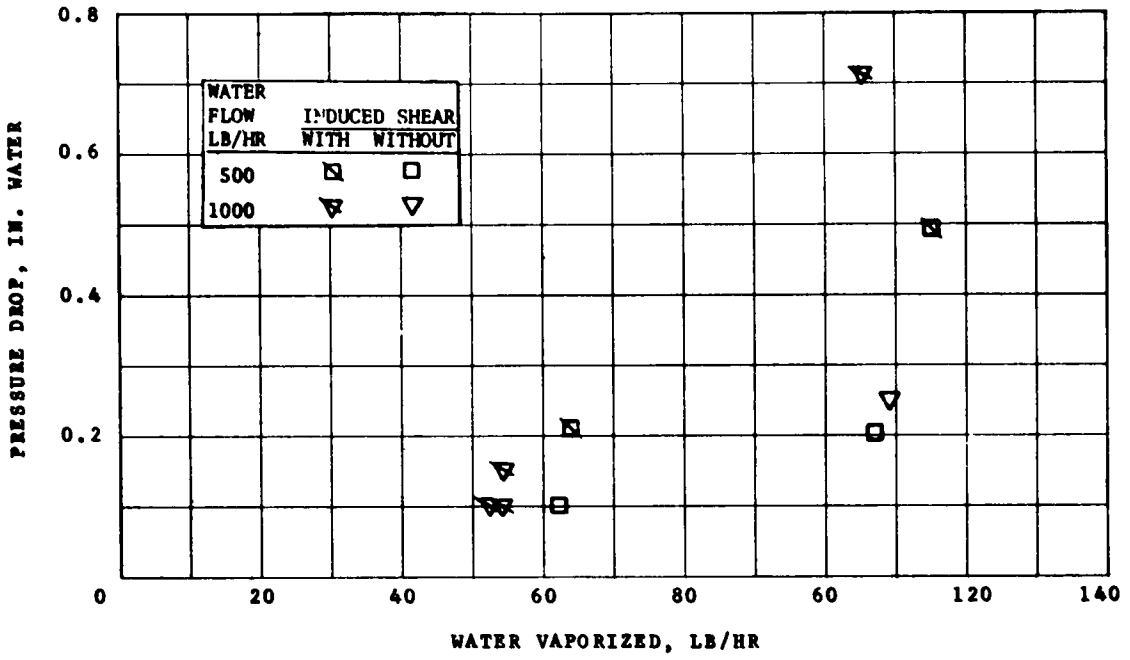

FIGURE 7.5. Comparison of pressure drop with and without 2 in. cylindrical insert (see Figure 7.1) at 18 in. Hg vacuum with fresh water.

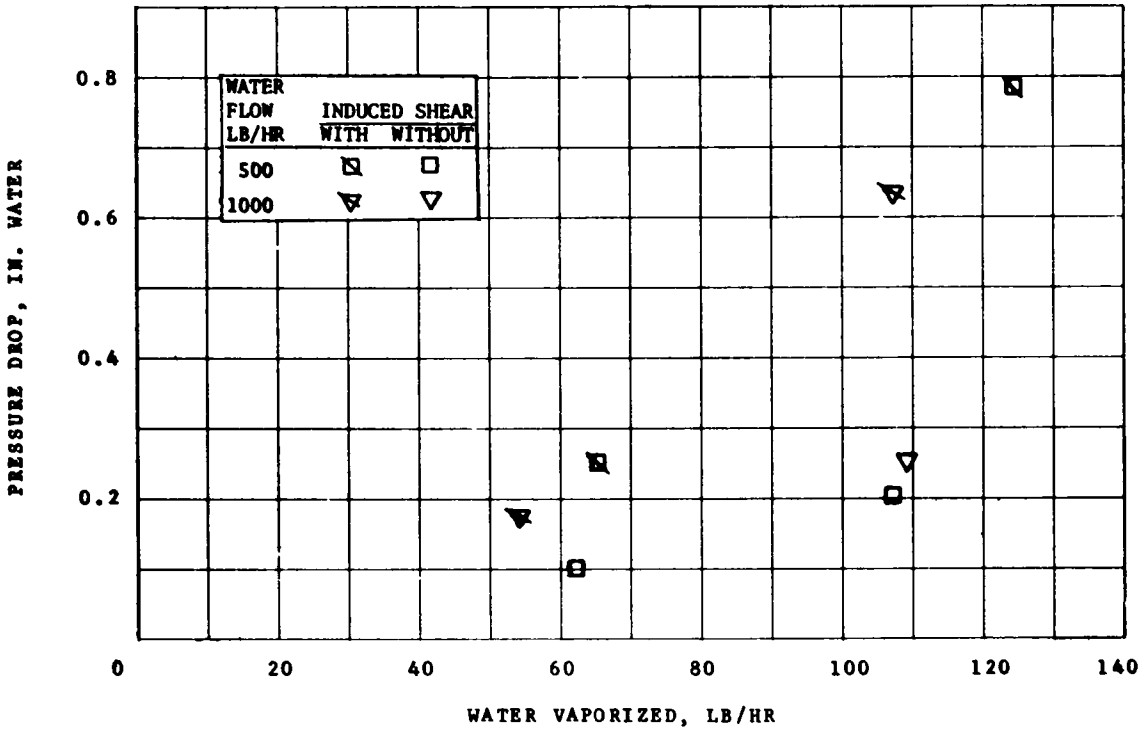

FIGURE 7.6. Comparison of pressure drop with and without 2 in. diameter balls (see Figure 7.2) at 18 in. Hg vacuum with fresh water.

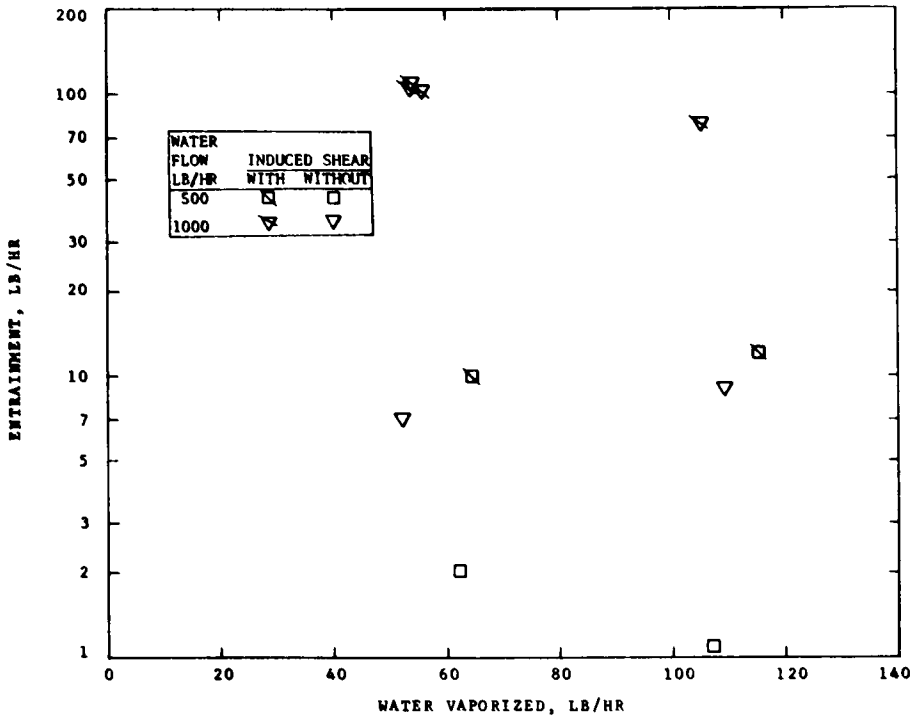

FIGURE 7.7. Comparison of entrainment with and without 2 in. diameter cylindrical insert (see Figure 7.1) at 18 in. Hg vacuum with fresh water.

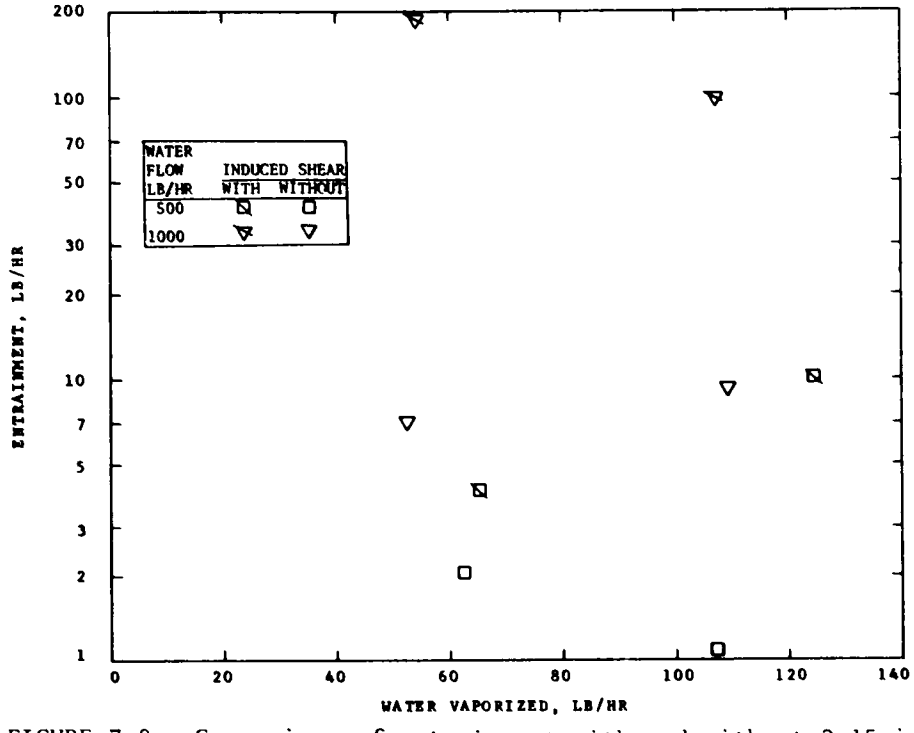

FIGURE 7.8. Comparison of entrainment with and without 2.15 in. diameter balls (see Figure 7.2) at 18 in. Hg vacuum with fresh water.

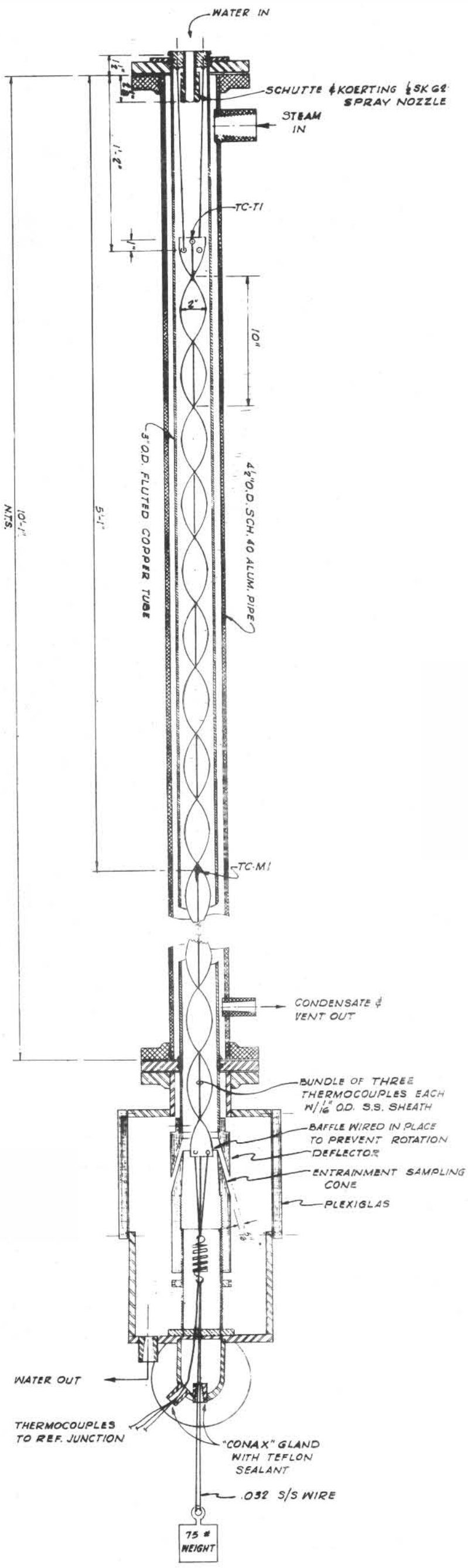

FIGURE 7.9 Spiral baffle installed in 3 in. by 10 ft fluted tube

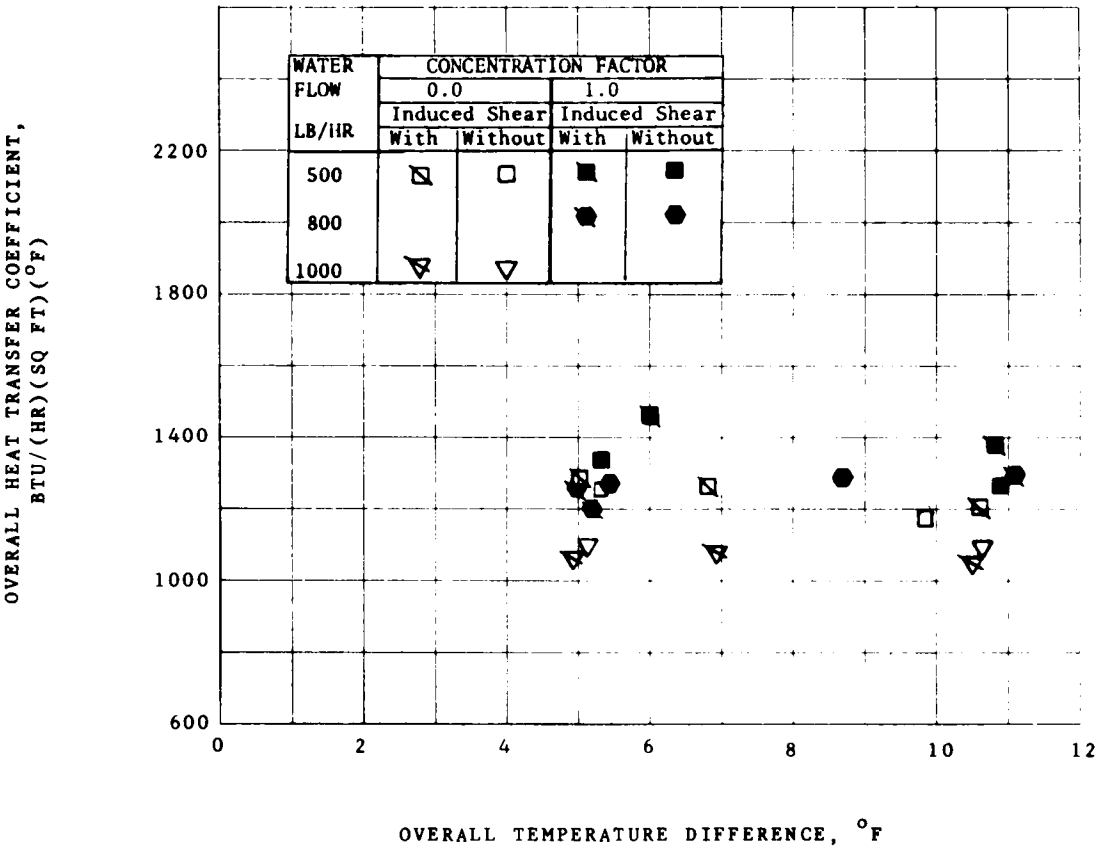

FIGURE 7.10. Comparison of heat transfer coefficient with and without the Sephton spiral baffle (see Figure 7.9) at 18 in. Hg vacuum with fresh water and brine. Coefficient based on mean temperature difference and developed heat transfer area of 1.00 sq ft/ft of length.

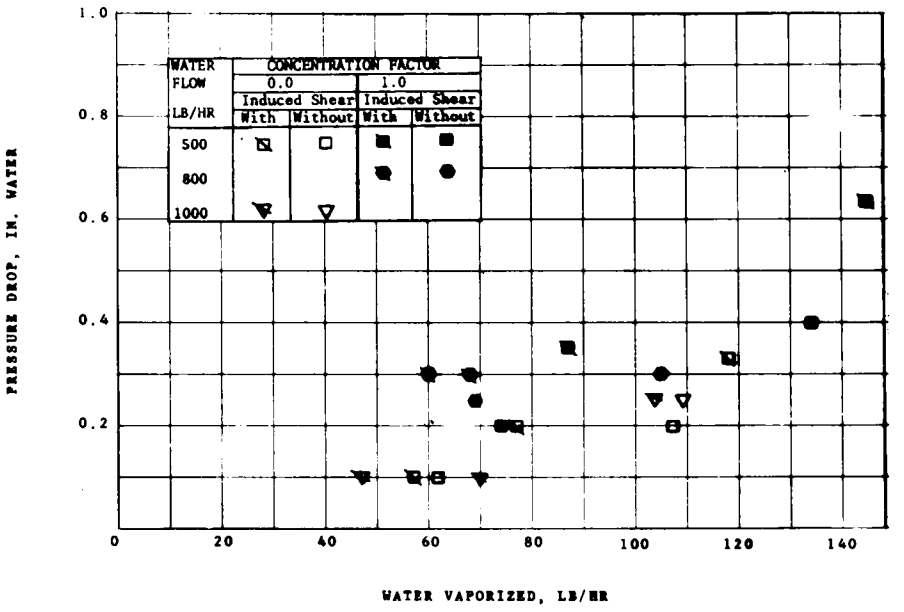

FIGURE 7.11. Comparison of pressure drop with and without the Sephton spiral baffle (see Figure 7.9) at 18 in. Hg vacuum with fresh water and brine.

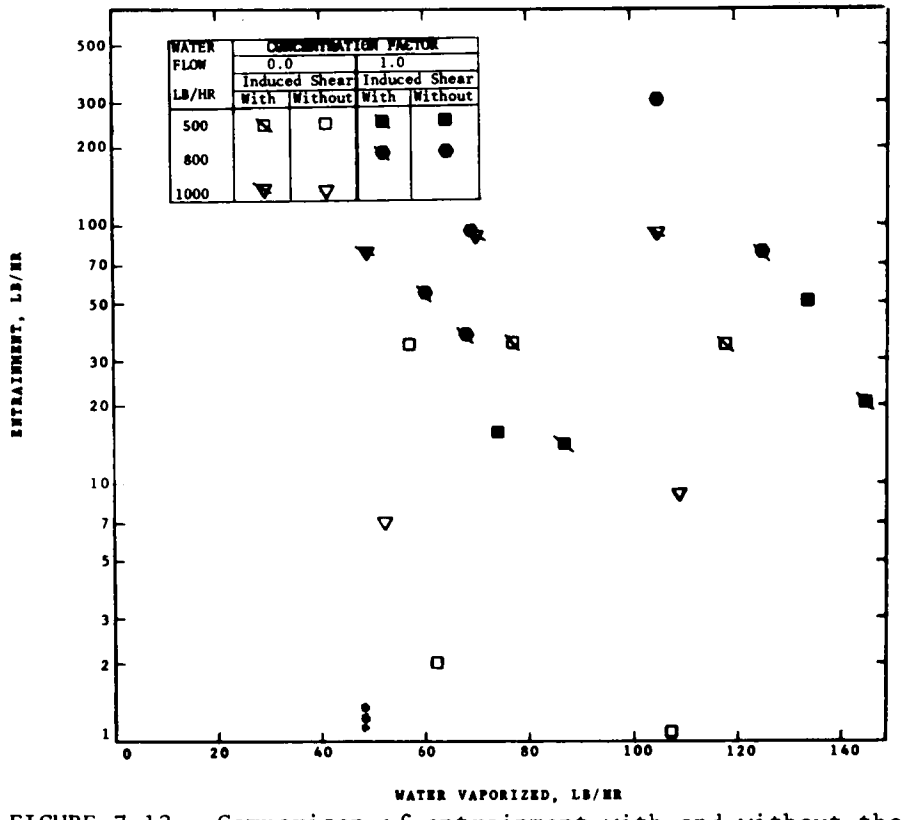

FIGURE 7.12. Comparison of entrainment with and without the Sephton spiral baffle (see Figure 7.9) at 18 in. Hg vacuum with fresh water and brine.

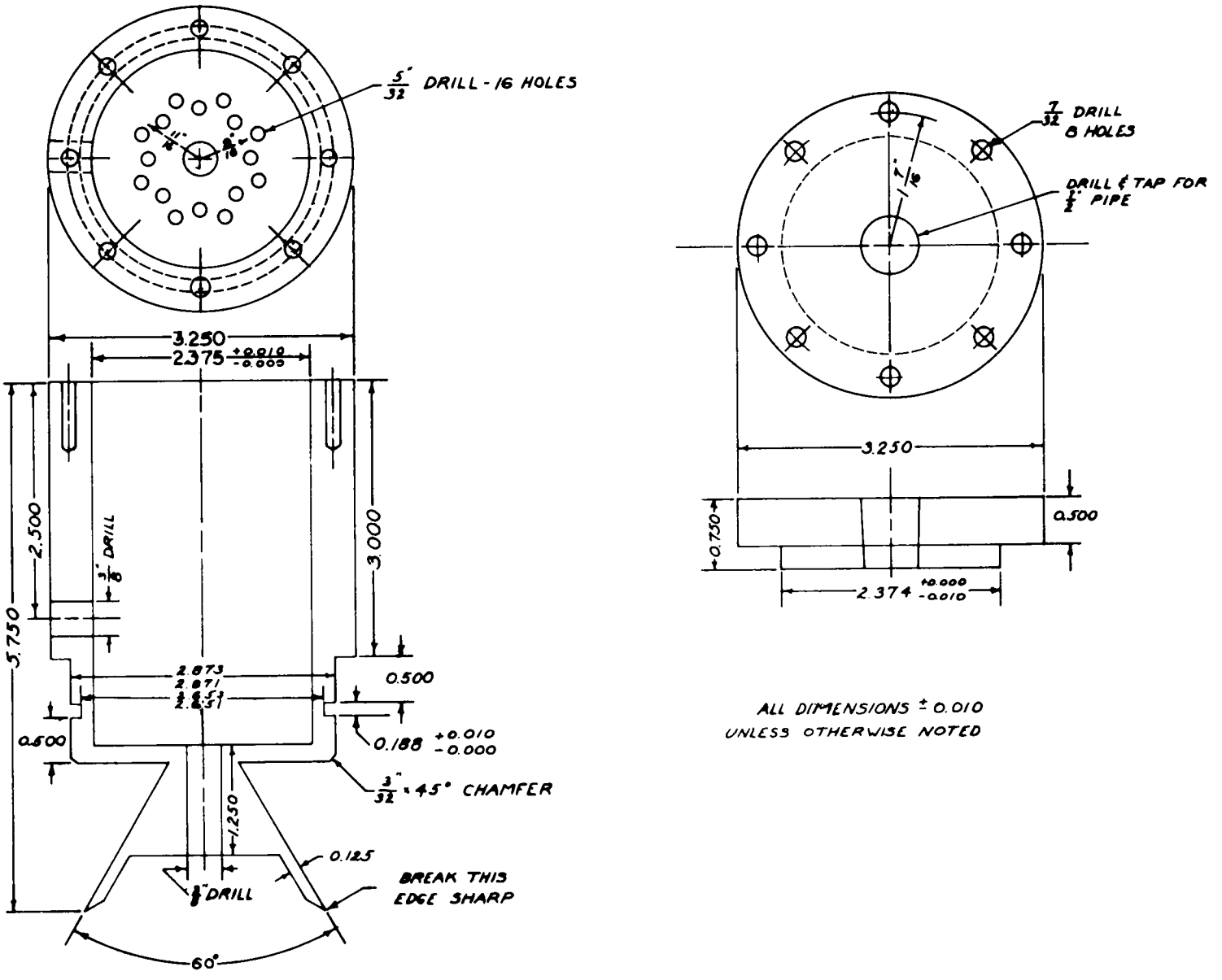

FIGURE 7.13. Detailed drawing of flow distributor.

APPENDIX

APPARATUS FOR DETERMINING CONCENTRATION OF AIR IN STEAM

Operation of the apparatus is as follows:

The steam-air sample is fed into a small water-cooled condenser. The condensate and air initially flow into a large aspirator bottle until the insulated sample line is thoroughly heated. The flow is then directed into the 50 ml buret by closing stopcock (C), opening stopcock (B) and redirecting flow through the three-way stopcock (A). The condensate separates out in the 50 ml buret leaving the air to flow into 1000 ml buret No. 1. This buret is initially full of water but the water is displaced by the incoming air into buret No. 2. When sufficient sample has been taken, the positions of stopcocks, (A), (B) and (C) are rapidly returned to their initial position and stopcock (D) is closed. The pressure over the liquid in buret No. 2 is adjusted by controlling needle valve (E) until the liquid levels in the two 1000 ml burets are the same. The manometer gives the pressure over the liquid in buret No. 2 which is the same as the air pressure in buret No. 1. The air concentration is calculated from the volume of condensate and the volume, pressure and temperature of the air.

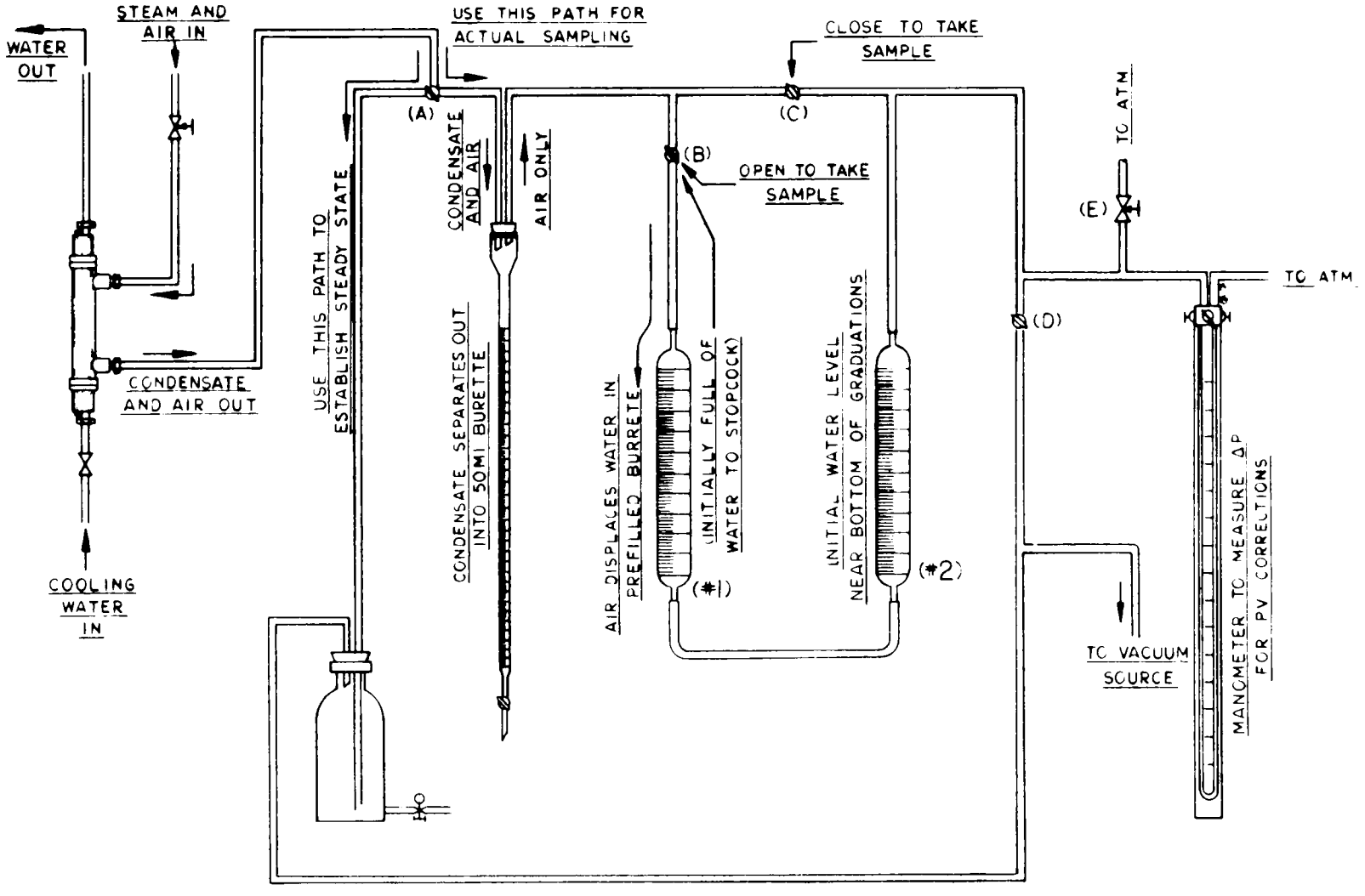

FIGURE A.1 Apparatus for measuring noncondensable content of steam.

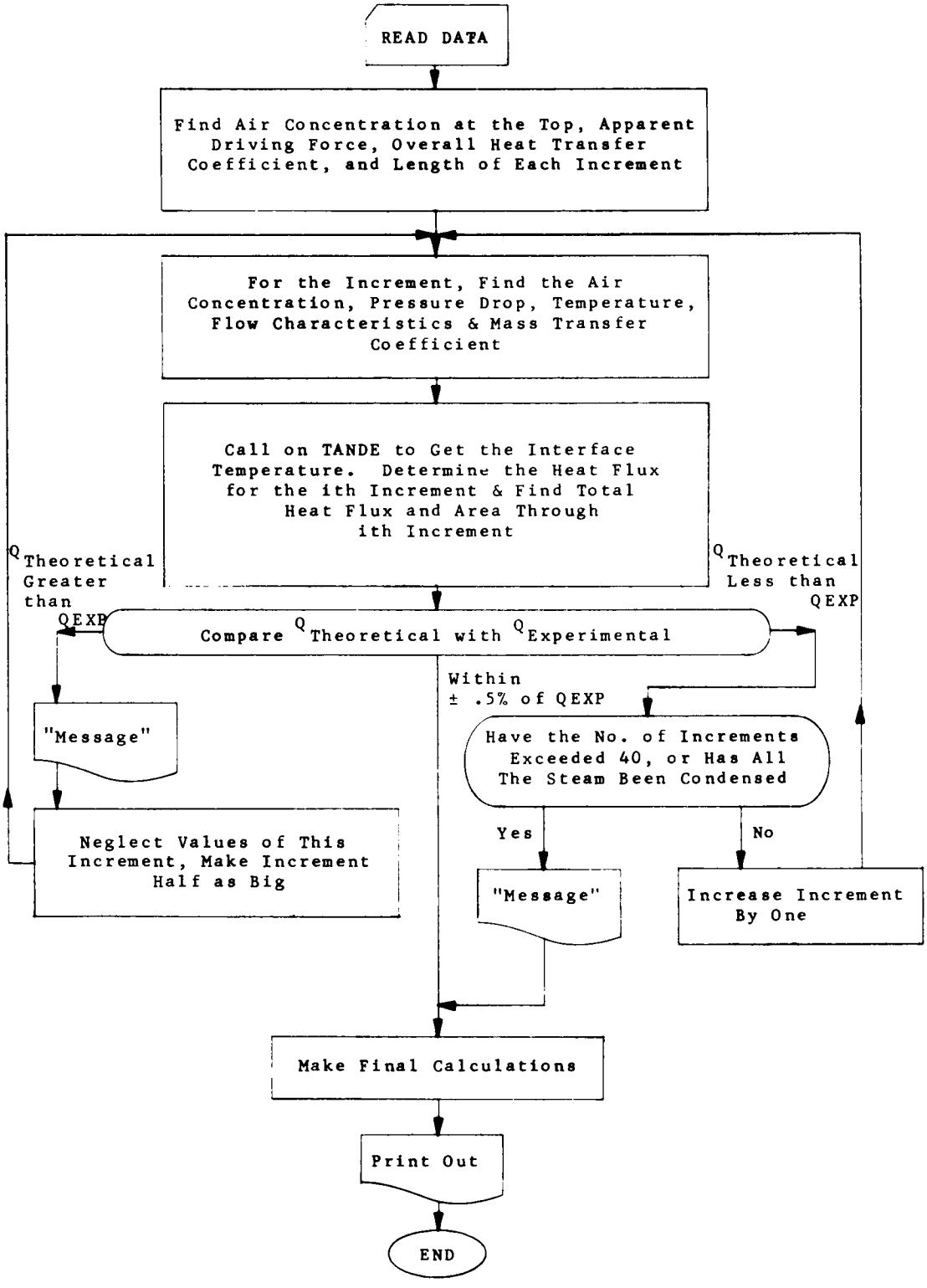

FIGURE A.2. Flowchart for computer program for predicting heat transfer by Colburn-Hongen method.

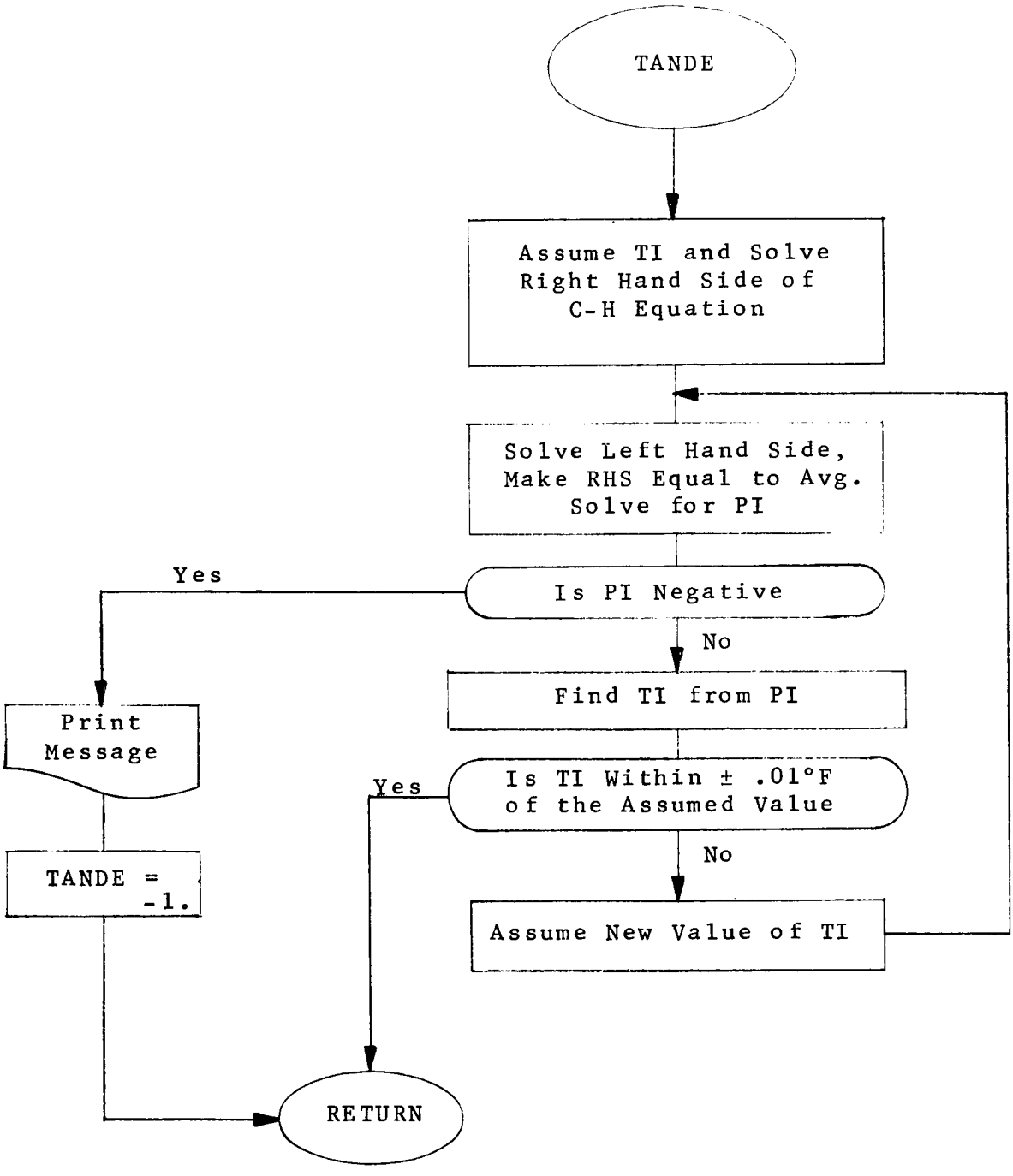

FIGURE A.3. Flowchart for Convergence Subroutine.

PROGRAM LISTING

```
-
      PROGRAM OSWRAIR(INPUT,OUTPUT,TAPE5=INPUT,TAPE6=OUTPUT)
C*****************************************************************************
C  EFFECT OF AIR IN STEAM ON HEAT TRANSFER IN THE FLUTED TUBE
C    USING COLBURN-HOUGEN CORRELATION
C*****************************************************************************
      REAL KG
      DIMENSION QFLUX(50),Q(50),RUNNO(8) ,S(3)
      DIMENSION QQ(50),HH(50)
      DIMENSION SU(3),CU(3)
      DATA SU(1),SU(2),SU(3),CU(1),CU(2),CU(3)/-5.0,-5.55,-10.5,
     1 1005.,930.,1353. /
      DATA DE,AC /0.1572,0.03931/
      FUNV(X)=0.019844 + 4.84E-5*X
      DATA S(1),S(2),S(3)/10.286E3,8.846E3,12.06E3/
 1    READ(5,99) RUNNO
 99   FORMAT(8A4)
      READ(5,100) TV,TL,UP,WST,WA,NI,DPOA,ICTRL,VENT,KK
 100  FORMAT(5F10.3/I3,7X,F10.2,I2,8X,F10.2,I2)
      READ(5,101) QNC
 101  FORMAT(F10.0)
      WRITE(6,200) RUNNO
      WRITE(6,100) TV,TL,UP,WST,WA,NI,DPOA,ICTRL,VENT,KK
 200  FORMAT(1H1,1H ,10X,7HRUN NO.,3X,8A4//)
      WRITE(6,101) QNC
      WRITE(6,300)
 300  FORMAT(1H /////////)
      AI=9.833/FLOAT(NI)
      VENTA=VENT
      WRITE(6,203)
 203  FORMAT(1H ,10X,8HINTERVAL,6X,5HSTEAM,6X,10HCONDENSATE,7X,3HAIR,8X,
     13HAIR,9X,4HHEAT,8X,8HREYNOLDS/
     1                  26X,4HRATE,9X,4HRATE,9X,4HRATE,7X,5HCONC.,5X,10HTR
     2ANSFERED,6X,6HNUMBER/
     2          24X,7H(LB/HR),6X,7H(LB/HR),7X,7H(LB/HR),1X,12H(WT PERCENT
     3),3X,8H(BTU/HR)//)
      WC=0.
      WS=WST - WC
      GASIN=WST + WA
      CAT=WA*100./GASIN
      XA=WA/29./((WST-WC)/18. + WA/29.)
      XV=1.0-XA
      PV=PSATL(TV)
```

```
      PS=PV/XV
      XAB=WA/29./((VENT - WA)/18. + WA/29.)
      PAB=PS*XAB
      PVB=PS - PAB
      TVB=TSATL(PVB)
      TS=TSATL(PS)
      ADF=TS - TL
      QS=S(KK)*ADF
      UP=CU(KK) + SU(KK)*ADF
      PT=PSATL(TL)
      QTOT=0.
      QFLT=0.
      X=AI*0.5
      AREA=0.
      IC=0
      SQSENS = 0.0
      DO 10 I=1,50
      AREA=AREA+AI
      IC=IC+1
      DPX=3.80E-04*X**3*DPOA /14.7
      PTI=PT - DPX
      TL=TSATL(PTI)
      XA=WA/29./((WST-WC)/18. + WA/29.)
      XV=1.0-XA
      CA=WA*100./(WST - WC + WA)
      PA=XA*PS
      PV=PS-PA
      IF (PA.LT.PV) GO TO 45
      X=X-AI+AI/2.
      AREA=AREA-AI
      AI=AI/2.
      I=I-1
      GO TO 10
45    CONTINUE
      TV1=TV
      TV=TSATL(PV)
      XLAM=HSATV(TV,PV) - HSATL(TV)
      XMUV=FUNV(TV)
      G=(WST-WC+WA)/AC
      RE=G*0.0855/XMUV
      H=0.023*0.4*G/(DE*G/XMUV)**0.2
      FAC=0.0343*XLAM*G/(DE*G/XMUV)**0.2
39    CONTINUE
      CALL TANDE(TL,UP,PV,FAC,TV,PA,PAB,KL,PS,KI,TI,H,QSENS)
      IF ( TI .LT. 0.) GO TO 26
      SQSENS = SQSENS + QSENS*AI
      QQ(I) = QSENS * AI
      HH(I) = H
      II = II + I
      QFLUX(I)=UP*(TI-TL)
      QFLT=QFLT+QFLUX(I)
```

```
 22   Q(I)=QFLUX(I)*AI
      QTOT=QTOT + Q(I)
      WC=WC + Q(I)/XLAM
      X=X + AI
      WRITE(6,204) I,WS ,WC,WA,CA,Q(I),RE,TI,KI
 204  FORMAT(13X,I3,8X,F6.1,8X,F6.1,9X,F5.2,5X,F4.1,6X,F9.0,4X,F8.0,
     15X,F8.2,1X,I3)
      WS=WST - WC
      TEST=(QNC - QTOT)/QNC
      IF (ABS(TEST).LE. 0.005)GO TO 30
      IF(TEST .GT. 0.) GO TO 35
      WRITE(6,225)
 225  FORMAT(1H /1H ,59H**THEORETICAL Q TOO BIG,ADJUST AND TRY A SMALLER
     1 INTERVAL**/)
      QTOT=QTOT - Q(I)
      SQSENS = SQSENS - QSENS * AI
      QFLT=QFLT - QFLUX(I)
      X=X - AI + AI*0.5
      WS=WST + WC
      WC=WC-Q(I)/XLAM
      AREA=AREA - AI
      AI=AI*0.5
      I=I-1
 35   CONTINUE
      IF(WS .LT. 0. .OR. IC .GT. 40) GO TO 40
 10   CONTINUE
      VENTC=WST - WC
      GO TO 30
 40   WRITE(6,230) WS,IC
 230  FORMAT(1H /1H ,5X,4HWS= ,F8.2,5X,4HIC= ,I3/)
 30   CONTINUE
      VENTC=WST - WC
      ETA=9.833/AREA*100.
      WRITE(6,205) ETA,QS,VENT,VENTC,QTOT,ADF,AREA,QNC,SQSENS
 205  FORMAT(1H ///10X,4HETA=,F7.2,5X,5HQEXP=,F9.0,5X,7HVENTEX=,F7.1,5X,
     18HVENTCAL=,F7.1/15X   ,5HQTOT=,F9.0,5X, 19HAPP. DRIVING FORCE=,
     3F7.2,5X,6HAREA =,F8.4/     10X, 5HQNC =,F9.0,
     45X,15HSENSIBLE HEAT= ,F9.0//)
      WRITE (6,250)(QQ(NN),NN=1,II)
      WRITE (6,250)(HH(NN), NN = 1,II)
250   FORMAT ( 9(2X,E10.3))
      ANOA=QNC/(UP*ADF)
      ACEF=(9.833 - ANOA)*100./ANOA
      CHEF=(AREA - ANOA)*100./ANOA
      WRITE(6,231) ANOA, ACEF, CHEF
 231  FORMAT(1H //1H ,6HANOA= ,F10.5,5X,6HACEF= ,F10.5,5X,6HCHEF= ,F10.5
     1/)
 26   IF (ICTRL .GT. 0) GO TO 25
      GO TO 1
 25   CONTINUE
      END
```

```
      SUBROUTINE TANDE (TL,UP,PV,FAC,TV,PA1,PA2,KL,PS,KI,TI,H,QSENS)
      TI = TV-1.0
      PI = PSATL(TI)
      DO 40 I=1,20
   17 FORMAT(1H ,10X,E12.5)
      PAI=PS - PI
      IF (PI .GE. PV) GO TO 42
      IF (KL .EQ. 0) GO TO 50
   50 PALM=(PAI-PA1)/ALOG(PAI/PA1)
51    CONTINUE
      XLHS = UP*(TI-TL)
      QSENS=H*(TV - TI)
      XRHS = FAC*(PV-PI)/PALM  + QSENS
      TEST=(XLHS - XRHS)/XLHS
      PI=PV-((XRHS+XLHS)*0.5 - QSENS)*PALM/FAC
      IF (PI .LE. 0.) GO TO 42
      TI=TSATL(PI)
      IF ( TI.LT. TL) GO TO 42
      IF ( ABS(TEST).LE. 0.005) GO TO 41
   40 CONTINUE
   41 CONTINUE
      KI=I
      GO TO 43
   42 CONTINUE
      WRITE=6*550(
  55% FORMAT(1H ,29HTANDE FOUND NEGATIVE PRESSURE/)
      WRITE(6,17) TI
      WRITE(6,17) PI
      TI=-1.
   43 CONTINUE
      RETURN
      END
      FUNCTION TSATL(P)
      DIMENSION A(10)
      DATA(A(I),I=1,9)    /35.15789,24.592588,2.1182069,-0.3414474,0.1574
     11642,-3.1329585E-2,3.8658282E-3,-2.4901784E-4,6.8401559E-6/
      C=P*14.696
      TSATL=A(1)
      DO 200 I=1,8
  200 TSATL=TSATL+A(I+1)*((ALOG(10.*C))**I)
      RETURN
      END
      FUNCTION HSATL(T)
C   FUNCTION SUBPROGRAM HSATL
      DIMENSION A(10)
      DATA(A(I),I=1,6)    /-3.2179105E1,1.0088084,-1.1516996E-4,4.8553836
     1E-7,-7.3618778E-10,9.6350315E-13/
      HSATL=A(1)
      DO201 I=1,5
  201 HSATL=HSATL+A(I+1)*(T**I)
      RETURN
      END
```

```
      FUNCTION HSATV(T,P)
C     FUNCTION SUBPROGRAM HSATV
      DATA A,B,C,D,E,F,G/1.89,2641.62,10.,80870.,82.546,1.6246E5,.21828/
      DATA XH,XJ,XK,XL,XM,XN,Q,R,U,V,W,Y,C1,XLC,HP,XKP/1.2697E5,3.635E-4
     1,6.768E-8,1.4720,7.5566E-4,47.8365,.101325,4.55504,.43,.2388888,-6
     298.65,0.0160185,14.6959,2.30258509,2502.36,273.16/
      TT=(T-32.)/1.8
      Z=P
      TAU=1./(XKP+TT)
      ALFA=B*(C**(D*TAU*TAU))
      BETA=D*XLC*TAU*TAU
      GAMA=ALFA*(1.+2.*BETA)
      DEL=E-F*TAU
      EPSI=G-XH*TAU*TAU
      R0=XJ-XK*((1000.*TAU)**24.)
      B0=A-TAU*ALFA
      XMU1=Z*Z/2.
      XMU2=(TAU*Z)**4./4.
      XMU3=(TAU*Z)**13./13.
      XLAM1=R0*TAU*TAU*(B0*(3.*DEL-F*TAU)-DEL*TAU*2.*GAMA)
      XLAM2=R0*B0*B0*(B0/TAU*(4.*EPSI-2.*XH*TAU*TAU)-4.*EPSI*GAMA)
      AA=(13.*R0-24.*XK*(1000.*TAU)**24)/TAU
      BB=13.*R0*GAMA
      IF (B0) 4,5,5
    4 B0=-B0
      XLAM3=R0**12*(B0*AA+BB)
      GO TO 7
    5 XLAM3=R0**12*(BB-B0*AA)
    7 HSATV=((
     1        Z*(A-2.*TAU*ALFA*(1.+BETA))+XLAM1*XMU1+XLAM2*XMU2+XLAM3*XMU
     13)*Q+XL/TAU+XM/TAU**2./2.-XN*ALOG(TAU)+W+HP)*U
      RETURN
      END
      FUNCTION PSATL(T)
      DATA A,B,C,D,AA,BB,CC,DD,EE/ 3243.7814E-3,586.826E-5,
     11170.2379E-11,2187.8462E-6,3346.313E-3,4141.13E-5,7515.484E-12,
     11379.4481E-5,6564.44E-14/
      TK=(T-32.)/1.8 + 273.16
      X=647.27 - TK
      IF (T .GT. 200.) GO TO 10
      XX=X/TK*( A + B*X +C*X*X*X)/(1. + D*X)
      GO TO 11
   10 XX=X/TK*(((EE*X + CC)*X*X  + BB)*X +AA)/(1. + DD*X)
   11 P=EXP(ALOG(218.167 ) - XX*2.30259)
      PSATL=P
      RETURN
      END
```

NOMENCLATURE

AC	Cross-sectional area (Sq Ft)
ADF	Apparent driving force (°F)
AI	Area of increment (Sq Ft)
ANOA	Total area of corresponding run without noncondensables (Sq Ft)
AREA	Total area Colburn-Hougen (Sq Ft)
CA	Air concentration at increment (Wt %)
CAT	Air concentration at the top (Wt %)
CHEF	% increase in area predicted by Colburn-Hougen
CU	Array of constants of the linear fit of UP vs. Δt
DE	Equivalent diameter (Ft)
DPOA	Overall experimental pressure drop (In. H_2O)
DPX	Pressure drop at increment (Atm)
ETA	Efficiency, area predicted by Colburn-Hougen/ experimental area (%)
G	Gas mass flux (Lb/Hr-Sq Ft)
GASIN	Rate of air and steam (Lb/Hr)
ICTRL	Control to terminate program
KG	Mass transfer coefficient through gas film (Lb Vapor Condensed/Hr-Sq Ft-Atm)
KK	Vacuum level code
NI	No. of increments
PA	Partial pressure of air (Atm)
PS	Shell pressure (Atm)
PT	Tube pressure (Atm)

PTI	Tube pressure at increment (Atm)
PV	Partial pressure of steam (Atm)
Q	Heat transferred at increment calculated by Colburn-Hougen (Btu/Hr)
QFLT	Total heat flux calculated by Colburn-Hougen (Btu/Hr-Sq Ft)
QFLUX	Heat flux calculated by Colburn-Hougen at increment (Btu/Hr-Sq Ft)
QNC	Experimental heat transfer of run with noncondensables (Btu/Hr)
QS	Experimental heat transfer on steam only run with the same driving force of noncondensable run (Btu/Hr)
QTOT	Total heat transfer rate (Btu/Hr)
RUNNO	Run identification number
S	Array of slopes of QA vs ΔT fit
SU	Array of slopes of UP vs ΔT fit
TI	Temperature at steam-air interface (°F)
TL	Saturation temperature of liquid side at PT (°F)
TS	Saturation temperature of vapor side at PS (°F)
TV	Saturation temperature of steam at PV (°F)
UP	Experimental overall heat transfer coefficient (Btu/Hr-Sq Ft-°F)
VENT	Experimental vent rate (Lb Gas/Hr)
VENTC	Calculated vent rate (Lb Gas/Hr)
WA	Air rate (Lb/Hr)
WC	Condensate rate (Lb/Hr)
WS	Steam rate at increment (Lb/Hr)
WST	Total steam rate (Lb/Hr)
X	Distance from the top of the tube to the middle of increment (Ft)

XA	Mole fraction of air
XLAM	Latent heat of steam (Btu/Lb)
XMUV	Viscosity of steam (Lb/Hr - Ft)
XV	Mole fraction steam

* U.S. GOVERNMENT PRINTING OFFICE : 1969 O—366-706